SYNTHETIC FUELS FROM CRACKING OF LDPE USING ZEOLITE BETA CATALYST IN CONTINUOUS PROCESS

BOONSUEB SONTAYAMARN

A THESIS SUBMITTED IN PARTIAL FULFILLMENT
OF THE REQUIRMENTS FOR THE DEGREE OF MASTER OF SCIENCE
IN PETROCHEMICALS AND HYDROCARBON CHEMISTRY
FACULTY OF SCIENCE
KING MONGKUT'S INSTITUTE OF TECHNOLOGY LADKRABANG
2010
KMITL-2010-SC-M-015-009

หัวข้อวิทยานิพนธ์	เชื้อเพลิงสังเคราะห์จากปฏิกิริยาการแตกตัวของพอลิเอทิลีนชนิดความหนาแน่นต่ำโดยใช้ซีโอไลท์บีต้าเป็นตัวเร่งปฏิกิริยาในกระบวนการแบบต่อเนื่อง
นักศึกษา	นายบุญสืบ สนธยามาลย์
รหัสประจำตัว	48068003
ปริญญา	วิทยาศาสตรมหาบัณฑิต
สาขาวิชา	ปิโตรเคมีและเคมีของไฮโดรคาร์บอน
อาจารย์ที่ปรึกษา	รศ.ดร.ตะวัน สุขน้อย

บทคัดย่อ

งานวิจัยนี้เป็นการพัฒนาและปรับปรุงเกลียวหนอนเดี่ยวภายในชุดปฏิกรณ์เบดเคลื่อนที่ในกระบวนการแบบต่อเนื่องเพื่อศึกษาการแตกตัวของพอลิเอทิลีนซึ่งมีความหนืดแตกต่างกันให้เป็นเชื้อเพลิงสังเคราะห์โดยใช้ตัวเร่งปฏิกิริยาซีโอไลต์บีต้า ชุดปฏิกรณ์เบดเคลื่อนที่ประกอบด้วย 4 ส่วน คือ ส่วนป้อนสาร (เครื่องอัดรีดพอลิเมอร์แบบเกลียวหนอนเดี่ยว) ถังปฏิกรณ์ ส่วนเก็บผลิตภัณฑ์ และส่วนเก็บกากที่เหลือจากการแตกตัว เกลียวหนอนเดี่ยวภายในถังปฏิกรณ์ที่ถูกสร้างขึ้นสามารถพาพอลิเอทิลีนตั้งต้นที่มีความหนืดที่แตกต่างกันและตัวเร่งปฏิกิริยาจากด้านบนเข้าสู่ภายในถังปฏิกรณ์และขับกากที่เหลือจากการแตกตัวออกทางด้านล่างของถังปฏิกรณ์โดยก๊าซผลิตภัณฑ์จะถูกก๊าซไนโตรเจนพาออกทางด้านบนของถังปฏิกรณ์ การศึกษาการแตกตัวของพอลิเอทิลีนเป็นเวลามากกว่า 5 ชั่วโมง ที่อุณหภูมิ 430 องศาเซลเซียสโดยใช้ก๊าซไนโตรเจนเป็นก๊าซตัวพาด้วยอัตราการไหล 50 มิลลิลิตรต่อนาที อัตราเร็วของเกลียวหนอนเดี่ยวภายในถังปฏิกรณ์ 46, 66 และ 130 รอบต่อนาที ปริมาณตัวเร่งปฏิกิริยา 1.0 และ 2.0 เปอร์เซ็นต์โดยน้ำหนักของพอลิเมอร์ อัตราการป้อนสารประมาณ 400, 600, 700 และ 800 กรัมต่อชั่วโมง ความหนืดของพอลิเอทิลีนตั้งต้น 2.7, 4.0 และ 20.3 พอยส์ จากการศึกษาพบว่าได้ผลิตภัณฑ์ก๊าซ 3-24 เปอร์เซ็นต์ ผลิตภัณฑ์ของเหลว 4-63 เปอร์เซ็นต์ และผลิตภัณฑ์แวกซ์ 0.3-16 เปอร์เซ็นต์ ความสามารถในการเกิดปฏิกิริยาเพิ่มขึ้นเมื่อเพิ่มอัตราเร็วของเกลียวหนอนเดี่ยวภายในถังปฏิกรณ์และปริมาณตัวเร่งปฏิกิริยา อย่างไรก็ตามการเพิ่มอัตราเร็วของเกลียวหนอนเดียวภายในถังปฏิกรณ์ทำให้เกิดการแตกตัวด้วยความร้อนเพิ่มขึ้นด้วย นอกจากนี้ความสามารถในการเกิดปฏิกิริยาจะเพิ่มขึ้นเมื่อทำการลดอัตราการป้อนสาร และเมื่อใช้พอลิเอทิลีนที่มีความหนืดมากซึ่งมีน้ำหนักโมเลกุลสูงเป็นสารป้อน ทำให้สายโซ่ของพอลิเอทิลีนที่แตกตัวแล้วส่วนมากยังคงมีขนาดใหญ่จนไม่สามารถแพร่และแตกตัวภายในรูพรุนของซีโอไลท์บีต้าได้ จึงส่งผลให้ความสามารถในการเกิดปฏิกิริยาลดลง พบว่าเชื้อเพลิงเหลวที่สังเคราะห์ขึ้นใน

งานวิจัยนี้มีค่าออกเทนประมาณ 96-115 โดยส่วนใหญ่ประกอบด้วยสารประกอบไฮโดรคาร์บอนประเภทโอเลฟินในปริมาณสูงในขณะที่มีปริมาณของสารประกอบไฮโดรคาร์บอนประเภทพาราฟินและอะโรเมติกต่ำเมื่อเปรียบเทียบกับแก๊สโซลีนทางการค้า

Thesis Title Synthetic fuels from cracking of LDPE using zeolite beta catalyst in continuous process

Student Mr. Boonsueb Sontayamarn

Student ID. 48068003

Degree Master of Science

Programme Petrochemicals and Hydrocarbon Chemistry

Thesis Advisor Assoc.Prof.Dr.Tawan Sooknoi

ABSTRACT

In this work, continuous catalytic cracking of polyethylene over zeolite beta were investigated in the moving bed screw reactor design for the production of liquid fuel from a feed with different viscosities. The moving bed screw reactor consisted of four sections: a feeder (single screw extruder), a reactor (screw reactor), a product collector, and a residue chamber. The single screw reactor carried feed and the catalyst down through the residue chamber at the bottom of the reactor and allowed cracked gases to exist from the top of the reactor. The catalytic cracking of polyethylene was carried out at 430°C for over 5 hours on stream. Zeolite beta was used as the catalyst, and nitrogen was fed as a carrier gas with a flow rate of 50 ml/min. The catalytic cracking of polyethylene can be continuously operated without deactivation in the design moving bed screw reactor. The effects of reactor screw speed (RSS; 46, 66 and 130 rpm), catalyst content (1.0 and 2.0 % wt.), polyethylene feed rate (~400, 600, 700 and 800 g/hr.) and viscosity of polyethylene feeds (2.7, 4.0 and 20.3 poise) were investigated. It was found that 3-24 % gas products, 4-63 % liquid products and 0.3-16 % wax products can be obtained. The cracking activity was increased with an increase in the reactor screw speed and catalyst loading. However, thermal cracking can be promoted by a better heat transfer at high reactor screw speed. In addition, the higher cracking activity occurred when the feed rate was decreased. Polyethylene fed at high viscosity with exceeding high molecular weight, cannot be easily cracked to the polyethylene fragments small enough to diffuse and further cracked within the pore of zeolite beta. The cracking activity was decreased. In addition, the liquid fuels from this work composed of mainly of olefins while the less paraffins and aromatics hydrocarbons showed the higher octane number, as compared with commercial gasoline 91.

ACKNOWLEDGEMENTS

I would like to thank and express my profound gratitude to my advisor, Assoc. Prof. Dr. Tawan Sooknoi for encouraging guidance, advice, discussion and helpful suggestions throughout this work. I am also grateful to Assist. Prof. Dr. Vanchat Chuenchom, Assoc. Prof. Dr. Ittipol Jangchud and Assoc. Prof. Dr. Sirirat Jitkarnka for serving as the chairperson and the committee members, and their valuable comments.

Special thanks are also given to Energy Policy and Planning Office of Thailand for financial support and TPI Polene Public Company Limited for supplying polyethylene. I also appreciate the supports from the Department of Chemistry, Faculty of Science, King Mongkut's Institute of Technology Ladkrabang for the equipment, chemicals and facilities.

I would like to extend my sincere appreciation to all of my teachers, and my friends for their support and encouragement.

Finally, I dedicates my work to my above parents, my family for their moral support.

Boonsueb Sontayamarn

CONTENTS

CONTENTS (Continued)

CONTENTS (Continued)

CONTENTS (Continued)

CONTENTS (Continued)

LIST OF TABLES

LIST OF TABLES (Continued)

LIST OF FIGURES

LIST OF FIGURES (Continued)

LIST OF FIGURES (Continued)

LIST OF FIGURES (Continued)

LIST OF ABBREVIATIONS

DSC	Differential Scanning Calorimeter
FID	Flame Ionization Detector
GC	Gas Chromatograph
GC/MS	Gas Chromatograph/Mass Spectrometer
MFI	Melt Flow Index
NMR	Nuclear Magnetic Resonance
LDPE	Low density polyethylene
RSS	Reactor screw speed
SEM	Scanning Electron Microscope
TGA	Thermogravimetric Analyzer
XRD	X-ray Powder Diffractometer
XRF	X-ray Fluorescence Spectroscopy

CHAPTER 1

INTRODUCTION

1.1 Statement and significance of the problems

Currently large amounts of waste plastics that resulted from a dramatic increase in polymer production gives rise to serious environmental concerns, as plastic does not degrade and remains in municipal refuse tips for decades. Plastic waste being more voluminous than the organic waste takes up a lot of landfill space that is becoming scarce and expensive. Incineration is not an acceptable solution to the problem, as toxic gases are produced and a solid waste problem leads to air pollution. The only sustainable solution is polymer recycling. Amongst various polymer recycling methods, thermal and/or catalytic degradation of plastic waste to fuel show the highest potential for a successful future commercial process. Especially plastic waste can be considered as a cheap source of raw materials for fuels, when depletion of natural resources is accelerated. This is particularly the case for community polyolefins, i.e. LDPE, HDPE and PP. Since, they cannot be easily depolymerized into the original monomers but readily transformed into hydrocarbon mixtures [3]. Catalytic degradation of plastic waste offers considerable advantages, as compared to the thermal degradation. This is because the latter demands relatively high temperatures and its products require further processing for their quality to be upgraded. Catalytic degradation occurs at considerably lower temperatures and forms hydrocarbons mainly in the range of motor gasoline over zeolite catalyst.

Most of previous research have been studied on thermal and thermo-catalytic degradation of low [9,14-15,26] and high [3,5-8, 10-12] density polyethylene in batch processes. For continuous process, catalytic cracking of low viscosity polyethylene was generally reported [25, 29-31, 39]. However, both in batch and continuous processes, the deactivated catalyst were disadvantage. Although attempt on FCC of polymer waste were made to cure the deactivated catalyst, the suitable particle sizes of both catalyst and polymer feed is crucial that may be laborious to use with general plastic waste [20]. Accordingly, the moving bed screw reactor was proposed in the previous work [39]. The limitation of particle sizes feeds was solved employing the screw extruder that mix and feed the catalyst with polymer into the reactor. With the screw at the bottom end of the rotating paddle within the reactor, the used catalyst can be continuously removed and replaced by newly fed one. However, the rotating paddle of reactor cannot controlled the resident time of feeds within the reactor. In addition, the general plastic waste was mainly composes of HDPE, LDPE and other polyolefins that possess different viscosity. This sometime makes it difficult for the system to handle the polymer feed with high viscosity as the used catalyst and polymer residue cannot be satisfactorily driven out of the reactor.

In this thesis, the moving bed was developed by incorporating a screw into the reactor for cracking the polyethylene samples with different viscosity and molecular weights. With the screw reactor, the resident time of the feeds can be readily controlled. Various hydrocarbons products including gas, liquid, wax products and residue can be separated and determined. The effect of reactor screw speed (RSS) and viscosity of polymer feeds were investigated, together with the typical reaction parameters, namely catalyst content and polymer feed rate.

1.2 Goal and Objectives

The objectives of this thesis were as follows:

1.2.1 To obtain vertical moving bed reactor for cracking of low-density polyethylene (LDPE) with variable viscosity.

1.2.2 To understand effect of factors in cracking process namely viscosity, catalyst (zeolite H-beta) content, polyethylene feed rate and residence time (reactor screw speed).

1.2.3 To obtain suitable operating condition for the production of motor gasoline with high selectivity.

1.3 Scopes of the study

The scopes of this thesis are as follows:

1.3.1 Characterization of zeolite catalyst by X-ray powder diffractometer (XRD), X-ray fluorescence spectroscopy (XRF), Scanning electron microscope (SEM) and Gas adsorption analyzer (Autosorb-1).

1.3.2 Characterization of polyethylene material and determination of viscosity by Differential scanning calorimeter (DSC) and Melt flow indexer (CEAST 6841.000 ASTM D1238, CEAST)

1.3.3 Development of the moving bed screw reactor for cracking of polyethylene samples with different viscosity.

1.3.4 Study on thermal and catalytic degradation of polyethylene by Thermogravimatric analyzer (TGA).

1.3.5 Study on effect of feed rate (400-800 g/hr), catalyst content (1.0 and 2.0 %wt), residence time (reactor screw speed 40-130 rpm) and viscosity (4-20 poise). It was be considered from conversion, selectivity, and yield and wax production of cracking reaction.

1.3.6 Analyse and evaluation of the liquid products from the reaction based on their compositions and quality as liquid fuel by, Gas chromatography (GC), Gas chromatograph/Mass spectrometer (GC-MS), Nuclear magnetic resonance spectrometer (NMR) and Automatic distillation analyzer.

1.3.7 Analyses and evaluation of the wax products from the reaction based on their the melting point and heat of fusion by Differential scanning calorimeter (DSC).

1.3.8 Study on thermal degradation of the residue using Thermogravimatric analyzer (TGA).

1.4 Expected results

1.4.1 This thesis would reduce the problem of the catalyst deactivation in the cracking of polyethylene with various viscosity and process severity (i.e. temperature, pressure and contact time) using the moving bed screw reactor.

1.4.2 This research would provide a process for high yield gasoline production from the cracking of plastic waste, from which an industrial scale process may be developed.

1.4.3 This research would provide an approach for alternative energy resource.

CHAPTER 2

THEORY AND LITERATURE REVIEWS

2.1 Zeolites

Zeolites are hydrated aluminosilicate minerals with micro-porous structure. Zeolites, is Greek in origin, coined from word "zein" and "lithos" meaning to boiling store. This is because, when zeolites was rapidly heated, it began to dance about as the water evaporated. Zeolites was first observed in the 18th century by a Swedish mineralogist named Axel Fredrik Cronstedt.

Natural and synthetic zeolites microporous possess ion exchange, sorption, and molecular sieving properties. Zeolites are built from an infinite extending three dimensional network, composed of SiO_4 and AlO_4 tetrahedra with O atoms connecting the neighboring tetrahedra. For a complete siliceous structure, combination of SiO_4 units in this fashion leads to silica (SiO_2), which is an uncharged solid. Upon incorporation of Al into the silica framework, the +3 charge on the Al makes the framework negatively charged, and requires the presence of extraframework cations (inorganic and organic cations can satisfy this requirement) within the structure to keep the overall framework neutral. The zeolite composition can be best described as having three components :

$M^{m+}_{n/m}$	•	$[Si_{1-n}Al_nO_2]$	•	nH_2O
exchangeable cations		framework		sorbed phase

The exchangeable cations give rise to the rich cation exchange chemistry of these materials. The novelty of zeolites stems from their microporosity and is a result of the topology of the framework.

The zeolites contain intracrystalline pores and apertures having dimensions approximately the same as molecular dimensions of organic compound. The zeolites are classified according to the size of these aperture.Table 2.1 shows the number of oxygen atom in the aperture of some zeolites and the aperture dimension (the smallest being 0.4 nm for zeolites A and the biggest being 0.74 for faujasite). The size of the aperture depends on for types of structure and also the size of the exchangeable cations.

Table 2.1 Zeolite and their pore (aperture) [40]

Zeolite	Number of Oxygenn in the ring	10 x Aperture Dimensions, nm
Chabazilte	8	3.6 x 3.7
Erionite	8	3.6 x 5.2
Zeolite A	8	4.1
ZSM-5 (or silicalite)	10	5.1 x 5.5; 5.4 x 5.6
ZSM-11	10	5.1 x 5.5
Heulandite	10	4.4 x 7.2
Ferrierite	10	4.3 x 5.5
Faujasite	12	7.4
Zeolite L	12	7.1
	12	7
Mordenite	12	6.7 x 7
Offretite	12	6.4

On the other hand, zeolites are further grouped into families on the basis of composition, namely, the Si/Al ratio. The amount of Al within the framework can vary over a wide range, with Si/Al = 1 to ∞. Lowenstein [49] proposed that the lower limit of Si/Al of a zeolite framework is one. This is because placement of adjacent AlO_4^- tetrahedra is not favored, due to electrostatic repulsions between the negative charges. Since the ion exchange capacity is equal to the concentration of Al^{3+} ions in the zeolite, the structures with low Si/Al ratios can have higher concentrations of catalytic sites than the others. There are other transitions in properties exemplified by the acid function from zeolites, those incorporating H^+ as the exchangeable ion. Postsynthesis modifications that insert Si in to the framework have also been developed, as in production of siliceous zeolite Y for catalytic cracking by removal of framework aluminum. As the Si/Al ratio of the framework increases, the hydrothermal stability as well as the hydrophobicity increases and enhanced catalytic properties.

Most industrial applications of zeolites are based upon technology adapted from the acid silica/alumina catalysts originally developed for the cracking reaction. This means that the activity required is based upon the production of brønsted sites arising the creation of "hydroxyls" within the zeolite pore structure.

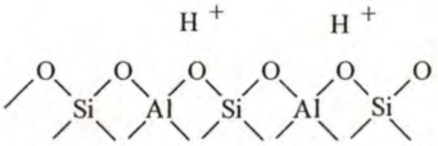

When a hydrogen form zeolite is heated to high temperature, water is driven off and coordinatively unsaturated Al^{3+} ions are formed with the consequent formation of Lewis sites. Over these strong acids sites, a base like pyridine is typically bonded strongly, as compared to strong proton-donor sites, as shown by infrared spectra and temperature-programmed desorption. Formation of the Lewis acid sites is depicted schematically as follows [49]:

Brønsted acid site

Lewis acid site

The Lewis sites in turn are unstable, especially in the continued presence of water vapour and an annealing process stabilizes the structure. This produces the so-called "true" Lewis sites by ejecting Al species from the framework, i.e. :

Lewis site

"True" Lewis site

Zeolites have very special pratical advantage over the more traditional catalysts, in that they will admit only certain reactant molecules and that is potentially tailored for selective products. This selectivity is known as 'shape selective catalysis' and is controlled by 'configurational diffusion' by which useful catalytic reaction are promoted by virtue of a matching of size, shape and orientation of reactant and products molecules to the geometry of the zeolites framework.

Reactant shape selectivity. The control of catalytic process based upon the exclusion of potential reactant can be simply illustrated for butanol dehydration. Using CaA, n-butanol can enter the zeolites and be are converted where as i-butanol cannot. However, both can enter NaX and both are dehydrated, as shown in Figure 2.1

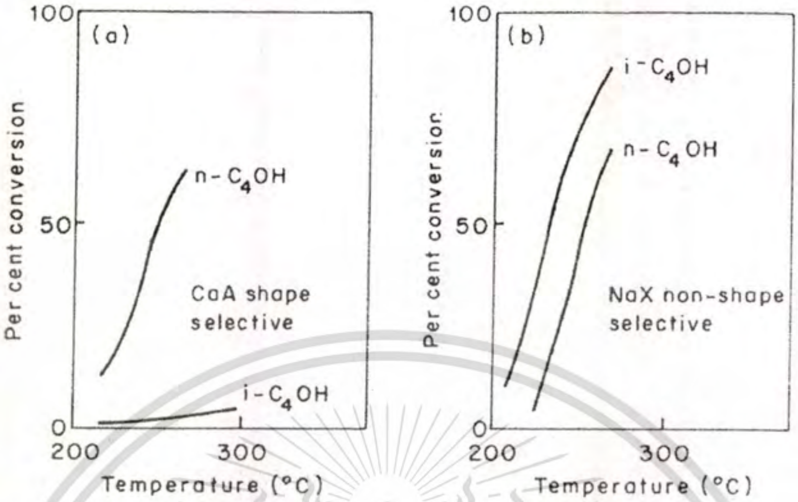

Figure 2.1 Shape-selectivity dehydration of n-butanol on (a) CaA (only n-butanol converted) and (b) NaX (both n- and i-butanol converted) [40]

Intermediate shape selectivity. Control of products shape can arise because the volume available round an active site in a zeolite framework is such as to preclude the formation a bulky intermediate products (transition state) of reactants meeting at the site.This was shown in Figure 2.2, that the acid-cataysed transalkylation of a dialkylbenzene is thought to proceed in modenite and forms a diaryl intermediate probably via:

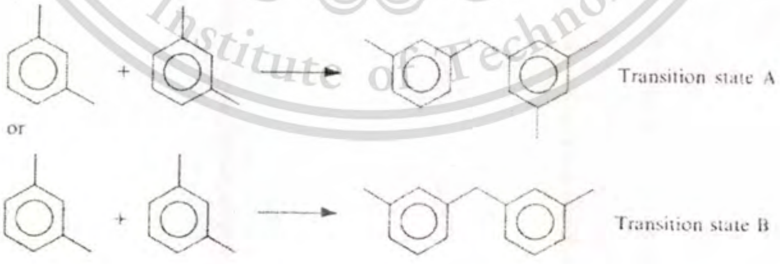

It can be seen that transition state A cannot fit in mordenite channel and so this precludes the production of molecule arising from scission of this transition state (i.e. 1,3,5-trimethylbenzene and toluene). On the other hand, transition state B can be accommodated within the channels and so its breakdown products (i.e. 1,2,4-trimethylbenzene and toluene) are the one which from.

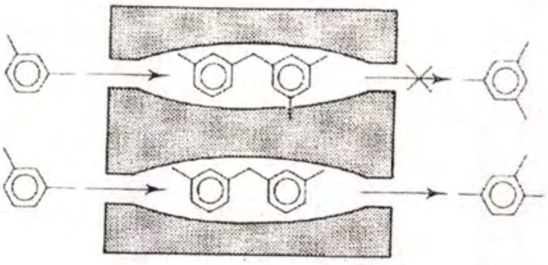

Figure 2.2 Transition state shape selectivity in zeolite channel [40]

Product shape selectivity. This is an essential function of rate of diffusion of products away from the reactive sites,through the crystal pores and out of the crystallites. Perhaps the best known of example of this type of selectivity is in preferred alkylation of toluene to p-xylene over H-ZSM-5, because the diffusivity of para isomer, in the zeolites, is much greater than that of the o- and m-xylene isomers for the same substrate.

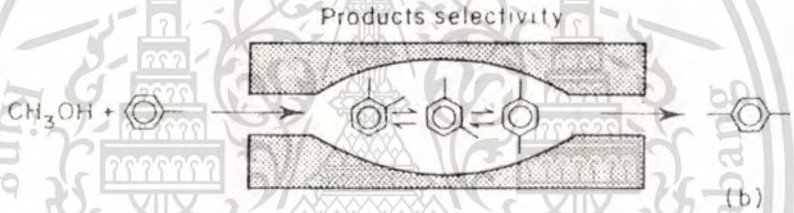

Figure 2.3 Products shape selectivity in zeolites channel [40]

Shape selectivity can be induced by altering other zeolites parameter, for instance crystallite size variation as mentioned earlier. Larger crystals provide longer diffusion path length and this can be used to modify catalytic products because product selectivity is a function of diffusion-limited process. Modification by P,Mg or B of ZSM-5 has been shown to create changes in the products from the alkylation and disproportionation reaction of toluene. These change in selectivity have also been assigned to alteration in effective diffusivities arising from the intrusion of carbon, or oxide, into the critical channel structures.

2.1.1 Applications of zeolites

2.1.1.1 Ion-exchange applications

The major use of zeolites as ion-exchange agents is for water softening applications in the detergent industry and substitute use of phosphates. Hydrated cations within the zeolite pores are bound loosely to the zeolite framework, and can be readily exchanged with other cations in aqueous media. The selectivity of zeolite A for Ca^{2+} provides a unique advantage. Natural zeolites find considerable use for removal of Cs^{+} and Sr^{2+} radioisotopes by ion exchange from radioactive waste streams.

2.1.1.2 Adsorbent applications

The geometry is the source of the ability of zeolites to separate mixtures of molecules (in both the gas and liquid phases) on the basis of their effective sizes-hence their description as "molecular sieves". Molecules have certain dimensions and allow them to enter the pores, such as *n*-paraffins from branched paraffins. This property can be fine-tuned by variation the structure by changing the size and number of cation around the pores.

2.1.1.3 Catalyst applications

Zeolites are extremely useful as catalysts for several important reactions involving organic molecules. Zeolites can promote a diverse range of catalytic reactions including acid-base and metal induced reactions. The reactions can take place within the pores of the zeolite, which allows a greater degree of product control. In the industrial application, the major employment of zeolite is as acid cracking catalysts. Zeolites are catalyst that offer the advantages of high densities of catalytic sites combined with stability at high temperatures. Almost the reactions catalyzed by acids in solutions and in polymer matrices can be catalyzed by zeolites incorporated with acidic groups. This generalization is based on experimental evidence for hundreds of catalytic reactions. The exceptions involve reactants too large to enter the zeolite pores and products too large to form in, or leave, the pores. The commercial processes using zeolite catalysts are listed in Table 2.2

Table 2.2 Commercial processes using zeolite catalysts [50]

Processes	Catalyst	Advantages in using zeolite-based catalysts
Catalytic cracking	REY (REX, REHY, REMgY, HY)	Selectivity and high conversion rates
Hydrocracking	X, Y, mordenite, erionite loaded with Co, Mo, W, Ni, also HY, US-Y, Ca MgY and H-ZSM-5	High conversion rates
Selectoforming	Ni erionite, clinoptilolite	Increase in octane number via LPG production
Hydroisomerization	Pt mordenite	Converts low octane, pentane and hexane feeds to higher octane yields
Dewaxing	Pt mordenite, ZSM-5	Improved pour points
Benzene Alkylation	ZSM-5	Ethylbenzene and styrene production with low by-product yield
Xylene isomerization	ZSM-5	Increase in p-xylene yield with low by-product yield
Methanol to gasoline conversion	ZSM-5	High gasoline yield with high octane rating
No_x reduction	H-mordenite	Effluent clean-up in nitric acid and nuclear reprocessing plants

2.1.2 Zeolite Beta [49]

A zeolite of substantial industrial importance is zeolite beta. It is a crystalline aluminosilicate molecular sieve zeolite which finds application in a number of industrial processes including as a catalyst in various hydrocarbon conversion reactions such as hydrocracking, hydroisomerization and dewaxing. The zeolite Beta has three-dimensional interconnecting channel system with 12-membered ring opening and with two different pore sizes of 5.5x5.5 and 6.4x7.6 diameter (Figure 2.4). It can be crystallized in a claimed range of silica to alumina ratio, $10 < SiO_2/Al_2O_3 < 200$, but the efficiency of crystallization is lower when it crystallizes at silica to alumina ratio lower than 19 (6 aluminium atoms per 1 unitcell).

Zeolite Beta, like many other molecular sieve zeolites, is synthesized by the hydrothermal digestion of a reaction mixture comprising silica, alumina, an alkaline earth metal and an organic templating agent. The organic agent acts as a template in the nucleating and growth of the zeolite Beta crystal. Once the crystals are formed, it is conventional practice to carry out a calcination treatment in order to remove the organic material from the interstitial channels of the molecular sieve network. In addition, it can be used in alkylation process. Alkylation process employing zeolite Beta which is said to be especially useful in the production of ethylbenzene from benzene and ethylene and production of cumene from benzene and propylene. Moreover, it may often be desirable to incorporate a metal component into the zeolite Beta. Suitable metal components include those found in groups VIB and VIII of the periodic table. Specific metals include chromium, molybdenum, tungsten, vanadium, iron, cobalt, nickel, copper, platinum and palladium.

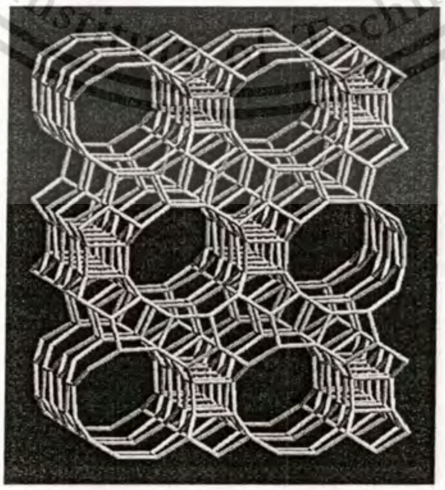

Figure 2.4 Structure formed by stacking of sequences of layers [61]

2.2 Cracking reaction

The term "cracking" usually applies to decomposition induced by elevated temperatures whereby the high molecular weight materials are converted into lower molecular weight products at elevated temperatures. Cracking reactions involve carbon-carbon bond cleavage and are thermodynamically favored at high temperatures. However, certain products may interact with one another to produce material of even higher molecular weight than that in the original feedstock. The cracking of petroleum products is of primary importance in the production of gasoline. Cracking also provides gasoline with sufficiently high octane number, although frequently further enhancement is needed [52-53]. Cracking is effected by one of three general methods, i.e., thermal cracking, catalytic cracking, or hydrocracking.

2.2.1 Thermal cracking [53-55]

One of the earliest processes used in petroleum, after distillation, is the noncatalytic conversion of higher boiling point petroleum stocks into lower boiling point products, known as thermal cracking. The mechanism of thermal cracking process generally proceed via free radical chain reaction and does not produce any degree of branching in the products other than that already present in the feedstock. However, certain products may interact with one another to produce higher molecular weight products than that in the original feedstock.

Two general types of reactions occur during cracking are:

1. Primary reactions in which decomposition molecules into small molecules :

$$\text{R-CH}_2\text{CH}_2\text{CH}_2\text{CH}_3 \longrightarrow \text{CH}_4 + \text{R-CH}_2\text{CH=CH}_2$$
$$\text{R-CH}_2\text{CH}_2\text{CH}_2\text{CH}_3 \longrightarrow \text{CH}_3\text{CH}_3 + \text{R-CH=CH}_2$$

2. Secondary reactions by which some of the active primary products interact to form higher molecular weight materials

$$\text{CH}_2\text{=CH}_2 + \text{CH}_2\text{=CH}_2 \longrightarrow \text{CH}_3\text{CH}_2\text{CH=CH}_2$$
$$\text{RCH=CH}_2 + \text{R}'\text{CH=CH}_2 \longrightarrow \text{tar, heavy oil, coke, others}$$

Free radicals are very reactive. A free radical reacts with a hydrocarbon by abstracting a hydrogen atom to produce a stable end product and a new free radical:

Initiation

$$CH_3CH_2CH_2CH_3 \longrightarrow CH_3CH_2CH_2^\bullet + CH_3^\bullet$$

Propagation

$$CH_3CH_2CH_2CH_3 + CH_3^\bullet \longrightarrow CH_3\overset{\bullet}{C}HCH_2CH_3 + CH_4$$

$$CH_3\overset{\bullet}{C}HCH_2CH_3 \longrightarrow CH_2{=}CHCH_2CH_3 + H^\bullet$$

$$CH_3^\bullet + CH_3CH_2CH_3 \longrightarrow CH_4 + CH_3CH_2CH_2^\bullet$$

Termination

$$2CH_3CH_2^\bullet \longrightarrow CH_3CH_2CH_2CH_3$$

$$CH_3CH_2^\bullet + H^\bullet \longrightarrow CH_3CH_3$$

Disproportionation

$$CH_2{=}CH_2 + CH_3CH_2^\bullet \longrightarrow CH_3CH_2CH_2CH_2^\bullet$$

$$2CH_3CH_2CH_2^\bullet \longrightarrow CH_3CH{=}CH_2 + CH_3CH_2CH_3$$

Other reactions, such as

$$CH_3CH_2CH_2CH_2^\bullet \longrightarrow CH_2{=}CH_2 + CH_3CH_2^\bullet$$

One of the significant features of hydrocarbon free radicals is their resistance to isomerization, for example, migration of an alkyl group:

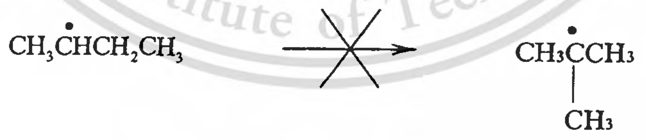

$$CH_3\overset{\bullet}{C}HCH_2CH_3 \not\longrightarrow CH_3\overset{\bullet}{\underset{\substack{|\\CH_3}}{C}}CH_3$$

An increase in pressure favours the shift of equilibrium towards the polymerzation of olefins and the alkylation of paraffins. Because of this, a high pressure prevents a deep cracking of the raw material, which inhibits the formation of low molecular weight gaseous products and therefore promotes the formation of higher molecular weight materials [46].

2.2.2 Catalytic cracking

Catalytic cracking is the most important and widely used in refinery process for converting heavy oils into more valuable gasoline and lighter products. But this reaction is not a major route to petrochemicals, except to insure and ample supply of propylene for the United States [54]. Catalytic cracking is basically the same as the thermal decomposition of hydrocarbons but it differs in the use of a catalyst, which is not consumed in the process [57]. Serveral reactions take place in a catalytic cracking unit with varying degree of importance. These include carbon-carbon bond breaking, disproportionation, olefin formation and cyclization. Thermal cracking has essentially been replaced by catalytic cracking as the process for gasoline manufacture. The main advantage of catalytic cracking over thermal cracking is the increased gasoline production and the formation of hydrocarbon components having more gasoline of higher octane and anti-knock properties than thermal cracking because gasoline produced by catalytic cracking is richer in branched paraffins, cycloparaffins, and aromatics [53,58]. This is due to the effect of the catalyst, which promotes isomerization and dehydrocyclization reactions. Another advantage of catalytic cracking process is the production of C_3 and C_4 hydrocarbons for LPG uses. Catalytic cracking also produces less methane and C_2 hydrocarbons than thermal cracking. These differences are due mainly to the presence of an acid catalyst which promotes carbonium ion intermediates that are more selective than the free radicals formed in the thermal cracking reaction.

Catalytic cracking may be regarded as the modern method for converting high boiling point petroleum fractions, such as gas oil, into high quality gasoline and other low boiling point fractions. Thus, catalytic cracking in the usual commercial process involves contacting a gas oil fraction with an active catalyst under suitable conditions of temperature, pressure, and residence time, so that a substantial part (50-60%) of the gas oil is converted into gasoline and lower boiling products, usually in a single-pass operation [58]. However, during the cracking reaction, formation of high molecular weight aromatic products called coke can be obtained. Solid deposits of coke accumulate in the catalyst; the deposits clog the pores and cover the catalytically active sites. Coke is a catalyst poison, which markedly reduces its activity, and removal of the deposit is extremely necessary. This is usually accomplished by burning the deactivated catalyst in the presence of air until the catalyst activity is reestablished.

A major difference between thermal and catalytic cracking is that reactions through catalytic cracking occur via carbonium ion intermediate, compared to the free radical intermediate in thermal cracking. Carbonium ions are longer lived and accordingly more selective than free radicals [51]. Moreover, the degradation products are distributed in a narrow range of carbon number compared with those obtained by thermal degradation. However, this type of catalyst is now being replaced by crystalline aluminosilicates (zeolites) or molecular sieves [53]. Low gas and coke yields, less sensitivity to poisoning, lower operation temperature, and low contact time are the main features of the new generation of cracking catalysts [52]. The formation of carbonium ions during catalytic cracking may be generated by:

1. By a proton from the Brønsted acid site (H^+) in zeolite adding to an olefin hydrocarbon which was formed by a cracking process.

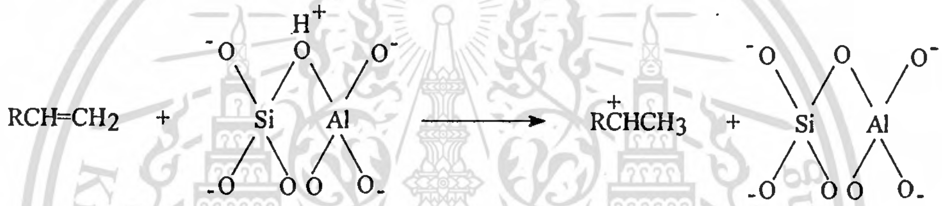

2. By a Lewis acid site abstracting a hydride ion (H^-) from a hydrocarbon.

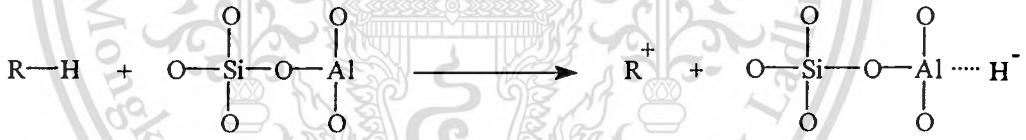

3. By a carbonium ion formed from step 1 or 2 abstracting a hydride ion from another hydrocarbon to form another carbonuim ion.

$$R^+ + R'C(CH_3)_2H \longrightarrow RH + R'C^+(CH_3)_2$$

However, carbonium ions are not formed by cleavage of a carbon-carbon bond:

$$RCH_2CH_2R \not\longrightarrow RCH_2^+ + RCH_2^- \qquad 260 \text{ kcal/mol}$$

but

$$RCH_2CH_2R \longrightarrow 2RCH_2^{\bullet} \qquad 76 \text{ kcal/mol}$$

Once the carbonuim ions are formed, can isomerize through either a hydride shift, a methide shift or both.

1,2 Hydride shift :

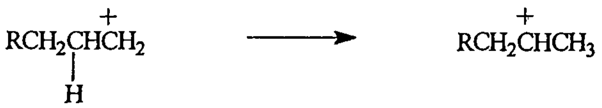

$$\mathrm{RCH_2\underset{\displaystyle H}{C}H\overset{+}{C}H_2 \longrightarrow RCH_2\overset{+}{C}HCH_3}$$

Methide shift-hydride shift :

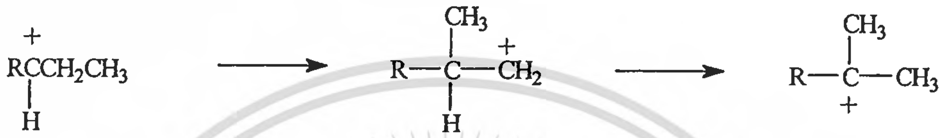

$$\mathrm{R\underset{\displaystyle H}{\overset{+}{C}}CH_2CH_3 \longrightarrow R{-}\underset{\displaystyle H}{\overset{\displaystyle CH_3}{C}}{-}\overset{+}{C}H_2 \longrightarrow R{-}\underset{+}{\overset{\displaystyle CH_3}{C}}{-}CH_3}$$

Abstraction of a hydride ion from a tertiary carbon is easier than from a secondary, which is easier than from a primary position. The formed carbonium ion can rearrange through a methide-hydride shift similar to catalytic reforming. This isomerization reaction is responsible for a high ratio of branched isomers in the products. The cracking rate is also influenced the structure of the molecule, with those containing tertiary carbon atoms cracking most readily while quaternary carbon atoms are most resistant.

Many reactions take place starting form a carbonium ion in addition to hydride and methide shifts. Among these are the important carbon-carbon beta bond scission and cyclization. The carbon-carbon beta bond scission is the most important cracking reaction of catalytic cracking. A bond at a position beta to the positively-charged carbon breaks heterolytically, yielding an olefin and another carbonium ion. This can be represented by the following example:

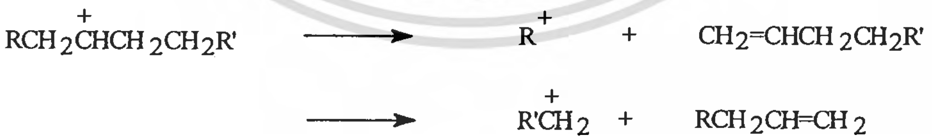

$$\mathrm{RCH_2\overset{+}{C}HCH_2CH_2R' \longrightarrow \overset{+}{R} + CH_2{=}CHCH_2CH_2R'}$$
$$\mathrm{\longrightarrow R'\overset{+}{C}H_2 + RCH_2CH{=}CH_2}$$

The new carbonium ion may experience another beta scission, rearrange to a more stable carbonium ion, or react with a hydrocarbon molecule in the mixture and produce a paraffin. Cyclization can take place by carbonium ion addition to a carbon-carbon double bond in the same molecule.

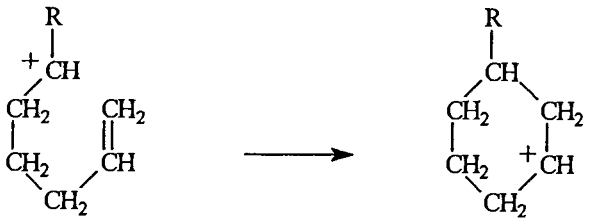

Cyclic olefins and aromatics can be produced by a two step hydrogen transfer sequence. The first is a proton transfer and the second is a hydride transfer. A continuation of these sequence converts the cyclic carbonium ion to an aromatic hydrocarbon and paraffins.

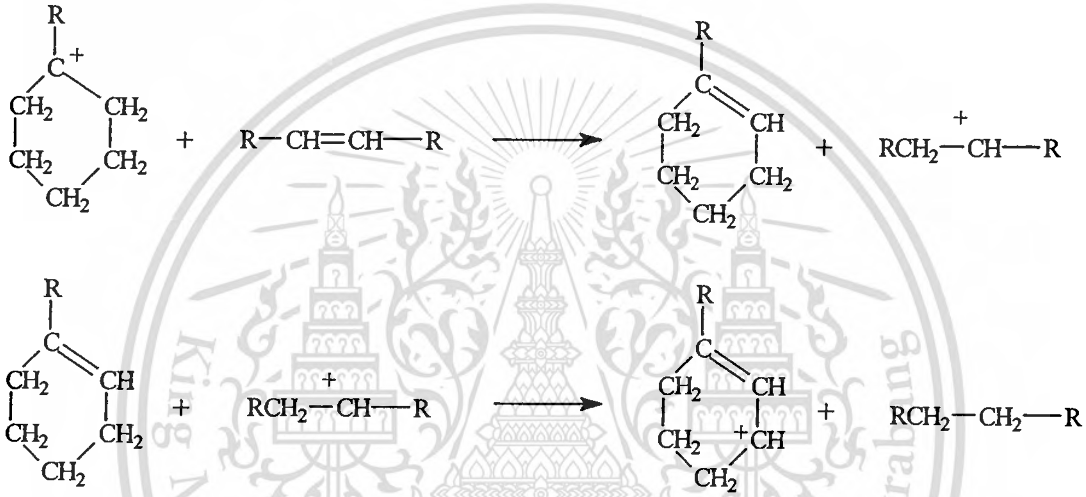

In essence, the use of a catalyst permits alternate routes for cracking reactions, usually by lowering the free energy of activation for the reaction. [58]

2.2.3 Hydrocracking

Hydrocracking is essentially catalytic cracking reaction whereby higher molecular weight hydrocrabons pyrolyze to lower molecular weight paraffins and olefins in the presence of hydrogen. Relatively high pressures of hydrogen (100-2000 psi) are employed, and the overall result is usually a change in the character or quality of the products. It produces less olefinic hydrocarbons whatsoever as the added hydrogen traps the intermediate species to yield saturated products. Since the hydrocarbon molecules in naphtha are relatively low molecular weight, hydrocraking forms molecules boiling in the gas range. Thus hydrocracking competes with the aromatization reaction by elimination hydrocarbons that can be aromatized. Such processes are generally expensive because of the considerable amount of hydrogen used and the high operating pressure [53, 58].

The wide range of product possible from hydrocracking is the result of combining catalytic cracking reactions with hydrogenation. The reactions are catalyzed by bifunctional catalysts used in hydrocracking provide high surface area cracking sites and hydrogenation-dehydrogenation sites. The cracking function is provided by an acid support such as silica-alumina or zeolite catalyst, whereas the hydrogenation-dehydrogenation function is provided by metals such as noble metals (palladium and platinum), or nonnoble metal sulfides from group VIA (molybdenum and tungsten) and group VIIIA (cobalt and nickel). [59] Catalysts with strong acidic activity promote isomerization, leading to a high iso/normal ratios. These metals catalyze the hydrogenation of the feedstock, making it more reactive for cracking and heteroatom removal, as well as reducing the coking rate. The metals also initiate the cracking by forming a reactive olefin intermediate via dehydrogenation.

Essentially all the initial reactions of catalytic cracking occur, but some of the secondary reactions are inhibited or stopped by the presence of hydrogen. The following is a representative hydrocracking reaction.

$$RCH_2CH_2CH_2CH_3 \xrightarrow{\text{zeolite}} RCH_2CH_2\overset{+}{C}HCH_3$$

$$RCH_2CH_2\overset{+}{C}HCH_3 \xrightarrow{\text{beta-scission}} RCH_2 + CH_2{=}CHCH_3$$

$$CH_2{=}CHCH_3 + H_2 \xrightarrow{\text{catalyst}} CH_3CH_2CH_3$$

The effect of hydrogen on naphthenic hydrocarbons is mainly that of ring scission followed by immediate saturation of each end of the fragment produced. The ring is preferentially broken at favored positions, although generally all the carbon-carbon bond positions are attacked to some extent.

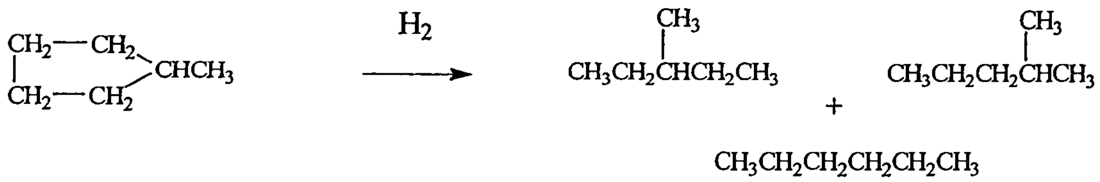

Aromatic hydrocarbons are resistant to hydrogenation under mid conditions, but under more severe conditions the main reactions are conversion of the aromatic to naphthenic rings and scissions within the alkyl side chains. The naphthenes may also be converted to paraffins.

As anticipated, most products from hydrocracking are saturated. For this reason, gasolines from hydrocracking units have lower octane ratings than those produced by catalytic cracking units since they have a lower aromatic content due to the high hydrogenation activity. Products from hydrocracking units are suitable for jet fuel use. Hydrocracking also produces light hydrocarbon gases suitable as petrochemical feedstocks.

2.3 Polyethylene (PE)

2.3.1 History [62]

Polyethylene was first synthesized by the German chemist, Hans von Pechmann, who prepared it by accident in 1898 while heating diazomethane. When his colleagues Eugen Bamberger and Friedrich Tschirner, characterized the white, waxy substance he had created, they recognized that it contained long -CH_2- chains and termed it *polymethylene.*

The first industrially practical polyethylene synthesis was discovered (again by accident) in 1933 by Eric Fawcett and Reginald Gibson at the ICI works in Northwich, England. Upon applying extremely high pressure (several hundred atmospheres) to a mixture of ethylene and benzaldehyde, they again produced a white waxy material. Because the reaction had been initiated by trace oxygen contamination in their apparatus, the experiment was at first difficult to reproduce. It was not until 1935 that another ICI chemist, Michael Perrin, developed this accident into a reproducible high-pressure synthesis for polyethylene that became the basis for industrial LDPE production beginning in 1939. Subsequent landmarks in polyethylene synthesis have revolved around the development of several types of catalyst that promote ethylene polymerization at more mild temperatures and pressures.

The first of these was a chromium trioxide based catalyst discovered in 1951 by Robert Banks and J. Paul Hogan at Phillips Petroleum. In 1953, the German chemist Karl Ziegler developed a catalytic system based on titanium halides and organoaluminum compounds that worked at even milder conditions than the Phillips catalyst. The Phillips catalyst is less expensive and easier to work with, however, and both methods are used in industrial practice. By the end of the 1950s both the Phillips and Ziegler type catalysts were being used for HDPE production.

Phillips' initially had difficulties producing a HDPE product of uniform quality, and filled warehouses with off-specification plastic.

However, financial ruin was unexpectedly averted in 1957, when the hula hoop, a toy consisting of a circular polyethylene tube, became a fad among youth in the United States.A third type of catalytic system, one based on metallocenes, was discovered in 1976 in Germany by Walter Kaminsky and Hansjörg Sinn. The Ziegler and metallocene catalyst families have since proven to be very flexible at copolymerizing ethylene with other olefins and have become the basis for the wide range of polyethylene resins available today, including very low density polyethylene , and linear low density polyethylene . Such resins, in the form of fibers like Dyneema, have (as of 2005) begun to replace aramids in many high-strength applications. Until recently, the metallocenes were the most active single-site catalysts for ethylene polymerisation known — new catalysts are typically compared to zirconocene dichloride. Much effort is currently being exerted on developing new single-site (so-called post-metallocene) catalysts, that may allow greater tuning of the polymer structure than is possible with metallocenes. Recently, work by Fujita at the Mitsui corporation (amongst others) has demonstrated that certain salicylaldimine complexes of Group 4 metals show substantially higher activity than the metallocenes.

2.3.2 Description and Physical properties

Polyethylene is a polymer consisting of long chains of the monomer ethylene (IUPAC name ethene). The recommended scientific name 'polyethene' is systematically derived from the scientific name of the monomer. In certain circumstances it is useful to use a structure–based nomenclature. In such cases IUPAC recommends poly(methylene). The difference is due to the 'opening up' of the monomer's double bond upon polymerisation. In the polymer industry the name is sometimes shortened to PE, in a manner similar to that by which other polymers like polypropylene and polystyrene are shortened to PP and PS, respectively. In the United Kingdom the polymer is commonly called polythene, although this is not recognised scientifically. The ethene molecule (known almost universally by its common name ethylene), C_2H_4 is $CH_2{=}CH_2$, Two CH_2 groups connected by a double bond, thus:

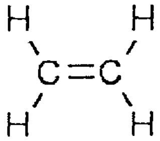

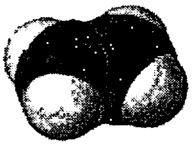

Polyethylene is created through polymerization of ethene. It can be produced through radical polymerization, anionic addition polymerization, ion coordination polymerization or cationic addition polymerization. This is because ethene does not have any substituent groups that influence the stability of the propagation head of the polymer. Each of these methods results in a different type of polyethylene.

Physical properties depending on the crystallinity and molecular weight, a melting point and glass transition may or may not be observable. The temperature at which these occur varies strongly with the type of polyethylene. For common commercial grades of medium-density and high-density polyethylene, the melting point is typically in the range 120 to 130 °C ((250 to 265 °F). The melt point for average commercial low-density polyethylene is typically 105 to 115 °C (220 to 240 °F). Most LDPE, MDPE, and HDPE grades have excellent chemical resistance and do not dissolve at room temperature because of the crystallinity. Polyethylene (other than cross-linked polyethylene) usually can be dissolved at elevated temperatures in aromatic hydrocarbons, such as toluene or xylene, or chlorinated solvents, such as trichloroethane or trichlorobenzene.

2.3.3 Product applications

Polyethylene not only finds many products but also because of the many forms in which it is produced as a resin. It may be obtained in granules, powders, film, rod, tube and sheet form and molded through such processes as injection molding, fluidized bed coating, blow molding, extrusion, vacuum forming, casting and calendering. Polyethylene is used for many purposes, including: containers, electrical insulation, house-wares, chemical tubing, toys, freezer bags, flexible ice cube trays, snap-on lids and battery parts. Two major applications of polyethylene are films for packaging soft goods and other nonperishable and blow molded bottles. Squeeze bottles from low densitypolyethylene and detergent bottles from high density are typical products.

2.4 Melt Flow Index [63]

The Melt Flow Index is a measure of the ease of flow of the melt of a thermoplastic polymer. It is defined as the mass of polymer in grams flowing in 10 minutes through a capillary of specific diameter and length by a pressure applied via prescribed alternative gravimetric weights for alternative prescribed temperatures.

The method is given in ASTM D1238 and ISO 1133 (similar). Melt flow rate is an indirect measure of molecular weight, high melt flow rate corresponding to low molecular weight.

At the same time, melt flow rate is a measure of the ability of the material's melt to flow under pressure. Melt flow rate is inversely proportional to viscosity of the melt at the conditions of the test, though it should be borne in mind that the viscosity for any such material depends on the applied force. Ratios between two melt flow rate values for one material at different gravimetric weights are often used as a measure for the broadness of the molecular weight distribution.Melt flow rate is very commonly used for polyolefins, polyethylene being measured at 190°C and polypropylene at 230°C. The plastics converter should choose a material with a melt index so high that he can easily form the polymer in the molten state into the article intended, but on the other hand so low that the mechanical strength of the final article will be sufficient for its use.The procedure for determining MFI is as follows:

1) A small amount of the polymer sample (around 4 to 5 grams) is taken in the specially designed MFI apparatus which is nothing but a miniature extruder.

2) The apparatus consists of a small die inserted into the extruder,diameter of the die generally being around 2 mm.

3) The material is packed properly inside the extruder barrel to avoid formation of air pockets.

4) A piston is introduced which acts as the medium that causes extrusion of the molten polymer.

5) The sample is preheated for a specified amount of time: 5 min at 190°C for polyethylene and 6 min at 230°C for polypropylene.

6) After the preheating a specified weight is introduced onto the piston. Examples of standard weights are 2.16 Kg,5 Kg,etc.

7) On account of the weight shear is exerted on the molten polymer and it immediately starts flowing through the die.

8) A sample of the melt is taken after desired period of time and is weighed accuarately.

9) MFI is expressed as grams of polymer/10 minutes of flow time.Synonyms of Melt Flow Index are Melt Flow Rate and Melt Index.

Actually, more commonly used are their abbreviations: MFI, MFR and MI. Be aware that, confusingly, MFR is also a term often used for the ratio between two melt flow rates at different gravimetric weights. More accurately, this should be reported at the FRR (flow rate ratio) or simply the flow ratio. The FRR is commonly used as an indication of the way in which rheological behaviour is inflenced by the molecular mass distribution of the material.

2.5 Fuel

The fuel products that are derived from petroleum supply more than half of the world's total supply of energy [60]. Gasoline, kerosene, and diesel oil provide fuel for automobiles, tractors, trucks, aircraft, and ships. Fuel oil and natural gas are used to heat homes and commercial buildings, as well as to generate electricity. The constant demand for products, such as liquid fuels, is the main driving force behind the petroleum industry. Other products, such as lubricating oils, waxes, and asphalt, have also added to the popularity of petroleum s a national resource. However, for the main part, the petroleum industry was inspired by the development of the automobile and the continued demand for gasoline, and other fuels. Such a demand has been accompanied by the demand for other products: diesel fuel for engines, lubricants for engine and machinery parts, fuel oil to provide power for the industrial complex, and asphalt for roadways.

2.5.1 Gaseous fuels

The principal types of gaseous fuels are oil gas, reformed natural gas, and reformed propane or liquefied petroleum gas (LPG). Mixed gas is a gas prepared by adding natural gas or liquefied petroleum gas to a manufactured gas, giving a product of better utility and higher. Liquefied petroleum gas (LPG) is the term applied to certain specific hydrocarbons and their mixtures, which exist in the gaseous state under atmospheric ambient conditions but can be converted to the liquid state under conditions of moderate pressure at ambient temperature. Thus, liquefied petroleum gas is a hydrocarbon mixture containing propane, butane, iso-butane and to a lesser extent propylene, or butylene. The most common commercial products are propane, butane, or some mixture of the two and are generally extracted from natural gas or crude petroleum. Propylene and butylenes result from cracking other hydrocarbons in a petroleum refinery and are two important chemical feed stocks

2.5.2 Gasoline

Gasoline is a mixture of volatile, flammable liquid hydrocarbons derived from petroleum that boil off over a range from about 25^{O}C (77 ^{O}F) to below 185^{O}C (365^{O}F). The hydrocarbon constituents in this boiling range are those that have four to twelve carbon atoms in their molecular structure. The hydrocarbons of which gasoline is composed fall in to three general types: paraffins (including the cycloparaffins and branched material), olefins, and aromatics. It is used as fuel for internal-combustion engines and also used as a solvent for oils and fats. Originally a byproduct of the petroleum industry (kerosene being the principal product), gasoline became the preferred automobile fuel because of its high energy of combustion and capacity to mix readily with air in carburetor. Gasoline was at first produced by distillation, simply separating, more valuable fractions of crude petroleum. Later processes, designed to raise the yield of gasoline from crude oil, split higher molecular weight products by processes known as cracking. And like typical gasoline, several processes (Table 2.3) produce the blending stocks for reformulated gasoline.

Table 2.3 Refining technologies for producing reformulated gasoline constituents

Technology	Objective
Catalytic reformer prefractionation	Reduce benzene
Reformate fractionation	Reduce benzene
Isomerization	Increase octane
Aromatics saturation	Reduce total aromatics
Isobutane dehydrogenation	Feedstock for oxygenate synthesis
Catalytic cracker naphtha fractionation	Increase alkylate and oxygenates Reduce olefins and sulfur

For use in motor vehicles, the gasoline must have certain chemical and physical properties, otherwise it will not pass satisfactorily up from the tank to the carburetor or injectors, form a suitable mixture with the air and burn efficiently in the cylinders to produce adequate power. These properties are:

1. Calorific value. The greater the quantity of thermal energy a fuel contains per unit of volume and weight, the smaller is the quantity required to be carried in the tank in the vehicle to provide enough energy to transport a given load at a given speed over a given distance. High density fuels contain the most energy and they have the lowest volatility.

2. Latent heat of vaporisation. A high latent heat of vaporisation causes the charge to be cooled, and therefore become more dense, as the fuel mixes with the air, so the charge passing into the cylinders of the engine will contain more energy than if that cooling had not taken place. However, it can also cause freezing of atmospheric moisture in carburetors, which can severely interfere with the running of engines.

3. Boiling point. The fuel must comprise a mixture of volatile liquids. Called fractions, each having a different boiling point over the previously mentioned range of ambient to 185^{O}C. Their individual boiling points affect not only its suitability for cold starting and use in both hot and cold ambient temperatures but also, if too high a proportion of the fractions have low boiling points, a risk arises of vapor lock occurring in the supply system.

4. Octane number. A high octane number is perhaps the most important of all the properties required for gasoline fuel. With a low octane number, it will burn explosively instead of progressively in the engine cylinders, and this can cause overheating and severe damage to the parts that are in any case very hot and their strength therefore reduces. Actually there are two different octane numbers. One is called the Research octane number (RON) because it is obtained in a single cylinder laboratory engine called the Co-operative Fuel Research Engine (CFR). However, in practice, the knock resistance of a fuel in multi-cylinder engine under normal running conditions is rarely as high as is indicated by the RON, so another method, called the Motor method. It was developed in which a more widely representative type of engine is used to determine the Motor octane number (MON). In the test methods used to determine the antiknock properties of gasoline, comparisons, are made with blends of two pure hydrocarbons, n-heptane and iso-octane (2,2,4-trimethylpentane). Iso-octane has an octane number of 100 and is high in its resistance to knocking. n-Heptane is quite low (with and octane number of 0) in its resistance to knocking.

2.5.3 Kerosene

Kerosene, also called paraffin or paraffin oil, is a flammable pale-yellow or colorless oily liquid with a characteristic odor. It is obtained from petroleum and used for burning in lamps and domestic heaters or furnaces, as a fuel or fuel component for jet engines, and as a solvent for greases and insecticides. Kerosene is also defined as a refined petroleum distillate that has a flash point of about 25^{O}C (77^{O}F) and is suitable for use as an illuminant when burned in a wide lamp. The term kerosene is also too often incorrectly applied to various fuel oils, but a fuel oil is actually any liquid or liquid petroleum product that produces heat when burned in a suitable container or that produces power when burned in an engine. Kerosene originated as a straight-run petroleum fraction that boiled between approximately 205 and 260^{O}C (400-500^{O}F). Chemically, kerosene is usually consists of about 10 different hydrocarbons, each containing from 10 to 16 carbon atoms per molecule; the constituents include *n*-dodecane (n-$C_{12}H_{26}$), alkyl benzenes, and naphthalene and its derivatives. Kerosene, because of its use as burning oil, must be free of aromatic and unsaturated hydrocarbons, as well as free of the more obnoxious sulfur compounds. It is a stable product, and additives are not required to improve the quality. Apart from the removal of excessive quantities of aromatics by the Edeleanu process, kerosene fractions may need only a lye wash or a doctor treatment if hydrogen sulfide is present to remove mercaptans. The essential properties of kerosene are flash point, fire point, distillation range, burning sulfur content, color, and cloud point.

In the case of the flash point, the minimum flash temperature is generally placed above the prevailing ambient temperature; fire point determines the fire hazard associated with its handling and use. The boiling range is of less importance for kerosene than for gasoline, but it can be taken as an indication of the viscosity of the product. The ability of kerosene to burn steadily and cleanly over an extended period is an important property and gives some indication of the purity or composition of the product. The significance of the total sulfur content of a fuel oil varies greatly with the type of oil and the use to which it is put. Sulfur content is of great importance when the oil to be burned produces sulfur oxides that contaminate the surroundings. The color of kerosene is of little significance, but a product darker than usual may have resulted from contamination or aging, and in fact a color dark than specified may be considered by some users as unsatisfactory. Finally, the cloud point of kerosene gives and indication of the temperature at which the wick may become coated with wax particles, thus lowering the burning qualities of the oil.

2.5.4 Diesel

Diesel fuel oil is also a distillate fuel oil. In general, it is a blend of straight-run gas oil and cracked gas oil to produce a product boiling in the 175-345^{O}C (350-650^{O}F) range. Diesel fuel oil is essentially the same as furnace fuel oil, but the proportion of cracked gas oil is usually less since the high aromatic content of the cracked gas oil reduces the cetane value of the diesel fuel. Cetane number is a measure of the tendency of a diesel fuel to knock in a diesel engine. The scale is based upon the ignition characteristics of two hydrocarbons n- hexadecane (cetane) and 2,3,4,5,6,7,8-heptamethylnonane. Cetane has a short delay period during ignition and is assigned a cetane number of 100; heptamethylnonane has a long delay period and has been assigned a cetane number of 15. Just as the octane number is meaningful for automobile fuels, the cetane number is a means of determining the ignition quality of diesel fuels and is equivalent to the percentage by volume of cetane in the blend with heptamethylnonane, which matches the ignition quality of the test fuel. The boiling range, carbon atom and phase of petroleum products are shown in Table 2.4.

Table 2.4 Boiling range of petroleum products

Products	Boiling range ^{o}C	Phase	Carbon atoms
Gas petroleum	< 10	Gas	1-4
Gasoline	30-185	Liquid	4-13
Kerosene	170-250	Liquid	10-14
Diesel	175-350	Liquid	14-19
Lubricant	350-500	Liquid	19-35
Wax	350-500	Solid	19-35
Fuel oil	> 500	Liquid	> 35
Bitumen	> 500	Solid	> 35

2.6 Literature reviews

In recent year, a number of authors have reported that the best recycling methods for waste plastics are catalytic and non-catalytic degradation processes. Furthermore, recycling of thermoplastics can reduce pollution problems. Catalytic degradation of polyolefin offers considerable advantages as compared to pure thermal degradation. Since the thermal degradation of polymers to low molecular weight materials requires high temperatures, typically more than 500 °C and even up to 900 °C, and has a major drawback in that a very broad product range is obtained. Catalytic pyrolysis provides a means to address these problems [63]. Catalytic degradation of polyolefin occurs at considerably lower temperatures and forms hydrocarbons in the range of motor gasoline [6].

Typical acid catalysts have been employed such as $AlCl_3$, amorphous silica-alumina and zeolites ZSM-5 and HY, MCM-41[4-6]. Amongst these, the zeoltie beta shows high selectivity to liquid fuel due to the high thermal stability and a 3-dimensional pore opening system that allow bulky molecules to diffuse and crack [3, 16]. Marcilla *et al* reported that the zeolite H-beta shows an important influence on the decomposition of polymer even at a very low zeolite concentrate [36]. Zeolite beta, which posses large crystal size (12 μm) and poor aluminium incorporation, has a low activity for the cracking of polyolefin. In contrast, zeolite beta, which consists of small crystallites (≤200 nm) give high conversion (40-60%) and good selectivity towards C_5-C_{12} hydrocarbons (60-70%). Heavier products is hardly obtained (<6%) [1].

In 2001, Mr. Chaiwat Tachakritikul reported the effect of pore size of zeolites which showed that a larger amount of gaseous products in a range of C_3-C_5 was produced over the medium pores of ZSM-5, while mainly liquid products in a range of C_5-C_9^+ were obtained over the large pores of Beta. This clearly showed that product distribution from polyethylene cracking can be controlled by the pore sizes of the zeolites used. The large pore size also caused the higher rate of coke formation than the medium pore size as shown in Figure 2.5.

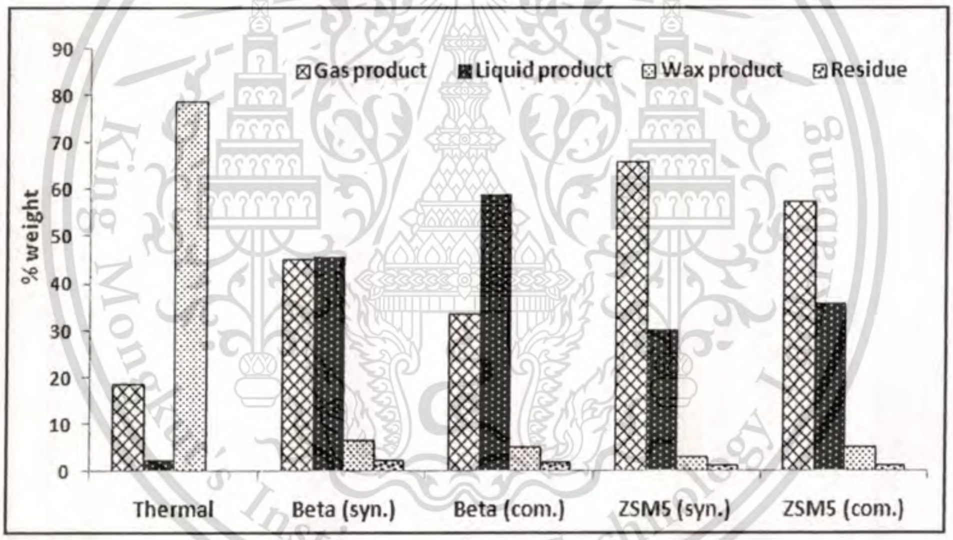

Figure 2.5 Yields of products from thermal and catalytic cracking of polyethylene using H-Beta and H-ZSM-5[48]

Young-Hwa Seo *et al* reported Catalytic degradation of waste high-density polyethylene (HDPE) to hydrocarbons by ZSM-5, zeolite-Y, mordenite and amorphous silica/alumina were carried out in a batch reactor [8]. Catalytic degradation of HDPE with zeolite-Y, mordenite and amorphous silica-alumina yielded 71-82 wt.% oil fraction, which mostly consisted of C_6-C_{12} hydrocarbons, whereas ZSM-5 yielded much lower oil fraction (~35%), which mostly consisted of C_6-C_{12} hydrocarbons. ZSM-5 showed the greatest catalytic activity on cracking waste HDPE to light hydrocarbons, whereas mordenite produced a high amount of coke. Amorphous silica-alumina also showed an activity on cracking HDPE to lighter olefins with high yield, but no activity on aromatic formation.

However, the deactivation of catalysts have been major obstacle of the cracking reaction in batch process [1-19]. Continuous process can be employed to solve this problem. More complicate designs have been applied including fixed beds, screw kilns, and conical spouted bed reactor [25, 29-31,39].

In 2007, Marcilla *et al* reported that the catalytic cracking of higher viscosity polyethylene (melt flow index was 20.0 g/10 min) by USY and HZSM-5 as catalysts in fixed bed reactor. The polyaromatic nature of the coke increases for both zeolites studied, as the temperature increases. The comparison between the soluble and insoluble content of the coke formed in the presence of USY and HZSM-5 zeolites reflects the different composition of the coke produced in both zeolites [31].

In 2002, Aguado *et al* reported both thermal and catalytic cracking of low-density polyethylene (LDPE) using a screw kiln reactor [29]. Thermal degradation gives rise to a broad product distribution, whereas catalytic cracking over Al-MCM-41 leads mainly to hydrocarbons within the gasoline range (C_5-C_{12}) with selectivities up to 80%. The increase of the screw speed between 3 and 15 rpm in the catalytic experiments allows the plastic feed rate to be varied in the range 20–41 g h^{-1}. The changes observed in the TOF values when varying the screw speed point out a decrease of the activity per site with increasing residence times, which may be due to the catalyst deactivation or to a contribution of the degradative extrusion at higher screw speeds.

In 2007, Elordi et al reported the catalytic pyrolysis of high density polyethylene (HDPE) on a HY zeolite catalyst. The reaction has been carried out in a conical spouted bed reactor (CSBR) at 500 °C. The 69 %wt. of the product stream corresponds to the gasoline fraction (C_5-C_{10}). It is noteworthy that this fraction fulfils European Union requirements for commercial gasoline and its RON index, 96.5, is of the same order as standard automotive fuel. The remaining products are mainly gases, especially propylene and butenes, although there is also a heavy fraction consisting of aromatics with more than one ring and waxes [30].

Although attempt on FCC of polymer waste were made, Y.H. Lin *et al* [20] reported catalytic degradation of high density polyethylene over mesoporous and microporous catalysts in a fluidised-bed reactor. HZSM-5 catalysed degradation resulted in much more amounts of gas products, as compared with degradation over non-zeolitic catalysts (MCM-41 and SAHA). The larger pore structure of the MCM-41 and SAHA catalysts showed deactivation in contrast to the more restrictive HZSM-5. MCM-41 with large mesopores and SAHA with weaker acid sites give high olefinic products and rise to the broad carbon range of C_3-C_7 [20]. However, suitable particle sizes of both catalyst and polymer feed is crucial. The FCC required particles that large enough to avoid entrainment but not too large to be inadequately fluidized [20]. To confront with a rapid deactivation and difficulty in the FCC operation, the moving bed reactor is proposed.

In previous thesis, cracking of polyethylene using zeolite beta catalyst in continuous process was reported by Mr. Teerawat Chalermsuksri. The melt flow index of polyethylene was 43.12 g/10 min. The liquid products obtained from catalytic cracking of polyethylene are distributed in a narrow range of gasoline fraction (80-90 %wt.). The carbon distribution of the products can be controlled by the pore size of the catalyst [39]. However, the direction of rotating paddles is changed to help driving molten polymer to though the reactor. The used catalyst can be continuously removed and replaced by newly fed one by the reactor screw. However, the remaining half of the waste plastic generated from household is in the forms of plastic mixtures, a mixture of waste plastics, particularly the hydrocarbon polyolefin that possesses various viscosity and molecular weights. The mixing speed of paddle cannot be controlled due to high torque of the viscous polymer melt when the polymer with various viscosity was used as feeds.

However, commodity plastic waste exhibits various viscosity because they are mixtures mainly composed of HDPE, LDPE and other polyolefin. To reduce separation cost, it is interesting to obtain a system that is applicable for polyethylene waste with various viscosity. Most of previous research have been studied on thermal and thermo-catalytic degradation of low [9,14-15,26] and high [3,5-8, 10-12] density polyethylene.

Both thermal and catalytic cracking of mixtures consisting of low-density polyethylene (LDPE) and a lubricating oil base have been investigated in a continuous screw kiln reactor by Serrano *et al.* The incorporation of the lubricating oil into the plastic leads to a significant decrease in its viscosity which favors the mixture flow through the reactor. Catalytic cracking of a 70/30 (%, w/w) LDPE–lubricating oil base mixture over mesoporous Al-MCM-41 catalysts at 400/450 °C proceeded with lower activity with regards to the pure LDPE catalytic cracking. This result is related to both the lower reactivity of the oil compared to the pure polyolefin and to the poisoning of the catalyst acid sites by sulfur/nitrogen-containing compounds present in the lubricant oil base [26].

Thermal and catalytic cracking of both high and low-density polyethylene (HDPE and LDPE, respectively) under mild conditions was reported by Van Grieken *et al* [3]. The best results achieved in the LDPE degradation with regard to stability and homogeneity of the waxy product were obtained using MCM-41 as catalyst. In addition, the product obtained from HDPE has a higher homogeneity than that coming from LDPE, leading to a waxy product with better quality for potential applications.

It can be seen that the polyethylene fed with various viscosity and molecular weight effect the cracking activity and the composition of product. In addition, the previous reported cracking process does not readily used for general plastic waste, which possesses various viscosities. In this thesis, the moving bed reactor with single reactor screw would also be designed for cracking general plastic waste that mainly composed of with various viscosity and molecular weight. Since, activation of these feed were obviously different, the process severity (i.e. temperature, pressure and contact time) can be easily controlled and adjusted in moving bed screw reactor. The effect of reactor screw speed (RSS), catalyst content, polymer feed rate and polymer viscosity was studied.

CHAPTER 3

EXPERIMENTAL DETAILS

3.1 Reagents

1. Air zero (99.9%, TIG)
2. Acetone (99.5%, Carlo Erba Reagenti)
3. Benzene (99.8 %, Carlo Erba Reagenti)
4. Cyclohexane (99.5 %, Carlo Erba Reagenti)
5. Cyclohexene (>99.0 %,Carlo Erba Reagenti)
6. Gasoline fuel, octane 91(PTT)
7. Isooctane (99.5 %, Carlo Erba Reagenti)
8. Helium gas (99.9%, TIG)
9. Liquid nitrogen (TIG)
10. *m*-Xylene (>99.0 %, Fluka)
11. Nitrogen gas (99.9%, TIG)
12. *n*-Heptane (99.5 %, Carlo Erba Reagenti)
13. *n*-Hexane (99.9 %, Mallinckrodt)
14. Methylcyclopentane (>98 %, Merck)
15. *n*-Nonane (>99.0 %, Merck)
16. *p*-Xylene (99.0 %, Fluka)
17. Low-density polyethylene (Melt flow index, MFI = 4.83, 24.58 and 36.83 g/10 min, pellets form, Global Connection Co., Ltd. and TPIPL)
18. Toluene (99.5%, Lab scan)
19. Zeolite Beta (Tosoh Corporation)

3.2 Apparatus

1. Automatic distillation analyzer (AD86 5G B.P.40 14790 version, ISL)
2. Bunsen burner
3. Condenser
4. Differential scanning calorimeter (Pyris Diamond DSC, Perkin Elmer)
5. Furnace (Vecstar Furnaces)
6. Gas adsorption analyzer (Autosorb-1, Quantachrome)

7. Gas chromatograph (5890 Series II Gas Chromatograph, HP)
8. Gas chromatograph/Mass spectrometer (6892N/5973N, Agilent Technologies, Instruments Service Centre, Kmitl)
9. Heating tape
10. Hotplate
11. Laboratory glassware
12. Motor
13. Melt flow indexer (CEAST 6841.000 ASTM D1238,CEAST)
14. Nuclear magnetic resonance spectrometer (AVANCE DPX300, Bruker)
15. Oven
16. Reactor (see Figure 3.3)
17. Scanning electron microscope (LEO 1455VP, LEO Electron Microscopy, Scientific Instruments Service Centre, Kmitl)
18. Single screw extruder (A.K. plastic and machinery Co.,Ltd.)
19. Single reactor screw (see Figure 3.1; A.K. plastic and machinery Co.,Ltd.)
20. Thermogravimetric analyzer (Pyris 1 TGA, Perkin Elmer, Scientific Instruments Service Centre, Kmitl)
21. Vacuum oven
22. Water circulator
23. Aspirator vacuum pump
24. Wax trap (see Figure 3.2)
25. X-ray fluoresence spectrometor (SRS 3400, Bruker AG, Scientific Instruments Service Centre, Kmitl)
26. X-ray powder diffractometer (D8 Advance, Bruker AG, Scientific Instruments Service Centre, Kmitl)

3.3 Experimental procedure

3.3.1 Development of continuous process.

3.3.2 Characterization of zeolite catalyst.

3.3.2.1 Determination of zeolite structure using X-ray Powder Diffractometer (XRD)

3.3.2.2 Determination of zeolite crystal morphology using Scanning Electron Microscope (SEM)

3.3.2.3 Determination of zeolites surface area using Gas Adsorption Analyzer (Autosorb-1C)

3.3.2.4 Determination of silicon/aluminium ratio of the zeolites using X-ray Fluorescence spectrometor (XRF)

3.3.2 Characterization of polyethylene material.

3.3.2.1 Determination of low-density polyethylene material heat of fusion and melt temperature using Differential Scanning Calorimeter (DSC)

3.3.2.2 Determination of melt flow index of low-density polyethylene material using melt flow indexer

3.3.3 Study on thermal and catalytic degradation of low-density polyethylene with different viscosity using Thermogravimatric analyzer (TGA).

3.3.4 Study on cracking reaction of low-density polyethylene in continuous process.

3.3.5 Analysis of products from cracking reaction of low-density polyethylene

3.3.5.1 Determination of product composition using Gas Chromatograph (GC).

3.3.5.2 Determination of product composition using Gas Chromatograph/Mass Spectroscopy (GC/MS).

3.3.5.3 Determination of the composition and predicted octane number of the gasoline products using Nuclear Magnetic Resonance (NMR).

3.3.5.4 Study on thermal degradation of residues from reaction using thermogravimetric Analyzer (TGA).

3.3.5.5 Determination of gasoline yield and distillation characteristics of the liquid products using Automatic distillation analyzer.

3.3.5.6 Determination of wax products heat of fusion and melt temperature using Differential Scanning Calorimeter (DSC)

3.4 Experimental details

3.4.1 Development of continuous process.

In this work, the high viscosity of polymer materials were used as fed in the continuous process. Hence, the new reactor screw (Figure 3.1) was incorporated in the reactor designed in previous work [49] for cracking reaction of low-density polyethylene with high viscosity. It can be seen that the screw flight is notched to allow the cracked gases to flow to an outlet line at the top of the reactor and the mixing speed of screw can be controlled for high torque of the viscous polymer melt. Hence, a better heat transfer is expected in the developed screw reactor.

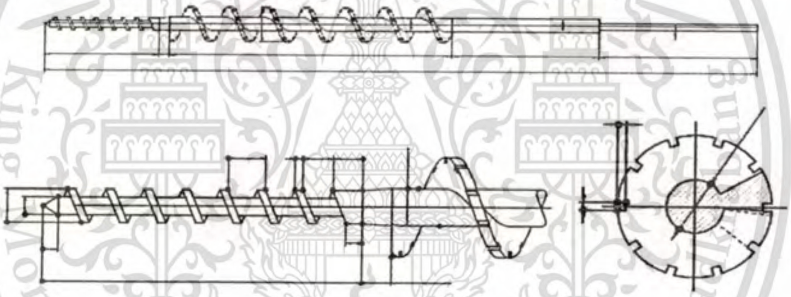

Figure 3.1 The single reactor screw

As discussed above, the high molecular of polyethylene materials was used and heat transfer was improved in this work. The thermal cracking may well participate in the reaction. It is expected that wax product is produced. Accordingly, wax trap (Figure 3.2) is attached to the exits of gaseous products from the top of the reactor to separated wax from liquid product. The wax trap connects to pump for collect the wax product from continuous process. The developed continuous process was showed in the Figure. 3.3.

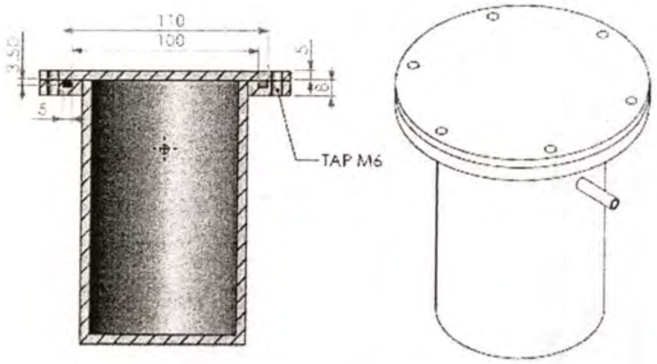

Figure.3.2 The wax trap

3.4.2 Characterization of zeolite catalyst.

3.4.2.1 Determination of zeolite structure using X-ray Powder Diffractometer (XRD)

The zeolite structure is determined by X-ray powder diffractometer. The sample is prepared by packing the zeolite in the sample holder. CuK$_{\alpha}$ X-ray beam is used for analysis at 40 kV, 40 mA. The sample is scanned from 2θ angle 5° to 50° with 1 second/step time and 0.02 2θ/step increment. X-ray diffraction pattern of the sample is compared with the X-ray diffraction pattern of standard zeolite for structure determination.

3.4.2.2 Determination of zeolite crystal morphology using Scanning Electron Microscope (SEM)

The crystal morphology and crystal size of zeolite is determined by scanning electron microscope. The sample is prepared by thoroughly placing zeolite powder onto the sample holder. It is then coated with gold by ion sputtering. The sample is placed in the sample chamber of SEM and evacuated from ambient pressure to 10^{-4} torr. The scanning electron micrographs is taken at the magnification of 6,000 and 10,000 times and scan speed of 9.

3.4.2.3 Determination of zeolites surface area using Gas Adsorption Analyzer (Autosorb-1C)

Surface area of the zeolites is determined by gas adsorption analyzer. The sample is prepared by weighing approximately 20 mg of zeolite sample into the clean and dry sample cell. The sample cell is attached to the out gassing station. Heating mantle is installed and the temperature is raised to 350 $^{\circ}$C under vacuum. The sample is out-gassed for 24 hours. The sample cell is then removed from the out-gassing station after the nitrogen is filled and is attached to the analysis station. The equilibration time is set to 3 minutes and the nitrogen adsorption is measured at the partial pressure (P/P_0) ranged from 10^{-6} to 1.0 at 77.4 K.

3.4.2.4 Determination of silicon/aluminium ratio of the zeolites using X-ray Fluorescence spectrometor (XRF)

The silicon/aluminium ratio of the catalysts is determined by X-ray fluorescence spectrometor. The sample is prepared by mixing 4.5 g of boric acid and 0.5 g of zeolite. The mixture is packed onto sample holder and compressed at 150 KN. The sample is then be placed in the sample chamber of X-ray fluoresence spectroscopy. Rhodium is used as source for analysis at 50 KV, 60 mA, and WDX of 0.3 to 188.5.

3.4.3 Characterization of low-density polyethylene material.

3.4.3.1 Determination of polymer material heat of fusion and melt temperature using Differential Scanning Calorimeter (DSC)

The heats of fusion of polyethylene with various viscosity are determined by differential scanning calorimeter. A small quantity of sample, usually 5-10 mg, is weighed into an inert capsule made of aluminum. The encapsulated sample is placed in the DSC sample holder furnace and reference is placed in the DSC reference holder furnace. Those are heated from 50°C to 200°C at a heating rate of 10°C/ min.

The crystallinity of polyethylene can be calculated by the following equation.

$$\%\ \text{crystallinity} = \frac{\Delta H_{\text{sample}}\ (\text{J/g}) \times 100}{293\ (\text{J/g})\ (\Delta H\ 100\%\ \text{crystallinity of LDPE})}$$

3.4.3.2 Determination of melt flow index of polymer material using melt flow indexer

The melt flow index of polyethylene with various viscosity are determined by melt flow indexer. The melt flow index apparatus is preheated at 190°C. The polymer material is then loaded into the cylinder from the top and a dead weight is placed on a piston with total weight of 2.16 Kg. The polymer material is allowed to flow through the die. Depending on the material or its flow rate, cuts for the test are taken at different time intervals. The extrudate is weighed and the melt index values was calculated in gram per 10 minutes.

3.4.4 Study on thermal degradation of polyethylene with different viscosity using Thermogravimatric analyzer (TGA).

Thermal degradation behavior of polyethylene is investigated using TGA. Approximately 30 mg of virgin polyethylene (SU 1018, LDPE1630J and LDPE 1905F pellets), polyethylene with various viscosity mixed with catalyst (catalyst content of 0, 0.5, 1 and 2 %) is placed in a platinum pan hanging from a thermobalance, and nitrogen is introduced as a carrier gas. The sample is then heated under a nitrogen flow (50 ml/min) from 50°C to 800°C at a heating rate of 10°C/ min. The %weight loss due to the degradation is measured with the sample temperature.

3.4.5 Study on cracking reaction of polyethylene in continuous process.

The schematic diagram of design continuous moving bed reactor is shown in Figure 3.3. Low-density polyethylene sample (100 grams) and zeolites beta (1 grams) are vigorously mixed in a small chamber. Then, the mixed low-density polyethylene samples with zeolite beta were loaded into the hopper (No.5). The barrel temperature of extruder was controlled by a three-zone horizontal heater at 100, 120 and 200 (at the top of the reactor) °C (No.6). The molten low-density polyethylene samples with zeolite beta were continuously fed into the top of the reactor (No.10) at 430 °C. The reactor was equipped with a single screw (No.9) designed for carrying feed and catalyst down through the residue chamber (No.15) at the bottom of the reactor and allow cracked gases to exist from the top of the reactor. Stirring of the polyethylene samples inside the reactor was achieved by means of an electric motor (No.7) and the rotating single screw.

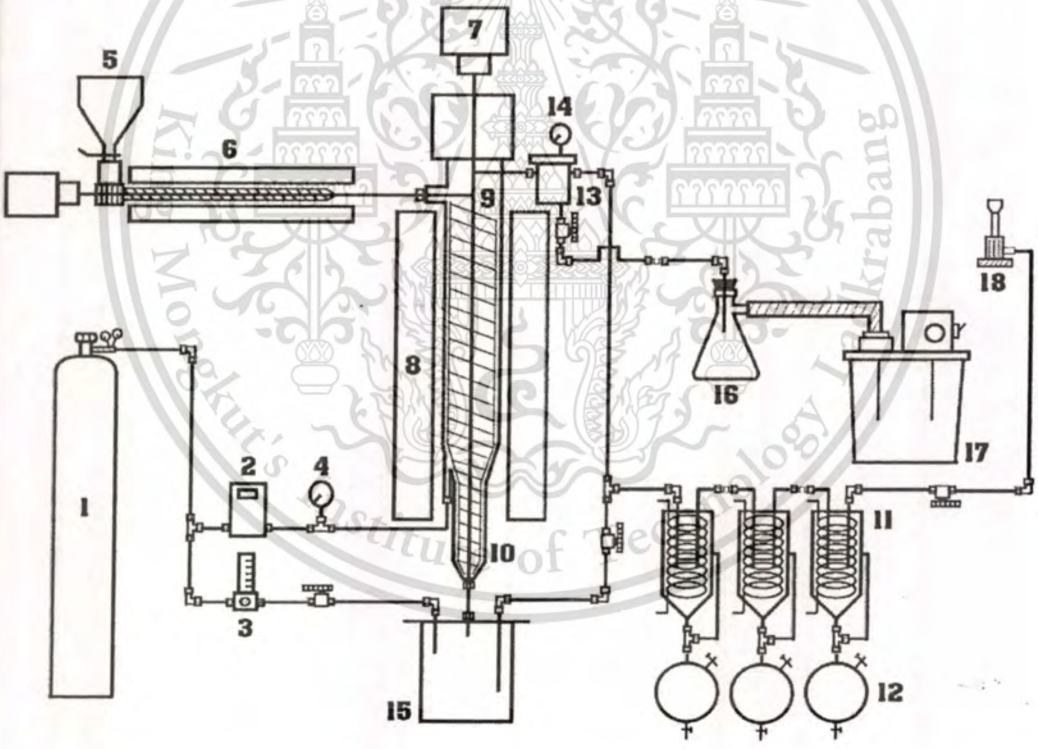

Figure 3.3 The developed continuous process; 1. Gas N_2, 2. Digital flow meter, 3. Flow meter, 4. Pressure gauge, 5. Hopper 6. Single screw extruder 7. Reactor motor, 8. Furnace, 9. Single reactor screw, 10. Reactor chamber, 11. Liquid trap condenser, 12. Liquid product collector, 13. Wax trap, 14. Wax trap pressure gauge, 15. Residue chamber, 16. Suction flask, 17. Aspirator vacuum pump, 18. Flair

Nitrogen (No.1) was used as a carrier gas with a flow rate of 50 ml/min. The vaporized wax can be trapped in wax trap unit (No.13) and the liquid products (No.12) were collected at approximately 40°C in the first cooling condenser (No.11) and at -5°C in the second and third condensers.

3.4.5.1 Effect of reactor screw speed (RSS).

The effect of reactor screw speed (RSS) was determined by the reactions using the reactor screw speed (RSS) of 46, 66 and 130. rpm. at reaction temperature of 430°C. The reactions were investigated using LDPE 1630J (MFI = 24.6, viscosity = 4.0 poise) as feed, an approximate polymer feeding rate; 600 g/hr, the catalyst content; 1.0 %wt.

3.4.5.2 Effect of catalyst content

The effect of catalyst content was determined by the reactions using catalyst contents of 1.0% and 2.0% at reaction temperature of 430°C. The reactions were investigated using LDPE 1630J (MFI = 24.6, viscosity = 4.0 poise) as feed, an approximate polymer feeding rate; 600 g/hr, the reactor screw speed (RSS); 46 rpm.

3.4.5.3 Effect of polyethylene feeding rate

The effect of polymer feeding rate was determined by the reaction using an approximate polymer feeding rate of 400, 600, 700, 800 g/hr at reaction temperature of 430°C. The reactions were investigated using LDPE 1630J (MFI = 24.6, viscosity = 4.0 poise) as feed, the reactor screw speed (RSS); 46 rpm, the catalyst content; 2.0%wt.

3.4.5.4 Effect of viscosity of polyethylene fed

The effect of viscosity of polyethylene fed was determined by the reaction using LDPE SU1018, LDPE 1630J. LDPE 1905F (MFI = 36.8, 24.6 and 4.8; viscosity = 2.7, 4.0 and 20.3 poise, respectively) as feed. The reactions were investigated the reactor screw speed (RSS) as 46 rpm, the catalyst content; 2.0%wt, feed rate; approximate 600 g/hr.

3.4.6 Analysis of products from cracking reaction of polyethylene

3.4.6.1 Determination of product composition using Gas Chromatograph (GC)

The liquid products was analyzed by gas chromatograph using 5890 Series II Gas Chromatograph, HP, with a capillary column (Equity-1, 30 m, 0.53 mm I.D.) and a flame ionization detector (FID). Nitrogen was used as carrier gas with a linear velocity of 30 cm/sec.. The liquid products, the 0.1 μl of sample was injected to the injection port (injection port temperature at 220°C). The oven temperature was started at 40°C and held for 5 minutes. Then, the temperature was raised to 160°C with a heating rate of 5°C/min and held at that temperature for 1 minutes. After that, the temperature was raised to 250 °C with a heating rate of 20 °C/min and held at that temperature for 18 minutes.

3.4.6.2 Determination of product composition using Gas Chromatograph/Mass Spectroscopy (GC/MS)

The structure of liquid products were confirmed by gas chromatograph/mass with a capillary column (HP-1, 30 m, 0.25 mm I.D.). Nitrogen was used as a carrier gas with an initial flow 0.6 ml/min and an average velocity of 28 cm/sec. Approximately 0.1 μl of the sample was injected to the injection port (injection port temperature at 220°C) using a split ratio of 200. The oven temperature was used the same with the FID gas chromatograph.

3.4.6.3 Determination of the composition and predicted octane number of the gasoline products using Nuclear Magnetic Resonance (NMR)

The content of paraffins, olefins and aromatics of liquid products were determined using the NMR method developed by Myers *et al* [36-37]. The liquid products were diluted in deuterated chloroform with tetramethylsilane (TMS) internal reference. The measurement was performed on a Bruker AVANCE DPX300 NMR spectrometer with 300-MHz proton resonance frequency. The integral spectra are obtained in separated scans from 0 to 10 parts per million (ppm). The RON and MON was also calculated using the equations as shown:

Isoparaffin index = CH_3/CH_2

RON = 80.2 + 8.90 (isoparaffin index) + 0.107 aromatics (vol.%)

MON = 70.8 + 10.0 (isoparaffin index) + 0.101 aromatics (vol.%)

Details of the method is described in appendix F

3.4.6.4 Study on thermal degradation of residues from reaction using thermogravimetric Analyzer (TGA).

The degradation behavior of the residue was studied using TGA. The residues from the reactor were cut into particles with 6 mm diameter. Approximately 30 mg of the sample was placed into a platinum pan hanging from a microbalance, then nitrogen was introduced as a carrier gas. The sample was heated under a nitrogen flow (50 ml/min) from 50°C to 800°C at a heating rate of 10°C/ min.

3.4.6.5 Determination of gasoline yield and distillation characteristics of the liquid product using Automatic distillation analyzer [38]

The distillation (volatility) characteristics of liquid product was determined by automatic distillation analyzer (AD86 5G B.P.40 14790 version, ISL) using ASTM D 86. A 100 ml of liquid product was distilled under prescribed conditions for the group in which the sample falls. The distillation was performed in a batch distillation unit at ambient pressure under conditions that was designed to provide approximately one theoretical plate fractionation. Systematic observations of thermometer readings and volumes of the condensate was made. The volume of the residue and the losses will also be recorded. The results of the test were calculated and reported. Measurement of the liquid product was carried out in program A, as shown in Tables 3.1. From the distillation data, yield of gasoline fraction could be calculated.

Table 3.1 Preparation of apparatus

Temp. of Stored Sample: °C	0 to 10
Flask, ml	125
Ip Distillation Thermometer	5C
Flask Support	B
Diameter of hole, mm	38
Flask and thermometer, °C	13 to 18
Flask support and shield	Not above ambient
Graduate and 10 ml charge, °C	13 to 18

Table 3.2 Distillation condition of liquid products

Method	ASTM D86
Group	2
Distillation rate, %/min	4.5
Condenser setpoint, °C	2
Bath temperature delta, °C	0
Graduate setpoint , °C	15
First level heating , W	18
First level heating time, min	3.0
Second level heating, W	39
Final heating adjustment, W	40
Barometric correction	1(1= yes, 0 = no)
Coefficient	0
Rounded temperature, °C	0
Expected volume – Hold up, %	98
FBP detection, °C	-5.0

3.4.6.6 Determination of wax products heat of fusion and melt temperature using Differential Scanning Calorimeter (DSC)

The heats of fusion of wax products from reaction are determined by differential scanning calorimeter. A small quantity of sample, usually 5-10 mg, is weighed into an inert capsule made of aluminum. The encapsulated sample is placed in the DSC sample holder furnace and reference is placed in the DSC reference holder furnace. Those are heated from 50°C to 200°C at a heating rate of 10°C/ min.

3.4.7 Calculation of the catalytic activity

3.4.7.1 Conversion

The conversion of product can be calculated as the fraction of the initial mass of polymer reacted to form gas and liquid products. It can be expressed as the following.

$$\% \text{ Conversion} = \frac{F - R}{F} \times 100$$

; F = Initial mass of polymer fed for a certain period of time

R = Mass of residue collected for a certain period of time

3.4.7.2 Liquid yield

The yield of liquid products was calculated as the mass of liquid collected divided by the initial amount of polymer. It can be expressed as the following.

$$\% \text{ Yield of liquid product} = \frac{L \times 100}{F}$$

; L = Mass of liquid product collected for certain period of time

F = Initial mass of polymer fed for certain period of time

3.4.7.3 Wax yield

The yield of wax products was calculated as the mass of wax collected divided by the initial amount of polymer. It can be expressed as the following.

$$\% \text{ Yield of wax product} = \frac{W \times 100}{F}$$

; W = Mass of wax product collected for certain period of time

F = Initial mass of polymer fed for certain period of time

3.4.7.4 Residue yield

The yield of residue from reaction was calculated as the mass of residue collected divided by the initial amount of polymer. It can be expressed as the following.

$$\% \text{ Yield of residue} = \frac{R \times 100}{F}$$

; R = Mass of residue collected for certain period of time

F = Initial mass of polymer fed for certain period of time

3.4.7.5 Gas yield

The yield of gas products was determined by subtracting the weight of all of liquids and residue. Yield of gas can be defined by the relation.;

$$\text{Gas (wt.\%)} = 100 - [\text{ liquid (wt\%)} + \text{wax (wt\%)} + \text{residue (wt\%) }]$$

3.4.7.6 Selectivity

The selectivity of liquid product is the ratio of mass of polymer that converted to liquid product over mass of polymer that converted to all of products. It can be expressed as the following.

$$\%\ \text{Selectivity of liquid product} = \frac{\%\ \text{Yield of the liquid product}}{\%\ \text{Conversion of the product}} \times 100$$

CHAPTER 4

RESULTS AND DISCUSSION

4.1 Characterization of zeolite catalyst

4.1.1 Determination of the zeolite structure using XRD

Catalyst used in this work was zeolite Beta type (HSZ-930NHA; Tosoh coporation). X-ray diffraction pattern of the zeolite as shown in Figure 4.1, was obtained from X-ray powder diffractometer using Cu-Kα-radiation.

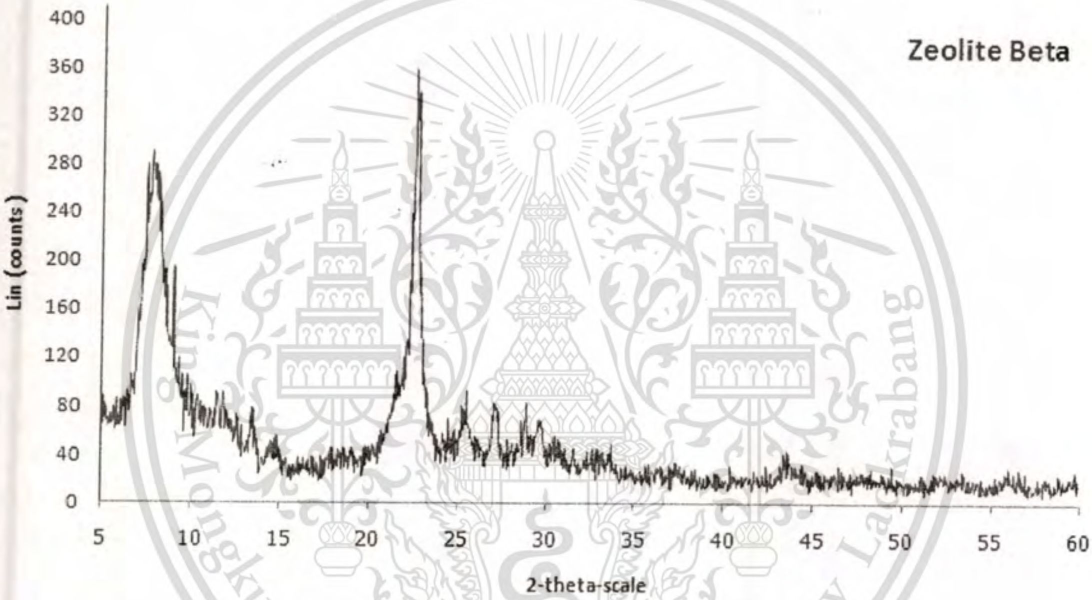

Figure 4.1 X-ray diffraction pattern of zeolite Beta

The X-ray diffraction pattern of zeolite Beta was compared to that of the standard zeolite Beta (Figure B.1, Appendix B). It revealed characteristic peaks at 2θ 7.68, 21.42, 22.50, 25.27, 26.93 and 29.51 in a manner similar to those of to the X-ray diffraction pattern of the standard Beta. The crystallite size of zeolite Beta is approximately 145 nm, as calculated by Scherrer's equation [72] (Table 4.1). Therefore, it was expected that this zeolite would have high external surface area.

4.1.2 Determination of the crystal morphology of zeolite using SEM

The electron micrograph of zeolite Beta showed a semi-spherical shape of agglomerate crystals with a particle size approximately 3 μm in diameter.

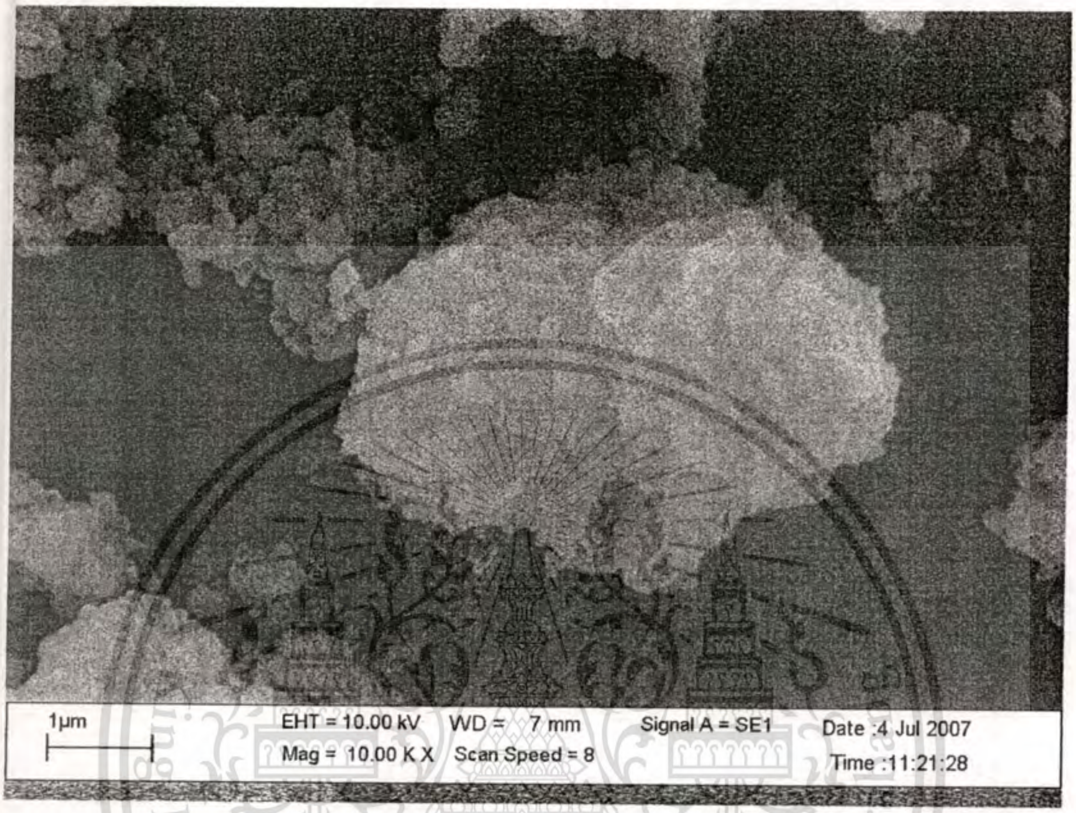

Figure 4.2 Scanning electron micrograph of the zeolite Beta

4.1.3 Determination of the surface area of zeolite using Gas Adsorption Analysis

The adsorption isotherm of nitrogen on zeolite sample was obtained using Autosorb-1C gas adsorption analyzer. The surface areas of zeolite Beta shown in Table 4.1 were determined by applying of the Brunauer-Emmet-Teller (BET) equation to the adsorption isotherm, measured at liquid nitrogen temperature. In consistent with XRD and SEM results, the zeolite beta possesses high surface area, as discussed previously.

Table 4.1 Crystal size, surface area, and Si/Al ratio of the zeolite beta

Catalyst	**Crystal size (XRD) (nm)**	**BET area (m^2/g)**	**Si/Al ratio**
Zeolite Beta	145	629.3	12.5

4.1.4 Determination of the silicon/aluminium (Si/Al) ratio of zeolite using XRF

The silicon/aluminium (Si/Al) ratio of zeolite Beta was determined by SRS 3400 X-ray Fluorescence Spectroscopy and the result is shown in Table 4.1. Zeolite Beta was classified as relatively high silica sample (Si/Al =12.5). It was expected that these zeolites would possess a high thermal stability and acid strength.

4.2 Characterization of polyethylene material

4.2.1 Determination of melt flow index of polymer material using melt flow indexer

Melt flow index of polyethylene samples (LDPE SU1018, LDPE 1630J and LDPE 1905F) was obtained from CEAST 6841.000, as shown in Table 4.2. The melt flow index is inversely proportional to the viscosity of the polyethylene melt, which can be calculated by the following equation [45].

$$\eta_0 * \text{MFI} = 0.0495\, W \rho$$

; where W is in gram., ρ in g/cm^3, η_0 in poise and MFI in g/10min.

Since all the polyethylene samples (LDPE SU1018, LDPE 1630J and LDPE 1905F) are long chain branching structure. It is suggested that the viscosity of polyethylene samples depends on the chain length and hence the molecular weight.

4.2.2 Determination of polymer material heat of fusion and melting temperature using DSC

The heat of fusion and melting temperature of polyethylene samples (LDPE SU1018, LDPE 1630J and LDPE 1905F) were obtained from Differential Scanning Calorimeter (Table 4.2). It is seen that heat of fusion and melting temperature of polyethylene samples were slightly increased when the viscosity and molecular weight were increased (decrease in melt flow index). This suggested that the crystallinity may be increased (16.02, 17.61 and 18.14%crystallinity, respectively) when molecular weight of polyethylene samples were increased. These polyethylene samples would be good representatives of commercial polyethylene waste that possesses various viscosity, and hence molecular weight.

Table 4.2 Melt flow index, Viscosity, T_m and heat of fusion of polyethylene fed.

Polymer materials	MFI (g/10min)	Viscosity (poise)	Melting temperature (°C)	Heat of fusion (J/g)
LDPE SU1018	36.8	2.7	106	47
LDPE 1630J	24.6	4.0	111	51
LDPE 1905F	4.8	20.3	113	53

* Calculation of melt flow index (load 2.16 kg/ temp 190°C) and data sheets of polyethylene samples were shown in Appendix A

4.3 Study on thermal degradation of polyethylene using Thermogravimatric analyzer (TGA).

Thermogravimetric analysis was applied to investigate the decomposition of polyethylene with different catalyst contents ranging (0, 0.5, 1.0 and 2.0%). Thermograms of polyethylene samples are shown in Figure 4.3 The initial degradation and degradation temperature of polyethylene are summarized in Table 4.3

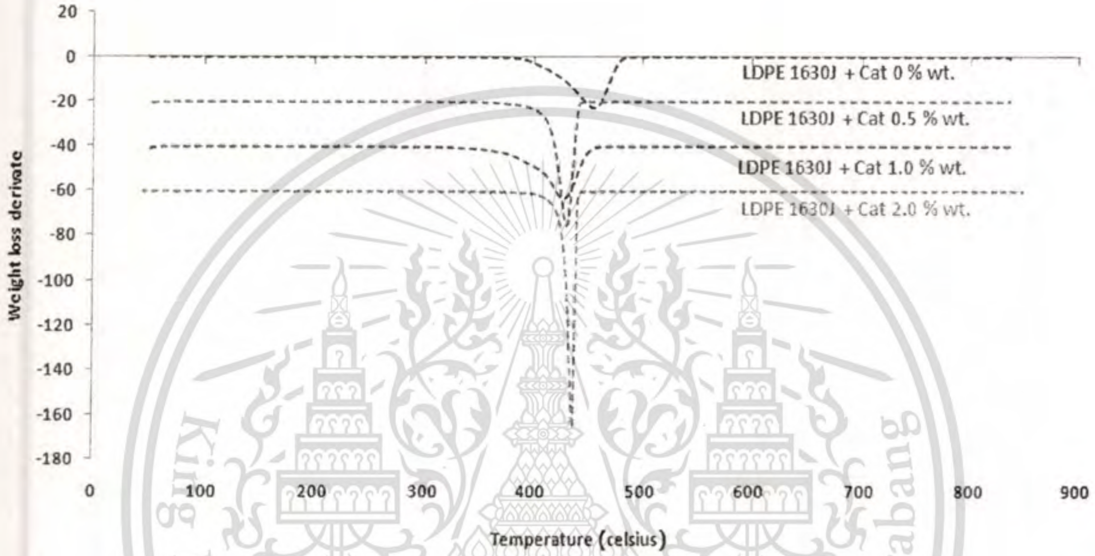

Figure 4.3 Thermogram curves of polyethylene sample (LDPE 1630J) with different % catalyst contents as a function of temperature; heating rate, 10 °C/min; nitrogen, 50 ml/min

The results observed from TGA show that reaction using catalyst leads to lower decomposition temperatures (432-437 °C), as compared to that with no catalyst (~ 460 °C). The catalyst shifts degradation temperature towards lower temperature because the reaction proceed via carbocation intermediate, of which the activation energy is reduced [4,30] while the thermal cracking required higher energies for cleavage of carbon-carbon and carbon-hydrogen bonds [26]. These results were in agreement with the fact that the catalytic cracking was promoted by acid sites. Over the strong acid catalysts, the protonation of polyethylene chains can be readily facilitated, giving carbocation intermediate. The C-C bonds cleavage via successive β-scission of the main chain produces fragments containing lighter hydrocarbons [17].

Table 4.3 Degradation data of polyethylene feds with different types and % catalyst contents.

Polymer	MFI (g/10min)	Viscosity (poise)	Catalyst content (%wt.)	Initial degradation temperature (°C)	Degradation temperature (°C)
LDPE SU1018	36.83	2.67	-	332	458
LDPE SU1018	36.83	2.67	2.0	307	432
LDPE 1630J	24.58	4.00	-	323	458
LDPE 1630J	24.58	4.00	0.5	304	431
LDPE 1630J	24.58	4.00	1.0	303	429
LDPE 1630J	24.58	4.00	2.0	343	437
LDPE 1905F	4.83	20.30	-	350	467
LDPE 1905F	4.83	20.30	2.0	280	434

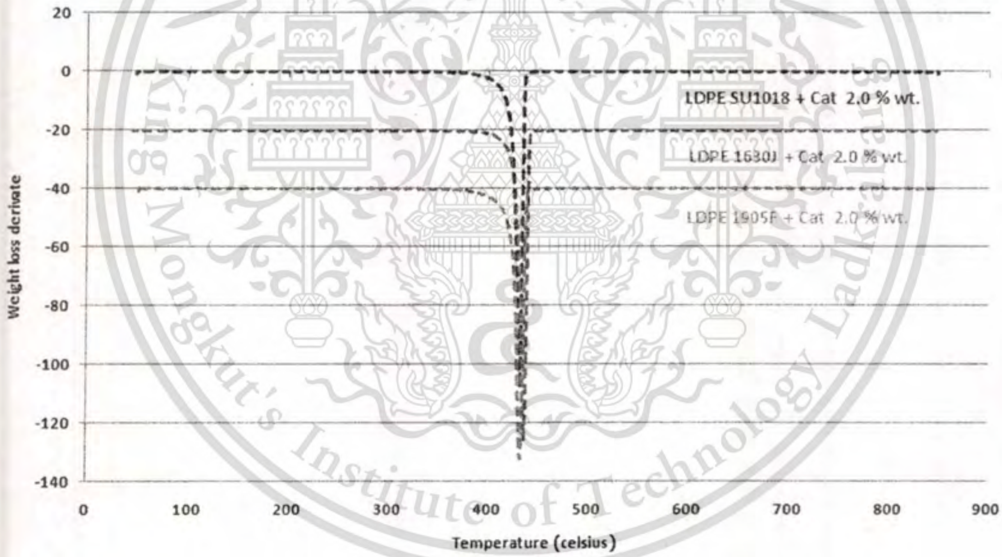

Figure 4.4 Thermogram curves of polyethylene samples with various viscosities (LDPE SU1018, LDPE 1630J and LDPE 1905F) as a function of temperature; heating rate, 10 °C/min; nitrogen, 50 ml/min

The degradation of different polyethylene samples (LDPE SU1018, LDPE 1630J and LDPE 1905F) are shown in Table 4.3. It can be seen that the temperature for either thermal or catalytic degradation of all polyethylene samples are similar. This is because a similar activation energy would be required for the homolytic C-C bond cleavage, despite molecular weight of polyethylene is not the same. This is also the case for heterolytic C-C bond cleavage when the catalyst is used.

4.4 Study on cracking of polyethylene in continuous process

In a continuous process, catalytic cracking of polyethylene samples with various viscosities (LDPE SU1018, LDPE 1630J and LDPE 1905F) was investigated using nitrogen as carrier gas with a flow rate of 50 ml/min at 430°C. The commercial zeolite beta was used as a catalyst for all experiments. The cracked products are classified into 4 groups: gaseous, liquid, wax products, and residue. The residue was determined from the weight of the output material obtained from the bottom of reactor chamber, excluding the spent catalyst weight. The amount of liquid fraction and wax products was determined by the product obtained from the condensers and the wax trap, respectively. The conversion was calculated as the fraction of the initial mass of polymer fed for certain period of time that converted to form gas and liquid products. The yield of liquid and wax products were calculated as the mass of liquid and wax collected divided by the initial mass of polymer fed for certain period of time. While yield of gas products was determined by subtracting the weight of all of liquids and residue from initial mass of polymer fed. In addition the selectivity of liquid product is the ratio of the mass of liquid product over the mass of all products obtained, as example in Appendix A.

4.4.1 Effect of reactor screw speed

The catalytic cracking of polyethylene (LDPE 1630J; MFI = 24.6 g/10 min. and viscosity = 4.0 poise) was investigated with a constant polymer feeding rate, approximately 600 g/hr using 1.0 %wt zeolite Beta as catalyst. The conversion of polyethylene was plotted versus time on stream as shown in Figure 4.5. It can be also noticed that the conversion at the start up were relatively low and gradually increased to constant values with time on stream. This phenomenon indicated that the reaction approached a steady state after 3 hours. It can be explained that at the start up the polymer materials with absence of the catalyst still accumulated in the reactor. This is because prior to starting of each reaction, only polyethylene was fed for material balance testing at 300°C. Therefore, at the beginning of the reaction the catalyst content in the reactor was small but gradually increased to a certain content as the polymer and catalyst were continuously fed. In addition, the reactor reach steady state more quickly than that observed in previous study [39]. This is because the single screw was incorporated in the reactor for cracking of polyethylene with high viscosity as discussed in Chapter 3. Hence, a better heat transfer can be obtained. After steady state, deactivation was not observed because the coking catalyst could be continuously removed and replaced by newly fed catalyst.

When the polyethylene sample was fed at approximately 600 g/hr. The whole polyethylene can be driven out from the reactor at the screw reactor speed as 46 rpm., as seen by the weight of polyethylene sample collected at the residue chamber (Appendix C; Table C.5). This suggests that, operating at the 46 rpm., the reactor screw speed was appropriately high to avoid holding up of polyethylene in the reactor. Therefore, no polyethylene would be retained/ accumulated in the reactor when the reactor screw speed was tested from 46 to 130 rpm.

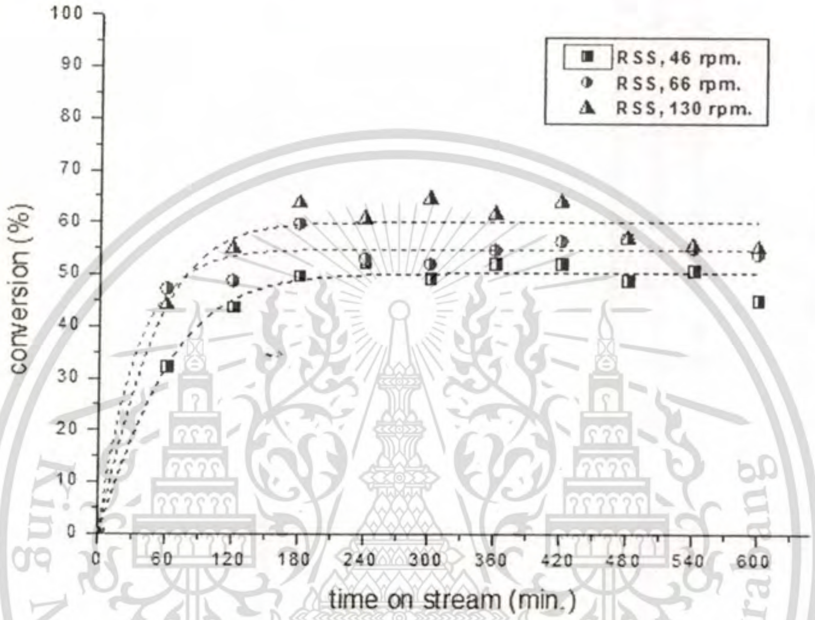

Figure 4.5 Conversion from catalytic cracking of polyethylene (LDPE 1630J; MFI = 24.6 g/10min. and viscosity = 4.0 poise) in continuous process with different the reactor screw speeds (RSS) as a function of time on stream; reaction conditions: temperature, 430^{o}C; polymer feeding rate, ~600 g/hr; nitrogen 50 ml/min; catalyst content, 1.0 % wt.

It was expected that the reactor screw speed would control the resident time of the polyethylene in the reactor and when reactor screw speed was increased, the contact time and conversion should be decreased. However, a relatively higher conversion was observed when the reactor screw speed (RSS) was increased from 46 to 66 rpm. (Figure 4.5). This suggests that the reactor screw speed cannot readily modify the contact time, as expected. This is because the screw flight was not completely filled with the polyethylene melts at the reaction temperature (430 ^{o}C). Instead, the observed increase in conversion can be attributed to a better heat transfer and additional heat that may well be generated from a higher shear rate of the reactor screw.

These would readily suppress a possible cold spot in the reactor which may well be arisen due to the endothermic nature of the cracking reaction. Hence, the conversion was increased with an increase in reactor screw speed.

Table 4.4 Yields and selectivity of liquid products from cracking of polyethylene using catalyst content as 1.0 % wt. in continuous process with different reactor screw speeds (RSS).

RSS (rpm.)	**Yields (%)**			**Selectivity (%)**		
	Liquid	**Wax**	**Gas**	**Liquid**	**Wax**	**Gas**
46	25.63	12.17	10.61	51.10	24.27	21.15
66	36.41	15.87	3.07	65.78	28.67	5.55
130	33.73	15.39	6.71	56.01	25.56	11.14

Due to the better heat transfer and additional heat from shear force, an increase in the reactor screw speed (RSS; from 46 to 66 rpm) can also provide higher liquid and wax yield, as shown in Table 4.4. This is because the primary cracking at external surface (produce wax product) and secondary cracking within the pore of zeolite (produce liquid product) were readily improved by a better heat transfer. The high reactor screw speed can also lead to better mixing of polyethylene and catalyst. This hence limits the random cracking of chain end that leads to gas products. It can be seen that the liquid and wax selectivities were increased while the gas selectivity was decreased when the reactor screw speed was increased from 46 to 66 rpm.

However, when the reactor screw speed was increased up to 130 rpm, the liquid and wax yields were slightly decreased. This is attributed to the exceeding heat transfer that facilitated thermal cracking that promotes random scission of the cracked species via radical intermediates, and also the secondary cracking within the pore of zeolite to produce lower molecular weight hydrocarbons. Accordingly, the gas yield was enhanced, as shown in Table 4.4. In addition, the wax product from the reaction with an increased reactor screw speed (RSS; from 46 to 130 rpm) possesses relatively lower molecular weight which is evidenced by lower T_m and heat of fusion (Table 4.5).

Table 4.5 The melting temperature and heat of fusion of the wax products from cracking of polyethylene in continuous process with different the reactor screw speed (RSS).

RSS (rpm)	Tm of wax product (^{o}C)	Heat fusion of wax product (j/g)
46.06	85.72	18.06
66.26	84.10	13.91
130.06	83.50	12.91

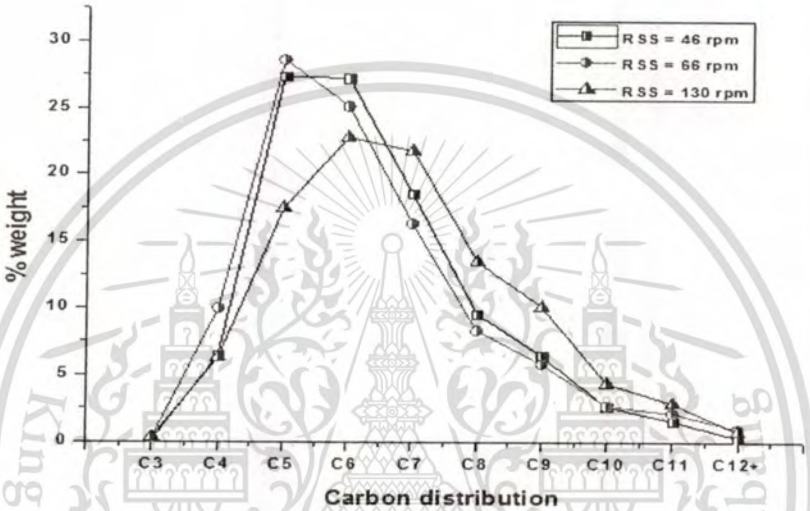

Figure 4.6. The carbon distribution of liquid products from the reaction using various of the reactor screw speed (RSS).

The carbon distribution of the liquid products at the steady state from catalytic cracking of polyethylene is shown in Figure 4.6. It can be seen that the carbon distribution of the liquid products from reaction using the reactor screw speed as 46 and 66 rpm was not significantly different because the molecular weight of liquid product was controlled by the pore of zeolite. However, the thermal cracking promoted by exceedingly heat transfer at high reactor screw speed (RSS; 130 rpm) also affect the carbon distribution of liquid products. It can be seen that the liquid product shifts to high molecular weight hydrocarbons and the wider carbon distribution can be obtained at the reactor screw speed of 130 rpm.

Nevertheless, the carbon distribution of all liquid products remain within the gasoline range (C_5-C_{13}), as shown by the distillation data Figure 4.7. According to the boiling profile, as compared to commercial gasoline 91, liquid product from the reaction with RSS of 46, 66 and

130 rpm contain 86.0, 82.0 and 82.0 %vol. of gasoline, respectively. It is obvious that zeolite beta plays important role in controlling molecular weight of cracked product from polyethylene to be in the range of C_5-C_9. This hydrocarbon range possess kinetic diameter within the same range of pore opening of zeolite beta (~7-8 °A) [39].

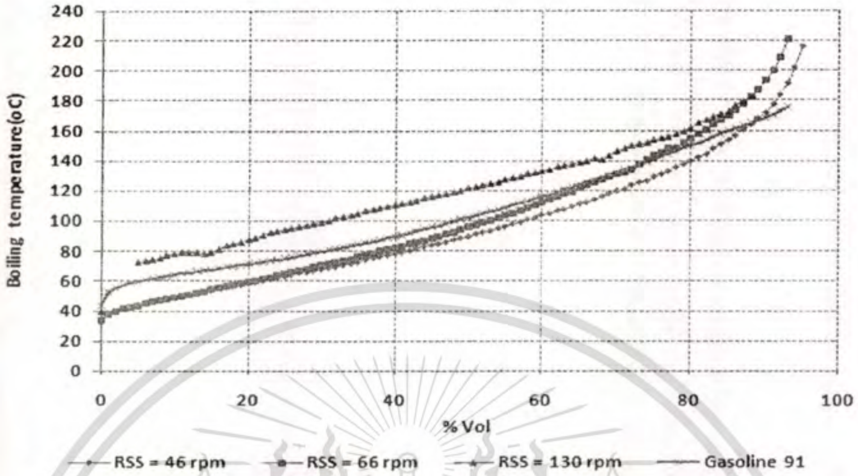

Figure 4.7 The distillation data of liquid products from the reaction using various of the reactor screw speed (RSS).

The liquid products obtained, compose mainly of paraffins, olefins and small aromatics hydrocarbons, as shown in Figure 4.8. It has been known that olefin is considered to be primary cracking products in most catalytic cracking because the β-scission itself ends up with hydrocarbons containing double bond. While paraffins and aromatics are considered to be produced mainly by hydrogen transfer, a secondary reaction of olefins. In addition, aromatization of cracked products leads to formation of aromatics and coke [39]. From the results, it suggests that the hydrogen transfer can be readily promoted by a better heat transfer. This is evidenced by an increase in paraffins content while olefins content is decreased when the reactor screw speed is increased (Figure 4.8). With this, aromatics content is in line with the paraffins content, except that at the reactor screw speed of 130 rpm. This is because additional activity due to thermal cracking does not lead to aromatization of cracked products. Accordingly, the aromatics selectivity in liquid product at the reactor screw speed of 130 rpm is less than that of 66 rpm. It is worth noting that all liquid products from this study, contain much less aromatics content, as compared to commercial gasoline 91.

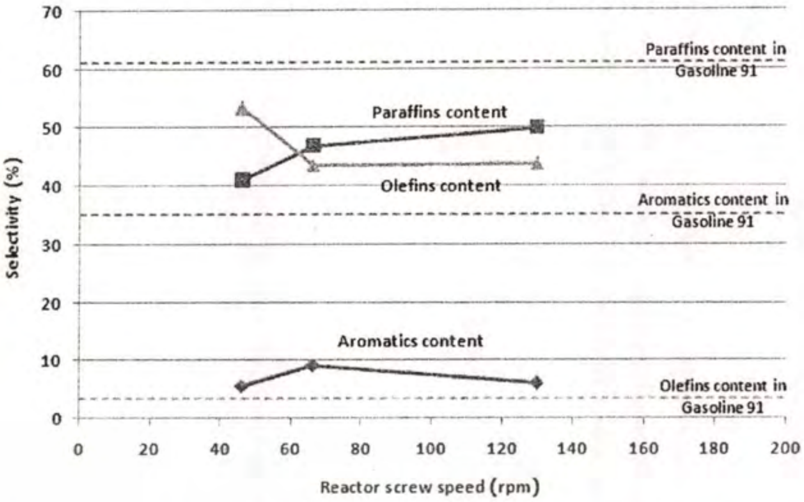

Figure 4.8 The hydrocarbon types of commercial gasoline and liquid products from cracking reaction of polyethylene with different reactor screw speeds (RSS).

Regarding with the quality of the liquid products (Figure 4.9), it can be seen that the octane number was decreased with an increase in the reactor screw speed. This is because the enhanced thermal cracking leads to the formation of saturated linear hydrocarbons. This is consistent with a decrease in olefin and aromatic content, which contribute high octane number. However, the octane number of all liquid products is higher than that commercial gasoline 91.

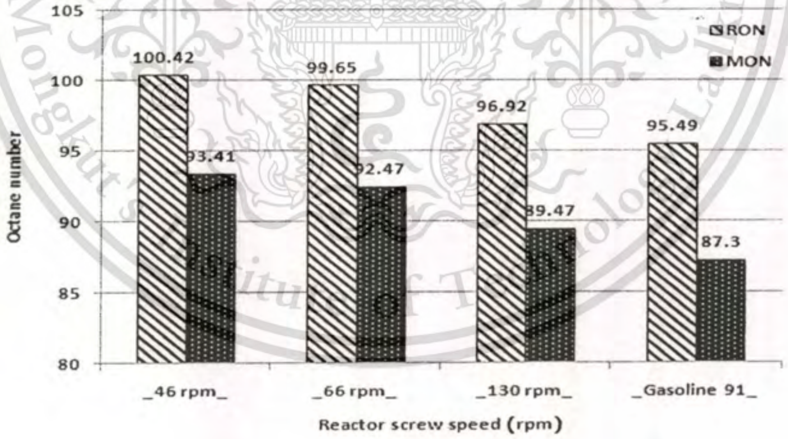

Figure 4.9 The octane number of commercial gasoline and liquid products from cracking reaction of polyethylene with different reactor screw speeds (RSS).

4.4.2 Effect of catalyst content

The catalytic cracking of polyethylene (LDPE 1630J; MFI = 24.6 g/10 min. and viscosity = 4.0 poise) over different catalyst contents were investigated with a constant polymer feeding rate, approximately 600 g/hr using the reactor screw speed of 46 rpm.

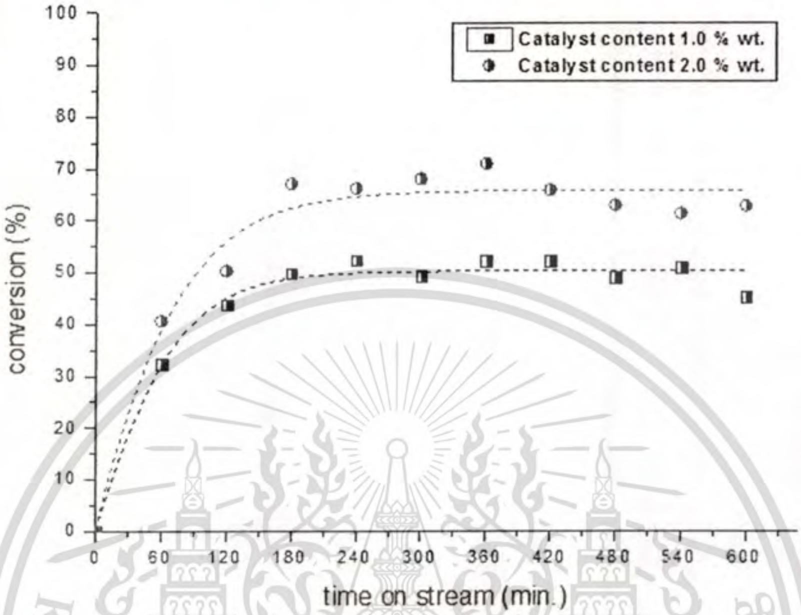

Figure 4.10 Conversion from catalytic cracking of polyethylene (LDPE 1630J; MFI = 24.6 g/10min. and viscosity = 4.0 poise) in continuous process with different the catalyst content as a function of time on stream; reaction conditions: temperature, 430°C; polymer feeding rate, ~600 g/hr; nitrogen 50 ml/min; the reactor screw speed (RSS), 46 rpm.

From Figure 4.10, the results show that an increase in the catalyst loading (from 1 to 2 % wt.) readily increases the conversion. This is because the number of active acid site is proportional to the loading amount of catalyst. Due to the fact that polyethylene molecules are much larger than the pore size of zeolite, the polyethylene chains must be initially cracked both thermally and catalytically by acid sites on the external surface of the zeolite particles. As catalyst content was increased, the external surface area and the number of acid sites at external surface area were increased. Accordingly, the thermal and catalytic cracking of polyethylene chains at external surface can be facilitated producing polyethylene fragments, which are small enough to diffuse into the pores of zeolite [9, 35, 40]. The random cracked products at the chain end and some of polyethylene fragments may leave from the external surface of the zeolite leading to the formation of gas and wax products. The fragments that diffuse into the pores of zeolite, can undergo secondary cracking and over-cracking forming the liquid and gas products, respectively. The cracking pathway can be proposed as in Figure 4.11.

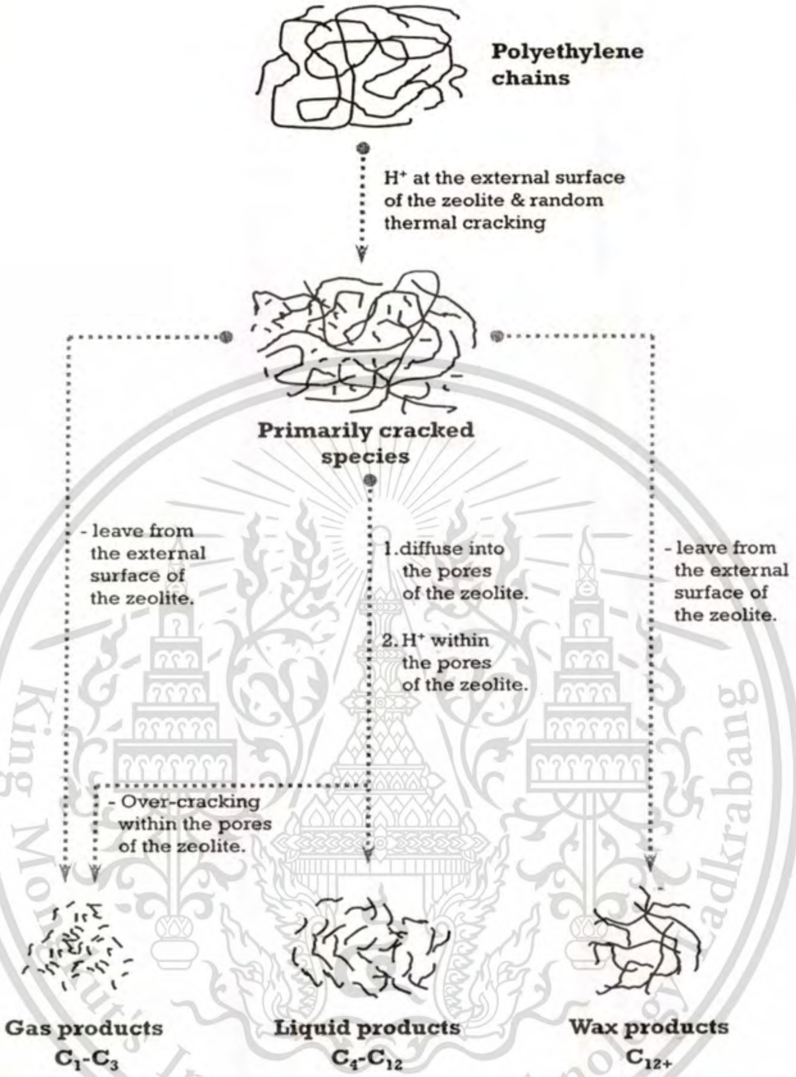

Figure 4.11 Thermal and catalytic cracking of polyethylene chains produce the lower molecular weight hydrocarbons.

Since, the crystal size of zeolite Beta is small (Table 4.1), high external surface area of the catalyst and high catalytic activity can be expected. The small crystal size does not only facilitate the diffusion of those hydrocarbon fragments to the acid sites within the zeolite pores but also help the diffusion of the cracked products out of the pores of the catalyst. This inhibits the over-cracking, particularly at short contact time. Therefore, the molecular weight of products would be mainly controlled within the range of liquid hydrocarbons by the restricted pores size of the catalyst [51].

As the cracking activity was improved by an increase in the catalyst content, the lower molecular weight residue from the reaction using 2.0 % wt. of catalyst content was expected. It can clearly seen that the lower degradation temperature was observed in the residue from reaction with 2.0 % wt. catalyst content, as compared to that with 1.0 %wt. (Figure 4.12).

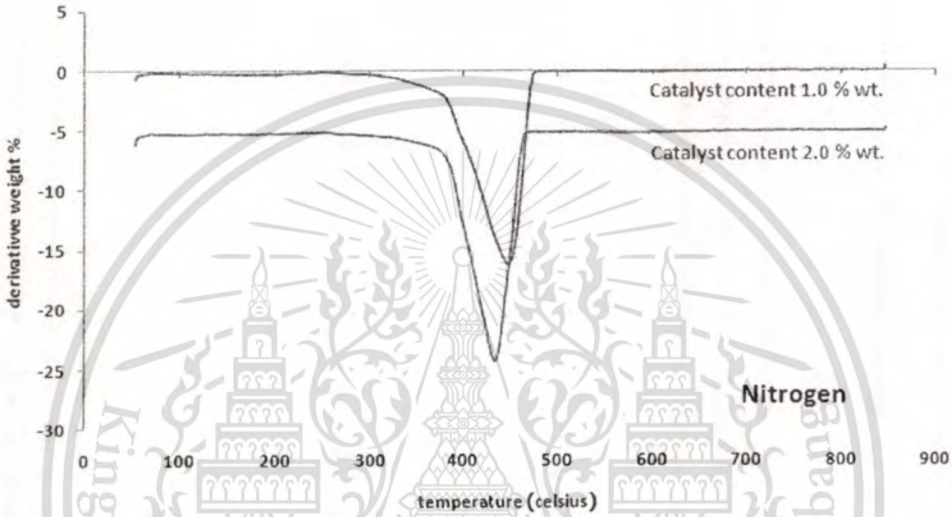

Figure 4.12 The DTG curve of residue from the reaction using different catalyst contents (1.0 and 2.0 wt.)

Table 4.6 Yields and selectivity of liquid products from cracking of polyethylene in continuous process with different catalyst contents (1.0 and 2.0 wt.)

Catalyst content	Yields (%)			Selectivity (%)		
(%wt.)	Liquid	Wax	Gas	Liquid	Wax	Gas
1.0	25.64	12.16	10.61	51.12	24.25	21.15
2.0	35.83	13.29	13.2	54.87	20.35	20.21

In line with an increase in conversion, the more polyethylene fragments can be produced when the catalyst content was increased. Together with an increase in the external surface, such the polyethylene fragments can readily be diffuse and further cracked in the pores of zeolite, in which the molecular weights of the cracked products were limited in the range of liquid product

(C_4-C_{10}). Accordingly, the liquid yield was increased when catalyst content was increased (Table 4.6). With relatively high conversion, more polyethylene fragments may well leave from the surface before entering the pore of zeolite beta. This leads to higher yield of wax products as shown. In addition, the small hydrocarbons fragments that were cracked at the chains end also leave from the surface as gas products. However, as the external surface was readily increased, the large portion of polyethylene fragments would diffuse into the pores rather than leaving from the surface of the zeolite. Hence, the liquid selectivity was increased while the wax and gas selectivity was decreased.

In addition, the shorter polyethylene fragments were probably obtained at reaction using 2.0 % wt. of catalyst loading. This leads to the lower molecular weight of wax product from reaction, using 2.0 % wt. of catalyst, as compared with 1.0 % wt. This was evidenced by the lower T_m and heat of fusion, as shown in Table 4.7.

Table 4.7 The melting temperature and heat of fusion of the wax products from cracking of polyethylene in continuous process with different catalyst contents (1.0 and 2.0 %wt.)

Catalyst (% wt.)	T_m of wax product (°C)	Heat fusion of wax product (J/g)
1.0	85.7	18.1
2.0	83.7	16.3

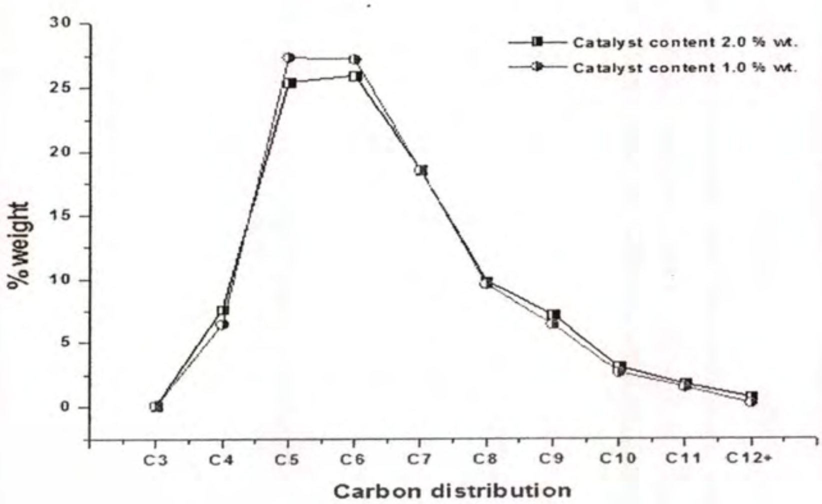

Figure 4.13 The carbon distribution of liquid products from the reaction using various of catalyst content (1.0 and 2.0 wt.)

The carbon distribution of liquid products (Figure 4.13) from cracking reaction were not significantly different for the reaction with various catalyst contents. It is because carbon distribution of liquid product can be controlled by the pore size of zeolite beta, as discussed earlier.

The distillation data suggests that the liquid products from catalytic cracking of polyethylene from reaction with 1 and 2 %wt. of catalyst content are in gasoline fraction (86.0 %vol. of liquid products (Figure 4.14)).

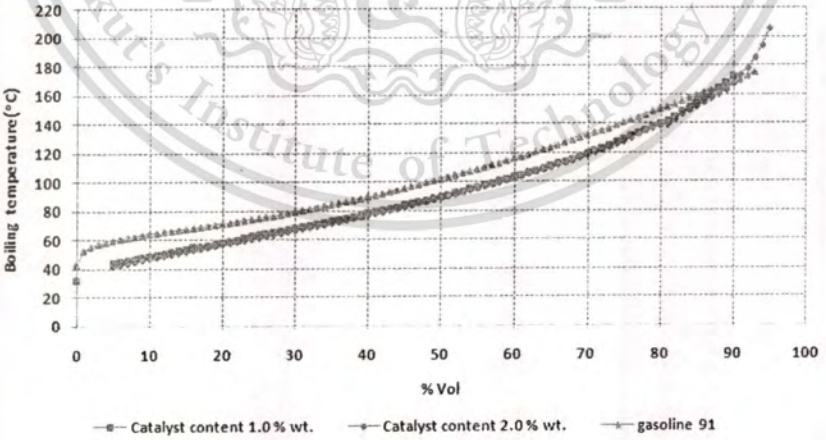

Figure 4.14 The distillation data of liquid products from the reaction with different the catalyst content (1.0 and 2.0 wt.)

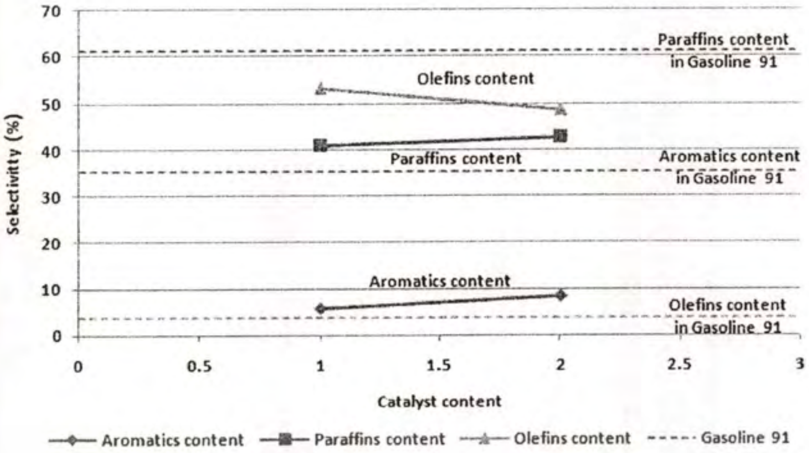

Figure 4.15 The hydrocarbon types of commercial gasoline and liquid products from cracking reaction of polyethylene with different the catalyst contents (1.0 and 2.0 wt.)

The increase in catalyst content does not only promote the secondary cracking of polyethylene fragments to but also oligomerization, aromatization and hydrogen transfer of the cracked products. This is clearly observed by a decrease in olefins content in liquid product while aromatics and paraffins content was increased in the reaction with 2.0 %wt (Figure 4.16). However, this does not significantly affect the octane number (Figure 4.16), presumably because the decrease in olefins content is compensated with an increase in aromatics content. With this, the octane number of all liquid products is still higher than commercial gasoline 91.

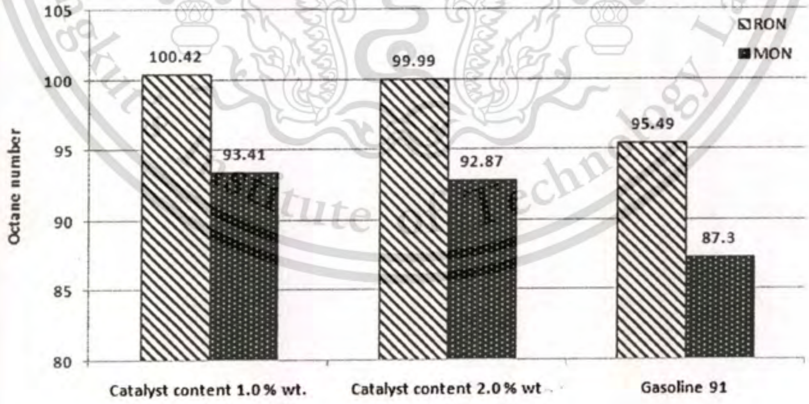

Figure 4.16 The octane number of commercial gasoline and liquid products from cracking reaction of polyethylene with different the catalyst content (1.0 and 2.0 wt.)

4.4.3 Effect of feed rate

The catalytic cracking of polyethylene (LDPE 1630J; MFI = 24.6 g/10 min. and viscosity = 4.0 poise) using various polymer feeding rate (approximately 400 – 800 g/hr.) was investigated.

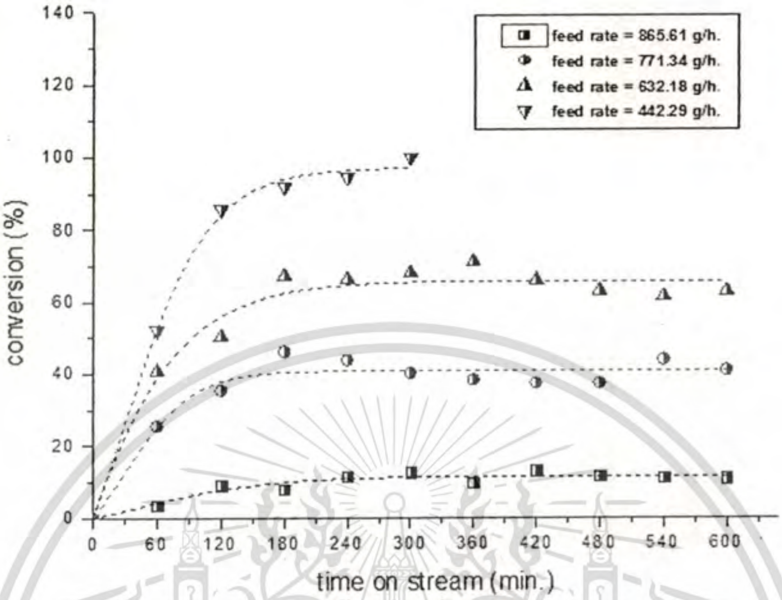

Figure 4.17 Conversion from catalytic cracking of polyethylene (LDPE 1630J; MFI = 24.6 g/10min. and viscosity = 4.0 poise) in continuous process with different feed rates as a function of time on stream; reaction conditions: temperature, 430°C; nitrogen 50 ml/min; the reactor screw speed (RSS), 46 rpm; catalyst content, 2.0 % wt.

From Figure 4.17, it can be seen that a decrease in the feed rate readily increase the conversion. This is because the contact time was increased when the feed rate was decreased. At longer contact time, i.e. low feed rate, a higher opportunity for the polyethylene chains to interact with the external surface of catalyst and further crack within the pores of catalyst in the reactor can be expected. This leads to an extensive cracking and hence higher conversion. However, the feed rate ~400 g/hr, as such provide 100% conversion, cannot be applicable for this system. It can be seen from Figure 4.17 that the reaction can be continuously operated for only 5 hours on steam. This is because the used catalyst cannot be driven out from the bottom end of the reactor since no residue were obtained. Therefore, the reaction cannot be further preceded. It is recommended that the operating conversion should be lower than 90% for this study.

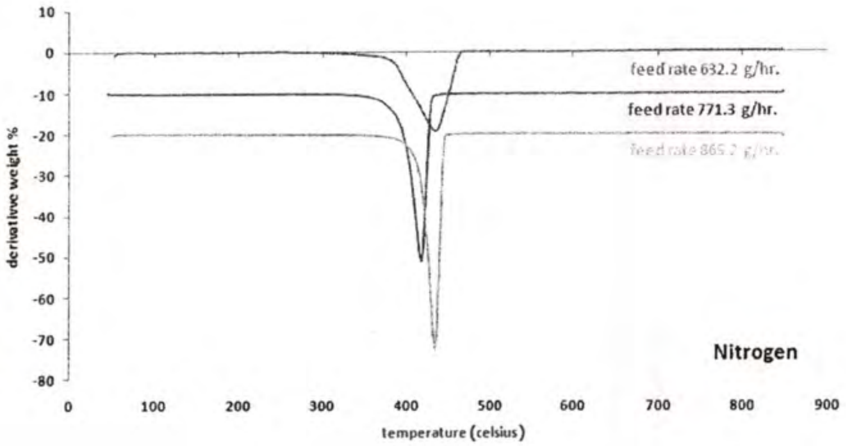

Figure 4.18 The DTG curve of residue from the reaction using different the feed rate

At the longer contact time, the cracking activity was improved by the low feed rate, as discussed previously. Therefore, the DTG of the residue at low feed rate (771.3 g/hr.) shows the lower degradation temperature, as compared with the feed rate 865.2 g/hr. (Figure 4.18). It is suggested that the residue from reaction with lower feed rate (771.3 g/hr.) posses low molecular weight, due to the extensive cracking. However, this is not the case for the feed rate of 632.2 g/hr. In turn, it can be seen that the higher degradation temperature was obtained for this sample despite low feed rate was used. This can be explained by the deactivation of the used catalyst within the residue, as the contact time is exceedingly high.

Table 4.8 Yields and selectivity of liquid products from cracking of polyethylene in continuous process with different feed rate.

Feed rate (g/hr)	Yields (%)			Selectivity (%)		
	Liquid	Wax	Gas	Liquid	Wax	Gas
865.6	3.98	0.25	6.94	35.60	2.24	62.08
771.3	12.67	9.81	18.27	31.09	24.07	44.83
632.2	35.83	13.29	13.20	54.87	20.35	20.21
442.3	62.58	10.21	24.34	64.43	10.51	25.06

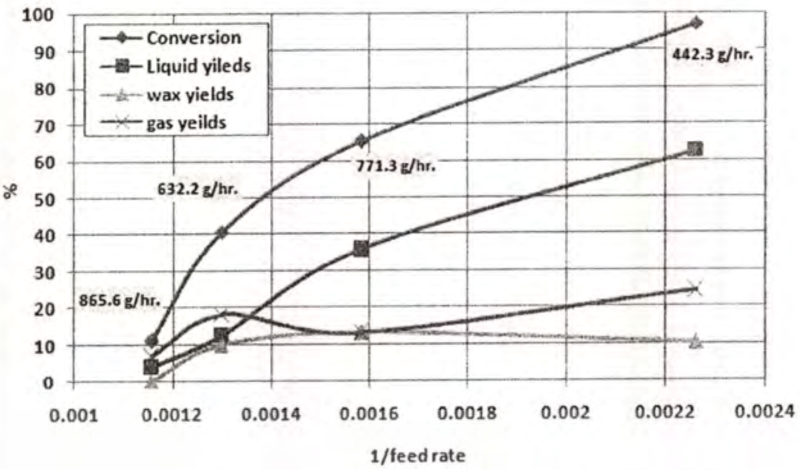

Figure 4.19 Products yields from the reaction using different the feed rate

In consistent with the conversion, liquid yields were increased when the feed rate was decreased (Figure 4.19). This is because the zeolite beta plays important role in cracking reaction. At the high feed rate (865.6 g/hr.), the cracking reaction mainly proceed via thermal pathway since the polyethylene and catalyst were rapidly driven out of the reactor. Only small amount of liquid and gas were observed. However, when the feed rate was decreased to 771.3 g/hr., the wax selectivity was markedly increased (Table 4.8). It is suggested that the cracking of polyethylene chains at external surface of the catalyst was improved by a decrease in the feed rate, leading to the formation of polyethylene fragments. However, such polyethylene fragments may well leave from the external surface, leading to the formation of wax product. This is because the contact time at feed rate of 771.3 g/hr is not appropriately high enough to allow the diffusion of such polyethylene fragments to diffuse and further crack in the pores of zeolite.

Decreasing in feed rate to 632.2 and 442.3 g/hr. readily improves the interaction of polyethylene fragments with the catalyst. Therefore, the primary cracked species easily diffuse into the pores of zeolite, leading to the secondary cracking in the pores of zeolite that limited the molecular weight of cracked species in the range of liquid products (C_4-C_{10}). It can be seen that the liquid yield was increased while wax yield does not significantly change. The exceedingly high contact time can also promoted the over-cracking that leads to the gas formation. Therfore, the gas yield was increased at feed rate of 442.3 g/hr.

Table 4.9 The melting temperature and heat of fusion of the wax products from cracking of polyethylene in continuous process with different polyethylene feed rate.

Feed rate (g/hr.)	T_m of wax product (°C)	Heat fusion of wax product (J/g)
771.3	91.0	18.0
632.2	83.7	16.3
442.3	85.3	13.9

As the cracking activity was improved when the feed rate was decreased, as discussed earlier. Therefore, the wax product from the reaction using the higher contact time possesses lower molecular weight. It is clearly seen that the melting temperature (T_m) and heat of fusion of wax product were decreased when feed rate was decreased, as shown in Table 4.9.

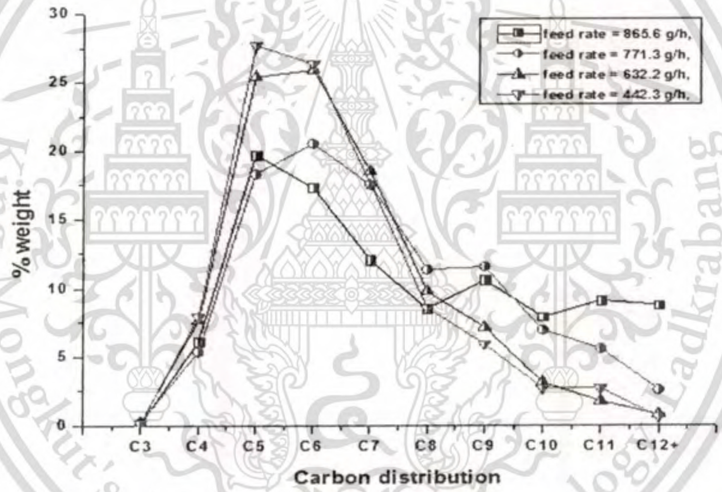

Figure 4.20 The carbon distribution of liquid products from the reaction with different feed rate

The effect of polyethylene feed rate on the carbon distribution of liquid products were shown in Figure 4.20. It can be seen that the carbon distribution at low feed rate (632.2 and 442.3 g/hr.) were significantly different due to the cracking mainly occurred within the pores of the zeolite that can be the molecular weight in the range of liquid products (C_4-C_{10}). In other hand, the carbon distributions were shift to high molecular weight when the contact time was decreased (771.3 and 865.6 g/hr.), i.e. high feed rate. This is because the further cracking within the pores of zeolite was limited by the low contact time.

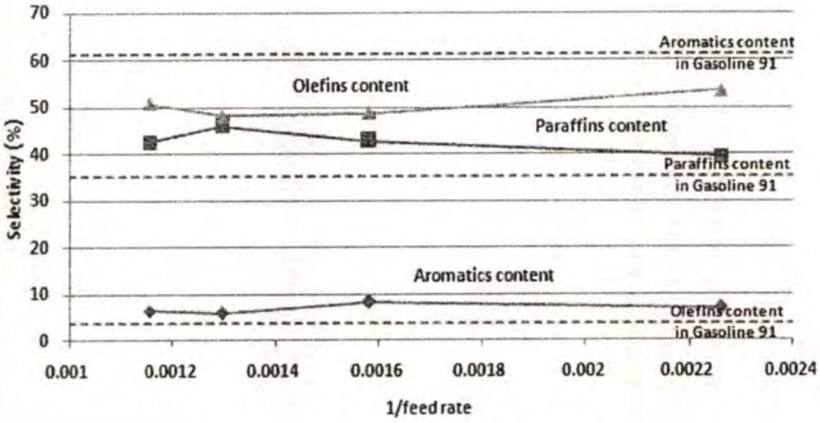

Figure 4.21 The hydrocarbon types of commercial gasoline and liquid products from cracking reaction of polyethylene with different the feed rate.

From Figure 4.21, it can be seen that the feed rate was decreased from 865.6 to 771.3 g/hr., the olefins content was decreased while the paraffins content was increased. This is because the hydrogen transfer, which convert olefins to paraffins, was promoted at high contact time. However, the olefins content was again raised at low feed rate (632.2 and 442.3 g/hr.). It is presumably because the intensive cracking mainly leads to unsaturated hydrocarbons. It can clearly seen that the paraffins content was decreased at 865.6 and 771.3 g/hr. of contact time. In addition, the aromatic content was slightly increased when the contact time was increased. This is because the aromatization of cracked products was also promoted at high contact time.

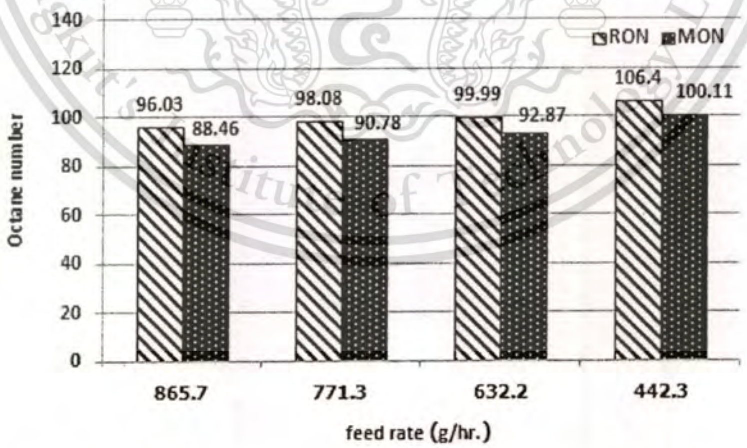

Figure 4.22. The octane number of commercial gasoline and liquid products from cracking reaction of polyethylene with different the feed rate.

In line with an increase in the olefin and aromatics content, the octane number of liquid product were slightly increased when the feed rate was decreased, as shown in Figure 4.22. Due to the formation of olefins and aromatic hydrocarbons was promoted at the high contact time, as discussed previously.

4.4.4 Effect of viscosity of polyethylene fed

The effect of viscosity of polyethylene fed on the catalytic cracking of polyethylene over zeolite beta was investigated with the reactor screw speed of 46 rpm using catalyst content 2.0 %wt and a constant polymer feeding rate, approximately 600 g/hr.

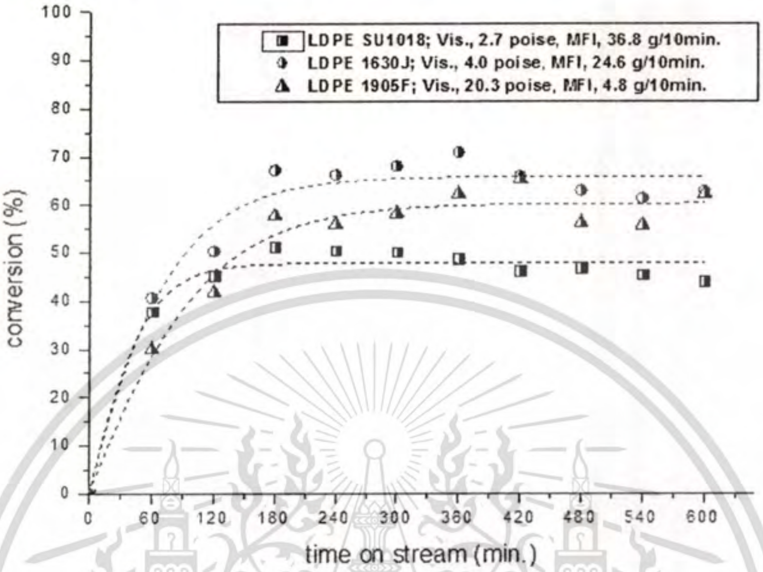

Figure 4.23 Conversion from catalytic cracking of polyethylene with different viscosity in continuous process as a function of time on stream; reaction conditions: temperature, 430$^{\text{o}}$C; the reactor screw speed (RSS), 46 rpm.; catalyst content, 2.0 %wt. ; polymer feeding rate, ~600 g/hr; nitrogen 50 ml/min.

From Figure 4.23, the conversion was increased (from 47.9 to 65.3 %) when the viscosity of polyethylene fed was increased from 2.7 to 4.0 poise. This is because the polyethylene fed with lower viscosity (2.7 poise) can be easily driven out from reactor while that with higher viscosity (4.0 poise) can be retained in the reactor, despite the same feed rate was applied. This is consistent to the melt flow index of polyethylene samples as shown in Table 4.2. However, when the polyethylene with 20.3 poise was used as fed the conversion was decreased (60.30 %). This is due to the high viscosity polyethylene fed possesses high molecular weight which cannot be easily cracked. Although the polymer can be primarily cracked at the external surface, less fraction of cracked intermediates can readily diffuse and further crack in the pore of zeolite beta.

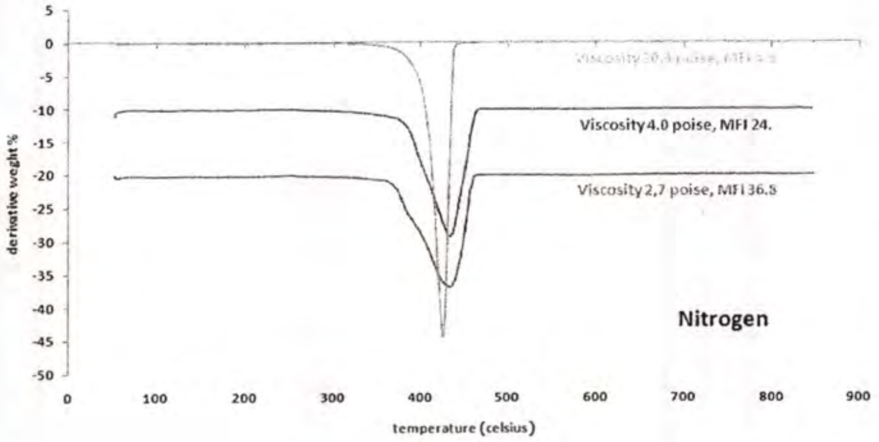

Figure 4.24 The DTG curve of residue from the reaction using polyethylene fed with different viscosities

In consistent with the observed low conversion using the high viscosity polyethylene (20.3 poise) as feed, the catalyst remained in the residue of is still reactive. This is seen by a shape degradation peak at relatively low temperature (Figure 4.24), as compared that of polyethylene fed with lower viscosity (2.7 and 4.0 poise) in which the catalyst have already been deactivated.

Table 4.10 Yields and selectivity of liquid products from cracking reaction in continuous process using polyethylene fed with different viscosities

MFI (g/10min.)	Viscosity (poise)	Yields (%)			Selectivity (%)		
		Liquid	Wax	Gas	Liquid	Wax	Gas
36.8	2.7	25.21	10.65	9.56	52.63	22.23	19.96
24.6	4.0	35.83	13.29	13.20	54.87	20.35	20.21
4.8	20.3	32.78	12.44	12.78	54.36	20.63	21.19

In line with the conversion, the liquid, wax and gas yield was increased when the viscosity polyethylene was increased from 2.7 to 4.0 poise (Table 4.10). This is because the feed with higher viscosity can be readily retained in the reactor. The polyethylene chains can be well interact with the external surface of catalyst and undergo cracking to the lower molecular weight polyethylene fragments. This intermediates can diffuse and were cracked within the pore of zeolite giving mainly liquid and gas products, as discussed previously. As the conversion of 20.3 poise of polyethylene viscosity was low, all product yields were dropped when the polyethylene with 20.3 poise of viscosity was used as feed. Due to the higher molecular weight of polyethylene fed, cracking of the main chain can be limited at both external surface and within the pore of zeolite. Therefore, the polyethylene can be mainly cracked at the chain end and branch via primary random cracking. However, all products selectivity was not significantly changed. This is because the cracking reaction of all polyethylene proceed via the same pathway, despite the molecular weight was increased.

Since, the molecular weight of polyethylene fed is high, the wax product would also possess higher molecular weight as evidenced by an increase in the melting temperature and heat of fusion of the wax products when the viscosity of fed was increased (Table 4.11).

Table 4.11 The melting temperature and heat of fusion of the wax products from cracking of polyethylene in continuous process using polyethylene fed with different viscosity.

MFI of feds (g/10min)	Viscosity of feds (poise)	T_m of wax product (°C)	Heat fusion of wax product (J/g)
36.8	2.7	78.2	15.0
24.6	4.0	83.7	16.3
4.8	20.3	88.1	20.9

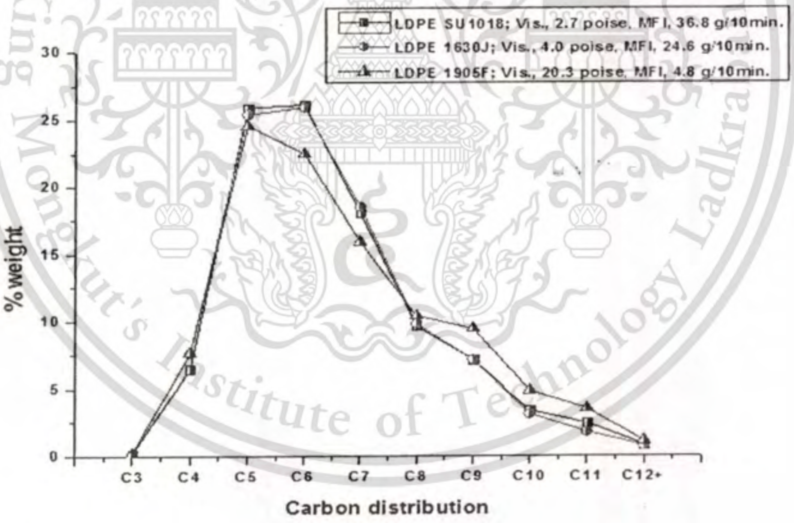

Figure 4.25 The carbon distribution of liquid products from the reaction using polyethylene fed with different viscosity.

As the cracking proceeds predominantly in the pore of zeolite, the carbon distribution of liquid products using polyethylene fed with 2.7 and 4.0 poise of viscosity remains similar (Figure 4.25). In the opposite view, the polyethylene fed with 20.3 poise of viscosity possesses higher molecular weight that the diffusion and secondary cracking in the pore of zeolite was limited.

Hence, the wider carbon distribution was observed. Nevertheless, the distillation data show that the all liquid products are in gasoline fraction (86.0-88.0%vol. of liquid products (Figure 4.26)).

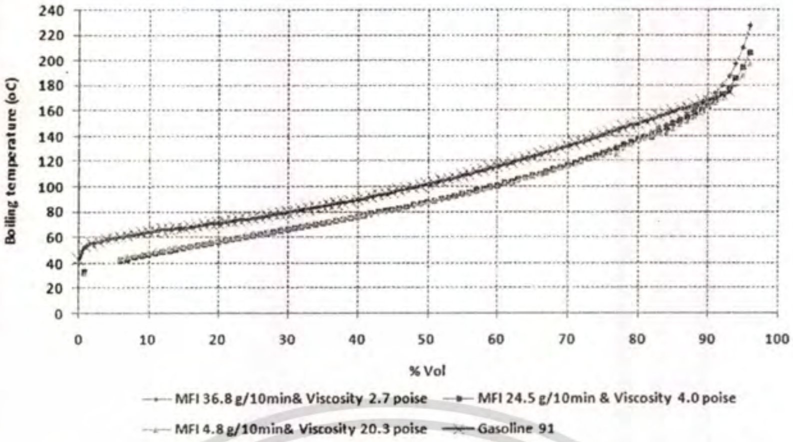

Figure 4.26 The distillation data of liquid products from the reaction using polyethylene fed with different viscosity.

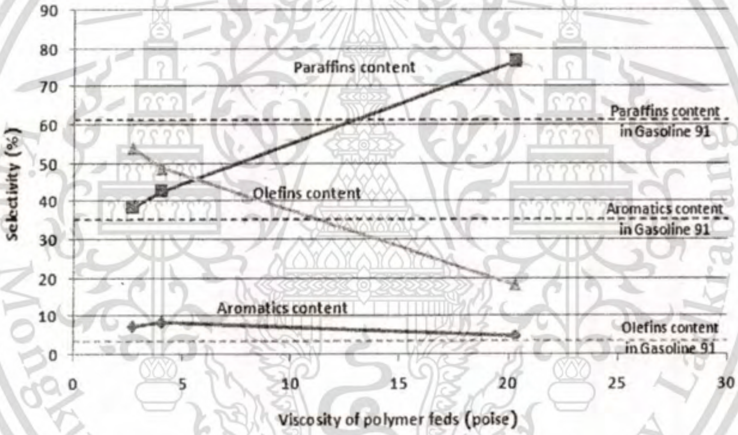

Figure 4.27 The hydrocarbon types of commercial gasoline and liquid products from cracking reaction using polyethylene fed with different viscosity.

As the viscosity of the polyethylene fed was increased, the paraffins and aromatics contents were increased while the olefins content was decreased (Figure 4.27). This is because the random cracking on the external surface of zeolite, would mainly take place in the reaction of feed with increased molecular weight. This leads to an increase in paraffins content, as clearly seen in Figure 4.27. While, the opposite is observed for the olefin content as the β-scission within the pores of zeolite was suppressed. As the aromatics are secondary products, the selectivity depends largely on the reaction severity in the pore of zeolite. Therefore, the trend of aromatics content is observed in a manner similar to that of conversion.

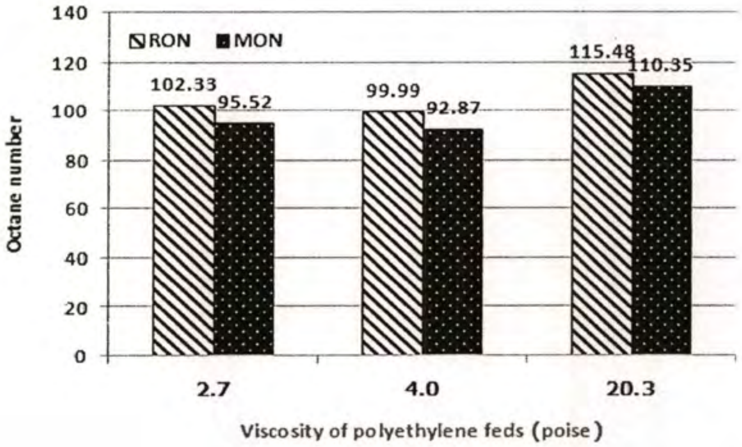

Figure 4.28 The octane number of commercial gasoline and liquid products from cracking reaction using polyethylene fed with different viscosity.

It can seen that the octane number of liquid product was slightly decreased when the polyethylene fed with 4.0 poise of viscosity was used as fed (Figure 4.28). This is because the olefin content that attribute the high octane number was decreased, as discussed above. However, the octane number of 20.3 poise feed is higher than that from low viscosity feed (2.7 and 4.0 poise) despite the olefins and aromatics content was decreased for polyethylene with high viscosity (20.3 poise). This can be attributed to the fact that the branching of liquid products was increased when polyethylene with high viscosity (20.3 poise) was used as feed. With low cracking activity, the reaction would only proceed via stable tertiary carbocation intermediate, leading to the branched hydrocarbons. It is clearly seen in Figure 4.29 that the isoparraffins index of liquid products from polyethylene of 20.3 poise was increased.

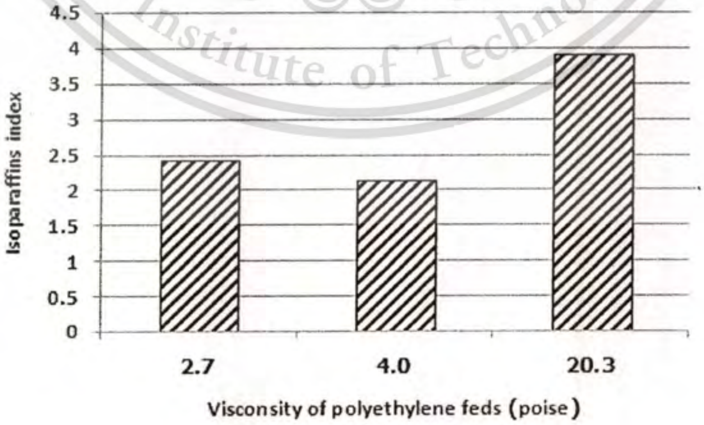

Figure 4.29 Isoparaffins index of liquid products from cracking reaction using polyethylene fed with different viscosity.

CHAPTER 5

CONCLUSION AND SUGGESTION

5.1 Conclusion

In this thesis, the catalytic and thermal cracking of low density polyethylene (LDPE) can be continuously operated without deactivation of catalyst in the design moving bed screw reactor. The polymer melt was continuously fed into the top of the reactor, whilst the residue was driven out of the reactor at the bottom end, together with the spent catalyst. This was collected by a residue chamber in a close system. Nitrogen gas can be used to carry the volatile products out of the reactor into a series of condensers. Catalytic cracking of polyethylene yielded mostly liquid products ranging from 4.0 to 63.0 %wt. The yield of gaseous and wax products was approximately 3.0-24.0, 0.3-16.0 %wt, respectively. The conclusions of the effect of factors in cracking process namely the reactor screw speed (RSS), the catalyst content, polyethylene feed rate and viscosity were reviewed as follows:

1) The cracking activity was improved due to a better heat transfer obtained when the reactor screw speed was increased. However, the severely high reactor screw speed (130 rpm) leads to a thermal cracking that promotes random scission of long chain hydrocarbon via radical intermediate. In this case, the molecular weight of products cannot be readily controlled.
2) An increase in catalyst content does not only increase in cracking activity, but also the higher yield of liquid products. Due to the external surface area and acid sites at the external surface were increased, the primary cracking of polyethylene chains at the external surface can be promoted, producing the polyethylene fragments that are small enough to diffuse into the pores of zeolite. The polyethylene fragments were further cracked within the pores of zeolite beta (~7-8 ^{o}A) that control the molecular weights of the cracked species in the range of liquid product s (C_4-C_{10}).
3) The higher cracking activity was obtained when the contact time was increased, i.e. a decrease in feed rate. The higher opportunities for the polyethylene chains to interact with the external surface of catalyst occur at the high contact time. Therefore, the polyethylene chains can be primarily cracked at the external surface and further cracked within the pores of zeolite beta. However, the extensive high contact time promote the over-cracking leading to the formation of gas products.

4) The cracking activity was increased when the viscosity of polyethylene feeds was increased. This is because the polyethylene fed and catalyst can be retained within the reactor. However, the cracking activity was decreased when the of polyethylene feeds was extensively high viscosity. This is because the polyethylene fed (20.3 poise) possesses exceedingly high molecular weight, producing the polyethylene fragments that are larger than the pores of zeolite beta. Therefore, a fewer fractions of polyethylene fragments can readily diffuse and further crack within the pore of zeolite beta.

In addition, the liquid fuels from this work compose mainly of olefins while the less paraffins and aromatics hydrocarbons. This is results in the higher octane numbers as the commercial gasoline 91. This becomes more important for the next generation of environmental friendly fuel. The optimum operating conditions for highly selective production of gasoline from this thesis are shown as follows;

Optimum operation condition		**Output (from average 8-10 hours on stream)**	
Reactor screw speed (rpm)	46	Liquid yield (%g/g polyethylene)	35.83
Catalyst content (%wt.)	2.0	Wax yield (%g/g polyethylene)	13.20
Polyethylene feed rate (g/hr)	632.2	Residue yield (%g/g polyethylene)	37.67
Carrier gas	Nitrogen	Liquid selectivity (%g/g polyethylene)	57.49
Flow rate (ml/min.)	50.00	Gasoline selectivity (%g/g liquid product)	86.0
Temperature (Celsius)	430	Paraffin content (% vol.)	42.81
Condenser 1, 2, 3 (Celsius)	40, -5, -5	Olefins content (% vol.)	48.83
Extruder temperature (Celsius)	120, 130, 200	Aromatics content (% vol.)	8.37
Conversion (%g/g polyethylene)	65.30	Gas yield (%g/g polyethylene)	13.29
Octane number (RON)		99.99	

5.2 Suggestions

1. In this thesis, the designed single reactor screw was incorporated within the reactor for carrying polyethylene feed with various viscosity and catalyst down though the residue chamber. This promotes the pressure build up within the reactor that lead to trouble operating of continuous process. Therefore, the flight of designed single reactor screw will excessively be noted that allow the large amount of cracked gases can flow to an outlet line at the top of the reactor. In addition, the outlet of cracked products will be enlarged for the cracked products readily flow out of the reactor.

2. The better heat transfer was obtained when the designed single reactor screw was used within the reactor. The exceedingly high temperature within the reactor can be expected leading to thermal cracking pathway. The effect of cracking reaction temperature should be investigated.

3. When the polymer feed with high molecular weights was used, the high yield of wax products was expected. Therefore, the wax separator unit should be developed. The rubber stopper of suction flask was in place of stainless dice that connect to line from wax trap for the wax products could be easily collected.

4. The high quality gasoline in liquid products can be obtained from catalytic cracking in this research. However, all liquid products mainly composed of the olefins which contain the less stability. The hydrogenation and stability of the liquid product should be studied in the future work.

Reference

[1] Aguado J., Serrano D.P., Escola J.M., Garagorri E. and Fernandez J.A. “Catalytic Conversion of Polyolefins into Fuels over Zeolite Beta” **Polymer Degradation and Stability**, vol. 69, 2000. pp.11-16

[2] Derrano D.P., Aguado J., Dscola J.M. and Garagorr E. “Conversion of Low Density Polyethylene into Petrochemical Feedstocks using a Continuous Screw Kiln Reactor ” **Journal of Analytical and Applied Pyrolysis,** vol. 58-59, 2001. pp. 789-801

[3] Grieken R.V., Serrano D.P., Aguado J., Garcia R. and Rojo C. “Thermal and Catalytic Cracking of Polyethylene Under mild Conditions” **Journal of Analytical and Applied Pyrolysis,** vol. 58-59, 2001. pp. 127-142

[4] Jerzy W., Mieczyslaw S. “Thermal and catalytic conversion of waste polyolefines” **Catalysis Today** vol. 65, 2001. pp. 323-330

[5] Seddegi] Z.S., Budrthumal U., Al-Arfaj A.A., Al-Amer A.M. and Barri S.A.I. “Catalytic Cracking of Polyethylene over all-silica MCM-41 Molecular Sieve” **Applied Catalysis A: General,** vol. 225, 2002. pp. 167-176

[6] Park J. W., Kim J. and Seo G. “The Effect of Pore Shape on the Catalytic Performance of Zeolites in the Liquid-phase Degradation of HDPE” **Polymer Degradation and Stability,** vol. 76, 2002. pp. 495-501

[7] Karagoz S., Yanik J., Ucar S., Saglam M. and Song C. “Catalytic and Thermal Degradation of High-Density Polyethylene in Vacuum Gas Oil over Non-Acidic and Acidic catalysts” **Applied Catalysis A: General,** vol. 242, 2003. pp. 51-62

[8] Young Hwa S., Kyong Hwan L., Dae Hyun S. “Investigation of catalytic degradation of high density polyethylene by hydrocarbon group type analysis” **Journal of Analytical and Applied Pyrolysis,** vol. 70, 2003. pp. 383-398

[9] Qian Z., Li Z., Yu Zhong W., Guo Ming Z., Bo W. “Catalytic degradation of low-density polyethylene and polypropylene using modified ZSM-5 zeolites” **Polymer Degradation and Stability**, vol. 84, 2004. pp.493-497

[10] Miskolczi N., Bartha L., Deaka G., Jover B., Kallo D. “Thermal and thermo-catalytic degradation of high-density polyethylene waste ” **Journal of Analytical and Applied Pyrolysis**, vol. 72, 2004. pp. 235-242

[11] Liliana B. Pierella , Soledad R., Oscar A. Anunziata "Catalytic degradation of high density polyethylene over microporous and mesoporous materials" **Microporous and Mesoporous Materials**, vol. 81, 2005. pp. 155-159

[12] Serrano D.P., Aguado J., Vicente G., Sanchez N. "Effects of hydrogen-donating solvents on the thermal degradation of HDPE" **Journal of Analytical and Applied Pyrolysis,** vol. 78, 2006. pp. 194-199

[13] Andras A., Norbert M., Laszlo B. "Petrochemical feedstock by thermal cracking of plastic waste " **Journal of Analytical and Applied Pyrolysis**, 2007.

[14] Aguado J., Serrano D.P., San Miguel G., Castro M.C., Madrid S. "Feedstock recycling of polyethylene in a two-step thermo-catalytic reaction system" **Journal of Analytical and Applied Pyrolysis**, vol. 79, 2006. pp. 415-423

[15] Mosio Mosiewski J., Marek W., Ireneusz M., Tadeusz D. "High-pressure catalytic and thermal cracking of polyethylene" **Fuel Processing Technology** vol. 88, 2007. pp. 359-364

[16] Hajekova E.,Spodova L.,Bajus M.,Mlynkova B. "**Separation and Characterization of Products from Thermal Cracking of Individual and Mixed Polyalkenes**" Faculty of Chemical and Food Technology, Slovak University of Technology, Radlinského 9, SK-812 37 Bratislava, Slovakia. 2007

[17] Marcilla A., Beltran M.I., Navarro R. "Study of the deactivation process of HZSM5 zeolite during polyethylene pyrolysis " **Applied Catalysis A: General**, vol. 333, 2007. pp. 57-66

[18] Serrano D.P., Aguado J., Rodriguez J.M., Peral A. "Catalytic cracking of polyethylene over nanocrystalline HZSM-5: Catalyst deactivation and regeneration study" **Journal of Analytical and Applied Pyrolysis**, vol. 79, 2007. pp. 456-464

[19] Lee K.H., Noh N.S., Shin D.H., Seo Y. "Comparison of plastic types for catalytic degradation of waste plastics into liquid product with spent FCC catalyst" **Polymer Degradation and Stability,** vol. 78, 2002. pp. 539-544

[20] Lin Y.H., Yang M.H., Yeh T.F., Ger M.D. "Catalytic degradation of high density polyethylene over mesoporous and microporous catalysts in a fluidised-bed reactor" **Polymer Degradation and Stability**, vol. 86, 2004. pp.121-128

[21] Nnamso S. A., Karishma G., George M. "Catalytic degradation of plastic waste to liquid fuel over commercial cracking catalystsEffect of polymer to catalyst ratio/acidity content" **Journal of Molecular Catalysis A: Chemical**, vol. 235, 2005. pp.67-73

[22] Salmiaton A., Garforth A. "Waste catalysts for waste polymer " **Waste Management**, 2006

[23] Mastral J.F., Berrueco C., Gea M., Ceamanos J. "Catalytic degradation of high density polyethylene over nanocrystalline HZSM-5 zeolite" **Polymer Degradation and Stability**, vol. 91, 2006. pp.3330-3338

[24] Lin Y.H., Yang M.H. "Catalytic pyrolysis of polyolefin waste into valuable hydrocarbons over reused catalyst from refinery FCC units" **Applied Catalysis A: General**, vol. 328, 2007. pp. 132-139

[25] Masuda T., Kuwahara H., Mukai S. R., Hashimoto K. "Production of high quality gasoline from waste polyethylene derived heavy oil over Ni-REY catalyst in steam atmosphere" **Chemical Engineering Science**, vol. 54, 1999. pp. 2773-2779

[26] Serrano D.P., Aguado J., Escola J.M., Garagorri E. "Performance of a continuous screw kiln reactor for the thermal and catalytic conversion of polyethylene–lubricating oil base mixtures" **Applied Catalysis B: Environmental**, vol. 44, 2003. pp. 95-105

[27] Nishino J., Itoh M., T. Ishinomori T., Kubota N., Uemichi Y. "Development of a catalytic cracking process for converting waste plastics to petrochemicals" **Journal Mater Cycles Waste Manage**, 2003

[28] Adil K., Bilgesu A.Y. "Catalytic and thermal oxidative pyrolysis of LDPE in a continuous reactor system" **Journal of Analytical and Applied Pyrolysis**, vol. 78, 2007. pp. 7-13

[29] Aguado J., Serrano D.P., Escola J.M., Garagorri E. "Catalytic conversion of low-density polyethylene using a continuous screw kiln reactor" **Catalysis Today**, vol. 75, 2002. pp. 257-262

[30] Elordi G., Olazar M., Aguado R., Lopez G., Arabiourrutia M., Bilbao J. "Catalytic pyrolysis of high density polyethylene in a conical spouted bed reactor" **Journal of Analytical and Applied Pyrolysis**, vol. 79, 2007. pp. 450-455

[31] Marcilla A., Gomez Siurana A., Valdes F.J. "Influence of the temperature on the composition of the coke obtained in the catalytic cracking of low density polyethylene in the presence of USY and HZSM-5 zeolites" **Microporous and Mesoporous Materials**, vol. 109, 2008. pp. 420-428

[32] Marcilla A., Garcıa Quesada J.C., Sanchez S., Ruiz R. "Study of the catalytic pyrolysis behaviour of polyethylene–polypropylene mixtures" **Journal of Analytical and Applied Pyrolysis**, vol. 74, 2005. pp. 387-392

[33] Aguado J., Serrano D.P, San Miguel G., Escola J.M., Rodrıguez J.M. "Catalytic activity of zeolitic and mesostructured catalysts in the cracking of pure and waste polyolefins" **Journal of Analytical and Applied Pyrolysis**, vol. 78, 2007. pp. 153-161

[34] Marcilla A., Ruiz Femenia R., Hernandez J., Garcıa Quesada J.C. "Thermal and catalytic pyrolysis of crosslinked polyethylene" **Journal of Analytical and Applied Pyrolysis**, vol. 76, 2006. pp. 254-259

[35] Sinfrônio1 F. S. M., Souza1 A. G., Ieda M. G. Santos1, Fernandes V. J. Jr.2, Cs. Novák and Zsuzsanna Éhen "Influence of H-ZSM-5, Al-MCM-41 and acid hybrid ZSM-5/MCM-41 on polyethylene decomposition" **Journal of Thermal Analysis and Calorimetry**, vol. 85, 2006. pp. 391-399

[36] Marcilla A., Gomez Siurana A., Valdes F. "Catalytic cracking of low-density polyethylene over H-Beta and HZSM-5 zeolites: Influence of the external surface. Kinetic model" **Polymer Degradation and Stability**, vol. 92, 2007. pp. 197-204

[37] Marcilla A., Gomez Siurana A., Berenguer D. "Study of the early deactivation in pyrolysis of polymers in the presence of catalysts" **Journal of Analytical and Applied Pyrolysis**, 2007.

[38] Jerzy Walendziewski "Continuous flow cracking of waste plastics" **Fuel Processing Technology**, vol. 86, 2005, pp. 1265– 1278

[39] Mark E. Myers, Jr., Janis Stollstelmer, and Andrew M. Wims "Determination of Hydrocarbon-Type Distribution' and Hydrogen-Carbon Ratio of Gasolines by Nuclear Magnetic Resonance Spectrometry" Research Laboratories, General Motors Technical Center, 12 Mile and Mound Rds, Warren, Mich. 48090

[40] Jeong-Geol Na · Byung-Hwan Jeong · Soo Hyun Chung Seong-Soo Kim " Pyrolysis of low-density polyethylene using synthetic catalysts produced from fly ash" **J Mater Cycles Waste Manag**, vol 8, 2006, pp. 126-132

[41] Juan Angel Botas, Mónica Bravo, José María Escola Pablo García "Catalytic upgrading of higher 1-alkenes from polyethylene thermal crackingby modified Wacker oxidation" **J Mater Cycles Waste Manag** , vol 8, 2006, pp.122–125

[42] J. Agullo, N. Kumar, D. Berenguer, D. Kubicka, A. Marcilla, A. Gómez "Catalytic Pyrolysis of Low Density Polyethylene over Hb, H-Y, H-Mordenite, and H-Ferrierite Zeolite Catalysts: Influence of Acidity and Structures" **Kinetics and Catalysis**, 2007, Vol. 48, No. 4, pp. 535–540.

[43] L. Soják, R. Kubinec, H.Jurdáková, E. Hájeková, M. Bajus "GC-MS OF POLYETHYLENE AND POLYPROPYLENE THERMAL CRACKING PRODUCTS" **Petroleum & Coal** vol 48 (1), 2006, pp.1-14.

[44] Siauw H. "Conversion of Polyethylene to Transportation Fuels through Pyrolysis and Catalytic Cracking" Energy & Fuels ,vol 9, 1995, pp.735-742.

[45] A. Dutta "On viscosity - melt flow index relationship" Polymer Science and Engineering Group, Chemical Engineering Division, National Chemical Laboratory, Pune (India)

[46] G. Elordi, M. Olazar *, G. Lopez, M. Amutio, M. Artetxe, R. Aguado, J. Bilbao "Catalytic pyrolysis of HDPE in continuous mode over zeolite catalysts in a conical spouted bed reactor" **J. Anal. Appl. Pyrolysis,** 2009

[47] Ali Sınagˇ,* Melike Sungur, Mustafa Gu¨llu¨, and Muammer Canel "Characterization of the Liquid Phase Obtained by Copyrolysis of Mustafa Kemal Pasüa (M.K.P.) Lignite (Turkey) with Low Density Polyethylene" **Energy & Fuels** 2006, vol 20 ,pp. 2093-2098

[48]Chaiwat Tachakritikul **"Synthetic Fuels from Cracking of Polyethylene using Zeolite Catalysts in Batch and Continuous Processes"** Thesis of Mater Degree of Petrochemicals and Hydrocarbon Chemistry Program, Faculty of Science, King Mongkut's Institute of Technology Ladkrabang. 2001

[49] Teerawat Chalermsuksri "**Synthetic Fuels from Cracking of Polyethylene Waste using Zeolite Beta Catalyst in Continuous Process**" Thesis of Mater Degree of Petrochemicals and Hydrocarbon Chemistry Program, Faculty of Science, King Mongkut's Institute of Technology Ladkrabang. 2005

[50] Dyer A. **An Introduction to Zeolite Molecular Sieves.** New York : John Wiley & Son, Inc. 1998

[51] Bruce C. G. **Catalytic Chemistry.** New York : John Wiley & Sons, Inc. 1992

[52] Olah G.A. and Molnar A. **Hydrocarbon Chemistry**. New York : John Wiley & Son, Inc. 1995

[53] Nelson W.L. **Petroleum Refinery Engineering.** 4th Ed., New York : Megraw-Hill book

company. 1985

[54] Wittcoff H.A. and Reaben B.G. **Industrial Organic Chemicals.** New York : John Wiley & Sons, Inc. 1996

[55] Bockhorn H., Hentschel J., Hornmg A. and Hornung U. "Environmental Engineering: Stepwise Pyrolysis of Plastic Waste" **Chemical Engineering Science**, vol. 54, 1999. pp. 3043-3051

[56] Lebeder N.N. **Chemistry and Technology of Basic Organic and Petrochemical Systhesis**. vol. 1, Moacow : MIR. 1984

[57] Speight J.G. **Fuel Science and Technology Handbook**. New York : Marcel Dekker. 1990

[58] Hatch L.F. and Matar S. **From Hydrocarbons to Petrochemicals**. Huston : Gulf Publishing Company Book Division. 1991

[59] Maxwell I.E. and Stork W.H.J. "Introduction to Zeolite Science and Practice" **Studies in Surface science and catalysts,** vol. 58, 1991. pp. 571-579

[60] Speight J.G. **The Chemistry and Technology of Petroleum,** 3rd Ed., New York : Marcel Dekker. 1999

[61] Newsam J.M. "Structural Characterization of Zeolite Beta." [Online]. Available : http://iza-sc.ithz.ch/IZA-SC/Atlas/data/models/BEA_mod.html. 1999

[62] Shenoy A. V.,. Saini D. R "Advances in Polymer Technology:" [Online] http://en.wikipedia.org/wiki/Polyethylene

[63] "A Guide to IUPAC Nomenclature of Organic Compounds, Blackwell Scientific Publications, Oxford (1993)" [Online] http://en.wikipedia.org/wiki/Melt_Flow_Index

[64] G. Manos, A. Garforth, J. Dwyer, Ind. Eng. Chem. Res. 39 (2000) 1203.

[65] G. Manos, A. Garforth, J. Dwyer, Ind. Eng. Chem. Res. 39 (2000) 1198.

[66] G. Manos, Y.I. Yusof, N. Papayannakos, H.N. Gangas, Ind. Eng.Chem. Res. 40 (2001) 2220.

[67] G. Manos, Y.I. Yusof, N. Papayannakos, H.N. Gangas, Energy Fuels16 (2002) 485.

[68] K. Gobin, G. Manos, Polym. Degrad. Stab. 83 (2004) 267.

[69] Vasile C, Onu P, Barboiu V, Sabliouschi M, Moroi G. Acta Polym 1985;36(10):543.

[70] Ivanova SR, Gumerova EF, Minsker KS, Zaikov GE, Berlin AA. Prog Polym Sci 1990;15:193.

[71] Songip AR, Masuda T, Kuwahara M, Hashimoto K. Energy & Fuels 1994;8:136.

[72] www.nhn.ou.edu/~bumm/NanoLab/ppt/X-ray_Diffraction.ppt

APPENDICES

APPENDIX A

Melt flow index of low-density polyethylene

Table A.1 Calculation of melt flow index of low-density polyethylene

LDPE SU1018			LDPE 1630J			LDPE 1905F		
times	g/min.	g/10min.	times	g/min.	g/10min.	times	g/min.	g/10min.
1	3.84	38.4	1	2.38	23.8	1	0.49	4.9
2	3.78	37.8	2	2.49	24.9	2	0.48	4.8
3	3.42	34.2	3	2.43	24.3	3	0.48	4.8
4	3.69	36.9	4	2.53	25.3	4	0.48	4.8
average		36.8±1.86	average		24.6±0.66	average		4.8±0.05

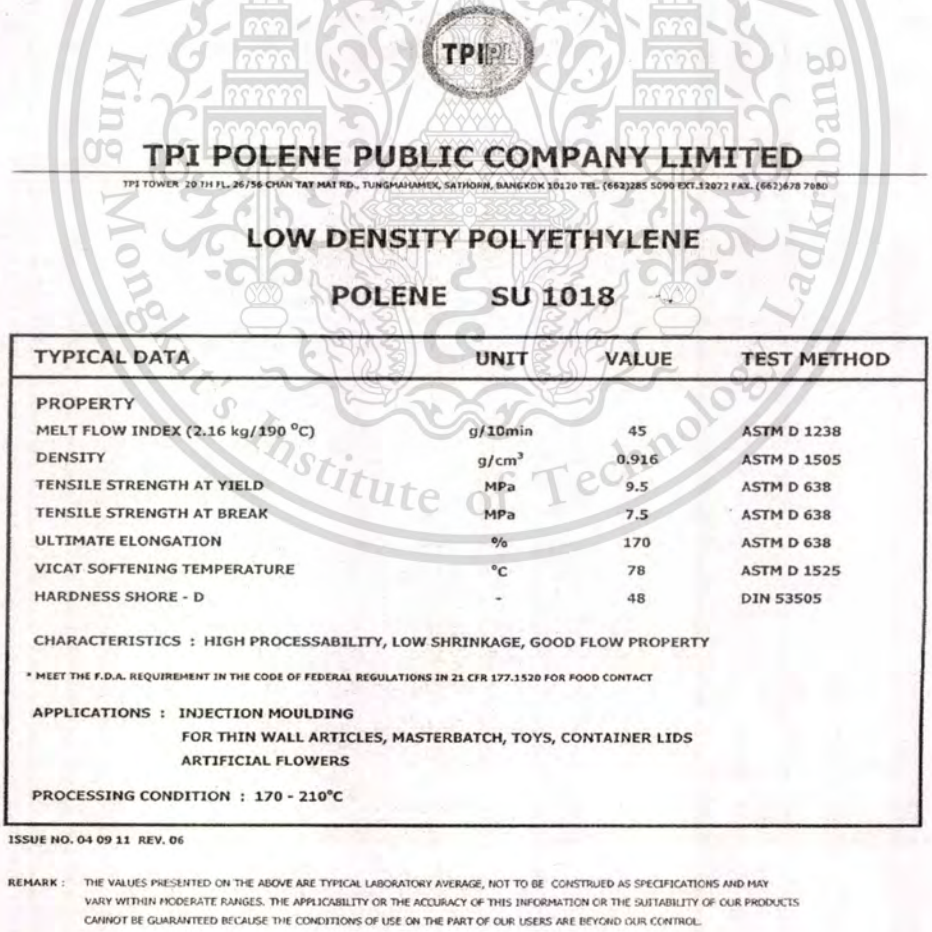

TPI

TPI POLENE PUBLIC COMPANY LIMITED

TPI TOWER 20 TH FL. 26/56 CHAN TAT MAI RD., TUNGMAHAMEK, SATHORN, BANGKOK 10120 TEL. (662)285 5090 EXT.12072 FAX. (662)678 7080

LOW DENSITY POLYETHYLENE

POLENE SU 1018

TYPICAL DATA	UNIT	VALUE	TEST METHOD
PROPERTY			
MELT FLOW INDEX (2.16 kg/190 °C)	g/10min	45	ASTM D 1238
DENSITY	g/cm^3	0.916	ASTM D 1505
TENSILE STRENGTH AT YIELD	MPa	9.5	ASTM D 638
TENSILE STRENGTH AT BREAK	MPa	7.5	ASTM D 638
ULTIMATE ELONGATION	%	170	ASTM D 638
VICAT SOFTENING TEMPERATURE	°C	78	ASTM D 1525
HARDNESS SHORE - D	-	48	DIN 53505

CHARACTERISTICS : HIGH PROCESSABILITY, LOW SHRINKAGE, GOOD FLOW PROPERTY

* MEET THE F.D.A. REQUIREMENT IN THE CODE OF FEDERAL REGULATIONS IN 21 CFR 177.1520 FOR FOOD CONTACT

APPLICATIONS : INJECTION MOULDING
FOR THIN WALL ARTICLES, MASTERBATCH, TOYS, CONTAINER LIDS
ARTIFICIAL FLOWERS

PROCESSING CONDITION : 170 - 210°C

ISSUE NO. 04 09 11 REV. 06

REMARK : THE VALUES PRESENTED ON THE ABOVE ARE TYPICAL LABORATORY AVERAGE, NOT TO BE CONSTRUED AS SPECIFICATIONS AND MAY VARY WITHIN MODERATE RANGES. THE APPLICABILITY OR THE ACCURACY OF THIS INFORMATION OR THE SUITABILITY OF OUR PRODUCTS CANNOT BE GUARANTEED BECAUSE THE CONDITIONS OF USE ON THE PART OF OUR USERS ARE BEYOND OUR CONTROL.

Figure A.1 Data sheet of LDPE SU1018

บริษัท ไทยโพลิเอททีลีน จำกัด
THAI POLYETHYLENE CO.,LTD.

TEST CERTIFICATE

CERTIFICATE NO : QC0-CLD1-504200	DATE : 26/11/2007 PAGE : 1 / 1
PRODUCT : LD1630J	LOT NO : 0C461361
SAMPLE RECEIVING DATE : 18/11/2007	SAMPLE NO : 643600
PURCHASE ORDER NO : ____________	TEST DATE : 18/11/2007
INVOICE NO : ____________	AMOUNT : 3.000 TONS
DATE SHIPPED : ____________	PACKAGES : 0025 Kg

SAMPLE CHARACTERISTIS AND CAONDITION : White Pellet
CUSTOMER NAME AND ADDRESS : ไกลบอล คอนเน็กชั่นส์ (บมจ.)
13/1 หมู่ 2 ถนนกิ่งแก้ว ตำบลราชาเทวะ อำเภอบางพลี สมุทรปราการ 10540

L/C NO.
OF

TEST ITEM	UNIT	TEST RESULT	+/- U	TEST METHOD
MELT FLOW RATE AT 190 C/2.16KG	g/10min	28	2.2	ASTM D 1238
DENSITY	g/cm3	0.917	0.0008	ASTM D 1505

(Siripun Poorinutpong)
LABORATORY MANAGER
Date 19/11/2007

* Density : Sample was controlled at 120 +/-0.5C for 1 hour, cooled down with rate 1.5 C/min until 30 C

The above results are valid only for the analyzed / tested sample(s) as indicated in the report
The reported uncertainty of measurement was based upon standard uncertainty multiplied by a coverage factor K = 2, providing a level of confidence of approximately 95%
This certificate may not be reproduced except in full unless permission for the reproduction has been given in writing from the laboratory

QC-F-0782 - Rev.011

Figure A.2 Data sheet of LDPE 1630J

บริษัท ไทยโพลิเอททีลีน จำกัด
THAI POLYETHYLENE CO.,LTD.

TEST CERTIFICATE

CERTIFICATE NO : QC0-CLD1-520366
PRODUCT : LD1905F
SAMPLE RECEIVING DATE : 07/02/2009
PURCHASE ORDER NO : ____________
INVOICE NO : ____________
DATE SHIPPED : ____________

DATE : 12/02/2009 PAGE : 1/ 1
LOT NO : 2C060119
SAMPLE NO : 769692
TEST DATE : 08/02/2009
AMOUNT : 5.950 TONS
PACKAGES : 0025 Kg

SAMPLE CHARACTERISTIS AND CAONDITION : White Pellet
CUSTOMER NAME AND ADDRESS : โกลบอล คอนเน็คชั่นส์ (บมจ.)
13/1 หมู่ 2 ถนนกิ่งแก้ว ตำบลราชาเทวะ อำเภอบางพลี สมุทรปราการ 10540

L/C NO.
OF

TEST ITEM	UNIT	TEST RESULT	+/- U	TEST METHOD
MELT FLOW RATE AT 190 C/2.16KG	g/10min	5.1	0.47	ASTM D 1238
DENSITY	g/cm3	0.919	0.0008	ASTM D 1505

(Siripun Poorinutpong)
LABORATORY MANAGER
Date 08/02/2009

* Density : Sample was controlled at 120 +/-0.5C for 1 hour, cooled down with rate 1.5 C/min until 30 C

The above results are valid only for the analyzed / tested sample(s) as indicated in the report
The reported uncertainty of measurement was based upon standard uncertainty multiplied by a coverage factor K = 2, providing a level of confidence of approximately 95%
This certificate may not be reproduced except in full unless permission for the reproduction has been given in writing from the laboratory

QC-F-0782 - Rev.011

Figure A.3 Data sheet of LDPE 1905F

APPENDIX B

X-RAY DIFFRACTION OF STANDARD PATTERN

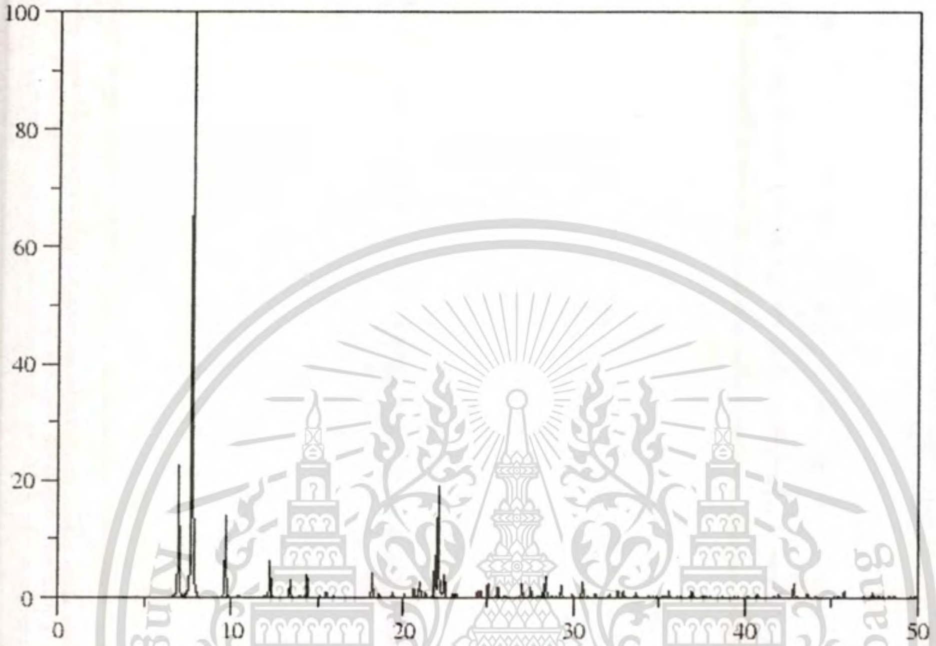

Figure B.1 X-ray diffraction pattern of standard Beta

APPENDIX C

REACTION DATA

Table C.1 The average conversion, yield of products and selectivity of liquid product from cracking of polyethylene in continuous process at 430 °C under nitrogen flow

Run	Viscosity of feds (poise)	MFI of feds (g/10min)	RSS (rpm)	Catalyst content (%wt.)	Feed rate (g/hr.)	Conversion	Liquid yield	Wax yield	Gas yield	Selectivity
1	4.0	24.6	130	1.0	633.8	60.22	33.73	15.39	6.71	60.41
2	4.0	24.6	66	1.0	635.6	55.35	36.41	15.87	3.07	65.78
3	4.0	24.6	46	1.0	639.5	50.15	25.63	12.17	10.61	53.01
4	4.0	24.6	46	2.0	632.2	65.30	35.83	13.2	13.29	57.49
5	4.0	24.6	46	2.0	442.3	97.13	62.58	10.21	24.34	64.29
6	4.0	24.6	46	2.0	771.3	12.67	12.67	9.81	18.27	31.03
7	4.0	24.6	46	2.0	865.6	3.98	3.98	0.25	6.94	35.67
8	20.3	4.8	46	2.0	607.7	60.30	32.78	12.44	12.78	56.58
9	2.7	36.8	46	2.0	639.9	47.90	25.22	10.65	9.56	55.52

Table C.2 The melting temperature and heat of fusion of the wax products from cracking of polyethylene in continuous process

Run	Viscosity of feds (poise)	MFI of feds (g/10min)	RSS (rpm)	Catalyst content (%wt.)	Feed rate (g/hr.)	Tm of wax product (^{o}C)	Heat fusion of wax product (J/g)
1	4.0	24.6	130	1.0	633.8	83.5	12.9
2	4.0	24.6	66	1.0	635.6	84.1	13.9
3	4.0	24.6	46	1.0	639.5	85.7	18.1
4	4.0	24.6	46	2.0	632.2	83.7	16.3
5	4.0	24.6	46	2.0	442.3	85.3	13.9
6	4.0	24.6	46	2.0	771.3	91.0	18.0
7	20.3	4.8	46	2.0	607.7	88.1	20.9
8	2.7	36.8	46	2.0	639.9	78.3	15.0

Table C.3 All products weight from cracking reaction of polyethylene at 430 ^{o}C under nitrogen flow

Reaction time on stream (min.)	Furnace temperature (^{o}C)	Polyethylene feed (g/hr.)	Weights (g)							Conversion
			Liquid products					Wax products	Residue	
			Fraction I	Fraction II	Fraction III	Fraction IV	Totals			
0	300	688.8	0.00	0.00	0.00	0.00	0.00	-	680.62	0.00
60	430	633.8	3.18	52.01	0.04	1.47	56.70	-	354.50	44.07
120	430	633.8	6.30	110.30	0.30	0.00	116.90	-	285.87	54.90
180	430	633.8	56.01	133.00	0.47	3.21	192.69	-	230.65	63.61
240	430	633.8	131.34	110.87	0.54	1.39	244.14	-	249.06	60.70
300	430	633.8	128.29	104.47	0.58	3.19	236.53	-	225.13	64.48
360	430	633.8	129.91	101.53	0.50	0.46	232.40	-	243.73	61.55
420	430	633.8	139.14	103.70	0.51	1.40	244.75	-	228.78	63.90
480	430	633.8	120.31	93.73	0.47	2.73	217.24	97.53	273.19	56.90
540	430	633.8	119.37	89.00	0.51	3.01	211.89	97.53	282.13	55.49
600	430	633.8	119.27	90.15	0.49	2.25	212.16	97.53	284.60	55.10

Reaction parameters; reactor screw speed, **130** rpm; catalyst content, 1.0 %wt.; polyethylene feed rate, 633.8 g/hr.; viscosity of polyethylene feed, 4.0 poise.

Table C.4 All products weight from cracking reaction of polyethylene at 430 °C under nitrogen flow

Reaction time on stream (min.)	Furnace temperature (°C)	Polyethylene feed (g/hr.)	Weights (g)							Conversion
			Liquid products					Wax products	Residue	
			Fraction I	Fraction II	Fraction III	Fraction IV	Totals			
0	300	699.6	0.00	0.00	0.00	0.00	0.00	-	709.75	0.00
60	430	635.6	42.34	41.67	0.00	0.00	84.01	-	398.41	37.32
120	430	635.6	6.78	80.04	0.88	1.68	89.38	-	325.48	48.80
180	430	635.6	4.89	71.13	0.42	0.57	77.01	-	256	59.72
240	430	635.6	4.14	62.92	0.59	1.09	68.74	-	298.76	52.99
300	430	635.6	162.00	48.50	0.43	1.32	212.25	-	305.1	52.00
360	430	635.6	141.54	60.57	0.57	1.50	204.18	-	288.05	54.68
420	430	635.6	148.64	78.16	0.35	1.30	228.45	-	276.96	56.42
480	430	635.6	154.26	82.54	0.49	1.26	238.55	100.88	272.96	57.05
540	430	635.6	151.96	75.95	0.42	1.26	229.59	100.88	285.60	55.07
600	430	635.6	149.50	74.00	0.39	2.21	226.10	100.88	292.80	53.93

Reaction parameters; reactor screw speed, **66** rpm; catalyst content, 1.0 %wt.; polyethylene feed rate, 635.6 g/hr.; viscosity of polyethylene feed, 4.0 poise.

Table C.5 All products weight from cracking reaction of polyethylene at 430 ^{o}C under nitrogen flow

Reaction time on stream (min.)	Furnace temperature (^{o}C)	Polyethylene feed (g/hr.)	Weights (g)							Conversion
			Liquid products					Wax products	Residue	
			Fraction I	Fraction II	Fraction III	Fraction IV	Totals			
0	300	660.6	0.00	0.00	0.00	0.00	0.00	-	614.16	0.00
60	430	639.5	2.29	24.75	0.03	8.39	35.46	-	432.72	32.33
120	430	639.5	4.24	68.01	0.26	10.31	82.82	-	358.84	43.88
180	430	639.5	4.66	68.76	0.30	10.85	84.57	-	320.97	49.81
240	430	639.5	5.15	75.20	0.39	12.74	93.48	-	304.98	52.31
300	430	639.5	31.00	71.11	0.39	12.24	114.74	-	324.12	49.31
360	430	639.5	81.65	73.16	0.37	15.13	170.31	-	306.32	52.10
420	430	639.5	82.11	73.91	0.38	14.66	171.06	-	306.31	52.10
480	430	639.5	81.09	70.30	0.38	12.60	164.37	77.82	325.69	49.07
540	430	639.5	84.07	71.92	0.43	12.99	169.41	77.82	313.55	50.97
600	430	639.5	66.94	75.00	0.56	15.59	158.09	77.82	350.28	45.22

Reaction parameters; reactor screw speed, **46** rpm; catalyst content, 1.0 %wt.; polyethylene feed rate, 639.5 g/hr.; viscosity of polyethylene feed, 4.0 poise.

Table C.6 All products weight from cracking reaction of polyethylene at 430 ^{o}C under nitrogen flow

Reaction time on stream (min.)	Furnace temperature (°C)	Polyethylene feed (g/hr.)	Weights (g)							Conversion
			Liquid products					Wax products	Residue	
			Fraction I	Fraction II	Fraction III	Fraction IV	Totals			
0	300	687.9	0.00	0.00	0.00	0.00	0.00	-	672.09	0.00
60	430	632.2	1.99	40.53	0.1	9.47	52.09	-	375.14	40.66
120	430	632.2	3.88	108.9	0.33	5.99	119.1	-	314.28	50.29
180	430	632.2	5.74	115.81	0.65	4.46	126.66	-	207.74	67.14
240	430	632.2	76.75	94.90	1.37	8.19	181.21	-	213.78	66.18
300	430	632.2	127.21	108.91	1.74	6.69	244.55	-	202.41	67.98
360	430	632.2	122.68	116.6	1.74	4.75	245.77	-	183.58	70.96
420	430	632.2	116.76	112.57	1.43	4.31	235.07	-	215.86	65.85
480	430	632.2	112.83	110.91	1.35	7.43	232.52	84.01	234.68	62.88
540	430	632.2	110.26	103.45	1.26	7.09	222.06	84.01	244.66	61.30
600	430	632.2	112.29	102.59	1.21	8.90	224.99	84.01	235.17	62.80

Reaction parameters; reactor screw speed, 46 rpm; catalyst content, **2.0** %wt.; polyethylene feed rate, 632.2 g/hr.; viscosity of polyethylene feed, 4.0 poise.

Table C.7 All products weight from cracking reaction of polyethylene at 430 °C under nitrogen flow

Reaction time on stream (min.)	Furnace temperature (°C)	Polyethylene feed (g/hr.)	Weights (g)							Conversion
			Liquid products					Wax products	Residue	
			Fraction I	Fraction II	Fraction III	Fraction IV	Totals			
0	300	460.4	0.00	0.00	0.00	0.00	0.00	-	395.84	0.00
60	430	442.3	2.26	54.36	0.25	7.68	64.55	-	211.75	52.12
120	430	442.3	4.71	153.28	0.58	0.00	158.57	-	63.57	85.63
180	430	442.3	9.48	134.69	0.61	0.00	144.78	-	36.01	91.86
240	430	442.3	133.81	128.23	0.43	0.00	262.47	45.14	24.63	94.43
300	430	442.3	144.52	146.24	0.35	0.00	291.11	45.14	0.78	99.82

Reaction parameters; reactor screw speed, 46 rpm; catalyst content, 2.0 %wt.; polyethylene feed rate, **442.3** g/hr.; viscosity of polyethylene feed, 4.0 poise.

Table C.8 All products weight from cracking reaction of polyethylene at 430 ^{o}C under nitrogen flow

Reaction time on stream (min.)	Furnace temperature (^{o}C)	Polyethylene feed (g/hr.)	Weights (g)							Conversion
			Liquid products					Wax products	Residue	
			Fraction I	Fraction II	Fraction III	Fraction IV	Totals			
0	300	798.3	0.00	0.00	0.00	0.00	0.00	-	612.76	0.00
60	430	771.3	0.00	0.33	0.00	0.00	0.33	-	573.95	25.59
120	430	771.3	2.06	36.66	0.38	3.30	39.1	-	498.04	35.43
180	430	771.3	2.95	28.77	0.12	5.68	37.52	-	414.67	46.24
240	430	771.3	3.50	29.31	0.23	6.83	39.87	-	432.67	43.91
300	430	771.3	4.10	21.69	0.2	9.53	35.52	-	460.81	40.26
360	430	771.3	6.40	28.86	0.26	8.01	43.53	-	475.67	38.33
420	430	771.3	11.17	29.95	0.28	9.29	50.69	-	482.97	37.39
480	430	771.3	48.39	26.73	0.30	7.80	83.22	75.70	483.09	37.37
540	430	771.3	63.89	30.10	0.33	9.85	104.17	75.70	432.63	43.91
600	430	771.3	58.63	33.58	0.43	13.10	105.74	75.70	455.28	40.98

Reaction parameters; reactor screw speed, 46 rpm; catalyst content, 2.0 %wt.; polyethylene feed rate, **771.3** g/hr.; viscosity of polyethylene feed, 4.0 poise.

Table C.9 All products weight from cracking reaction of polyethylene at 430 ^{o}C under nitrogen flow

Reaction time on stream (min.)	Furnace temperature (°C)	Polyethylene feed (g/hr.)	Weights (g)							Conversion
			Liquid products					Wax products	Residue	
			Fraction I	Fraction II	Fraction III	Fraction IV	Totals			
0	300	867.6	0.00	0.00	0.00	0.00	0.00	-	833.08	0.00
60	430	865.6	0.05	4.33	0.00	2.13	6.51	-	833.89	3.66
120	430	865.6	1.45	9.52	0.13	18.81	29.91	-	786.93	9.09
180	430	865.6	3.00	11.71	0.21	12.82	27.74	-	796.59	7.97
240	430	865.6	3.43	13.26	0.24	15.03	31.96	-	766.23	11.48
300	430	865.6	3.42	15.42	0.25	14	33.09	-	756.82	12.57
360	430	865.6	3.56	14.75	0.23	13.41	31.95	-	781.17	9.75
420	430	865.6	3.33	15.59	0.24	14.37	33.53	-	752.69	13.05
480	430	865.6	3.62	15.28	0.20	15.51	34.61	2.14	765.34	11.58
540	430	865.6	3.86	15.94	0.31	12.43	32.54	2.14	769.76	11.07
600	430	865.6	4.03	16.66	0.31	15.40	36.40	2.14	771.31	10.89

Reaction parameters; reactor screw speed, 46 rpm; catalyst content, 2.0 %wt.; polyethylene feed rate, **865.6** g/hr.; viscosity of polyethylene feed, 4.00 poise.

Table C.10 All products weight from cracking reaction of polyethylene at 430 ^{o}C under nitrogen flow

Reaction time on stream (min.)	Furnace temperature (^{o}C)	Polyethylene feed (g/hr.)	Weights (g)							Conversion
			Liquid products					Wax products	Residue	
			Fraction I	Fraction II	Fraction III	Fraction IV	Totals			
0	300	646.0	0.00	0.00	0.00	0.00	0.00	-	620.67	0.00
60	430	607.7	0.79	7.44	0.15	1.88	10.26	-	425.67	29.96
120	430	607.7	3.00	58.79	0.63	1.73	64.15	-	354.06	41.74
180	430	607.7	6.09	120.99	1.58	1.01	129.67	-	256.93	57.72
240	430	607.7	6.10	90.27	1.37	6.94	104.68	-	267.74	55.94
300	430	607.7	45.73	92.93	1.48	1.68	141.82	-	253.83	58.23
360	430	607.7	107.54	97.07	1.75	3.60	209.96	-	229.46	62.24
420	430	607.7	110.35	122.61	2.14	2.19	237.29	-	210.89	65.30
480	430	607.7	94.05	96.66	1.69	4.66	197.06	75.58	266.92	56.08
540	430	607.7	93.52	91.15	1.62	6.33	192.62	75.58	269.19	55.70
600	430	607.7	100.39	99.29	1.90	6.39	207.97	75.58	229.75	62.19

Reaction parameters; reactor screw speed, 46 rpm; catalyst content, 2.0 %wt.; polyethylene feed rate, 607.7 g/hr.; viscosity of polyethylene feed, **20.3** poise.

Table C.11 All products weight from cracking reaction of polyethylene at 430 ^{o}C under nitrogen flow

Reaction time on stream (min.)	Furnace temperature (^{o}C)	Polyethylene feed (g/hr.)	Weights (g)							Conversion
			Liquid products					Wax products	Residue	
			Fraction I	Fraction II	Fraction III	Fraction IV	Totals			
0	300	738.5	0.00	0.00	0.00	0.00	0.00	-	701.36	0.00
60	430	639.9	0.29	9.98	0.09	3.41	13.77	-	397.85	37.83
120	430	639.9	3.23	82.54	0.98	5.67	92.42	-	350.74	45.19
180	430	639.9	3.59	83.73	1.30	11.12	99.74	-	311.9	51.26
240	430	639.9	4.25	76.71	1.33	10.55	92.84	-	317.11	50.44
300	430	639.9	10.89	74.77	1.39	11.16	98.21	-	318.61	50.21
360	430	639.9	84.51	73.51	1.37	9.67	169.06	-	327.87	48.76
420	430	639.9	80.25	72.66	1.48	10.78	165.17	-	344.36	46.18
480	430	639.9	79.63	73.57	1.52	10.01	164.73	68.17	339.83	46.89
540	430	639.9	75.79	71.95	1.42	11.57	160.73	68.17	348.97	45.46
600	430	639.9	73.73	71.09	1.52	12.33	158.67	68.17	358.67	43.95

Reaction parameters; reactor screw speed, 46 rpm; catalyst content, 2.0 %wt.; polyethylene feed rate, 639.9 g/hr.; viscosity of polyethylene feed, **2.7** poise.

APPENDIX D

GAS CHROMATOGRAPH CONDITION AND DATA

D.1 Condition for liquid products

Column parameter

Type : Equity-1 capillary column

Length (meters) : 30

I.D. (mm) : 0.53

Film thickness (μm) : 0.3

Carrier gas : Nitrogen

Flow rate : 4.00 ml/min.

Injector temperature : 220°C

FID detector temperature : 220°C

Amount injected (μl) : 0.1

Column oven condition for liquid products

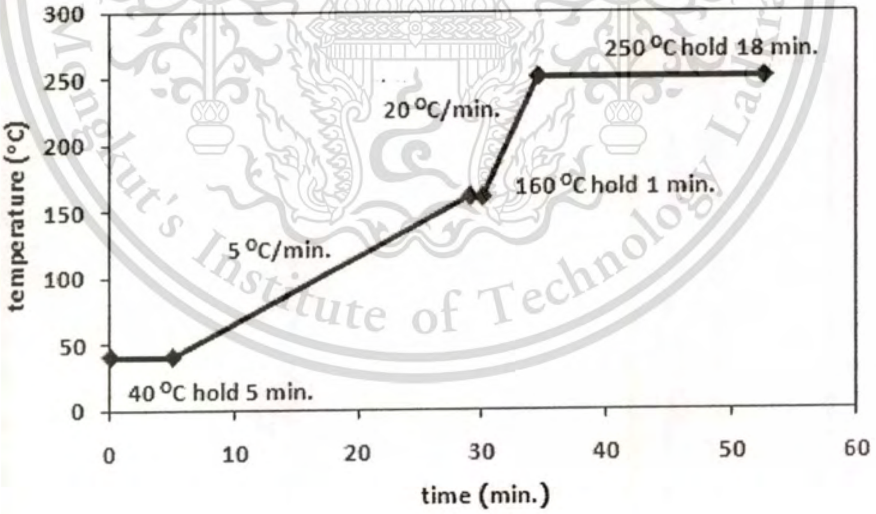

Figure D.1 Chromatogram of liquid products from cracking reaction of polyethylene at 430 °C under nitrogen flow

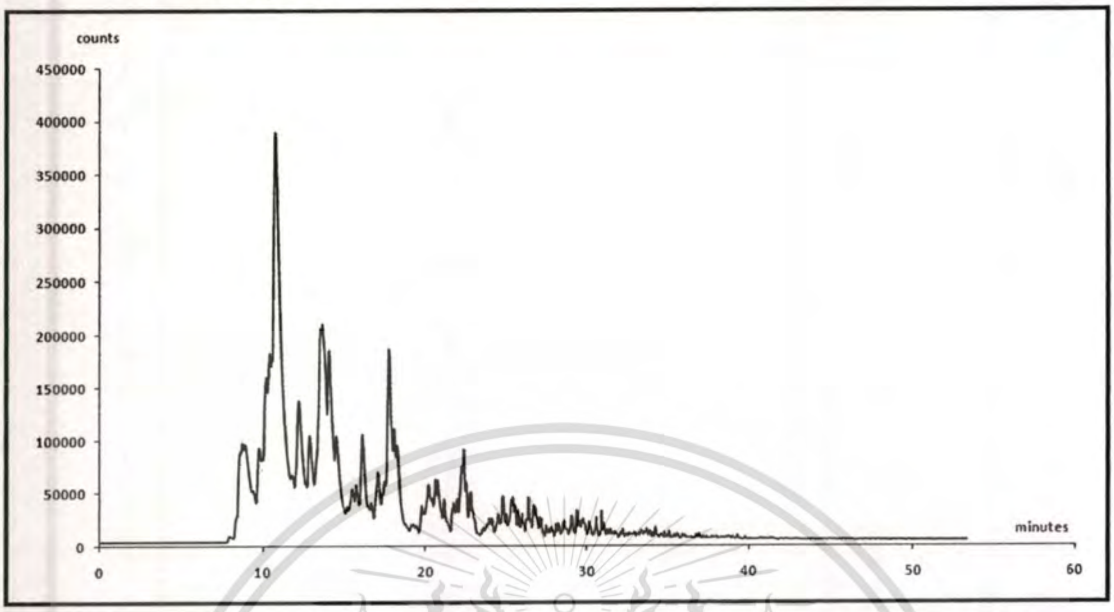

Reaction parameters; reactor screw speed, **130** rpm; catalyst content, 1.0 %wt.; polyethylene feed rate, 633.8 g/hr.; viscosity of polyethylene feed, 4.0 poise.

peak	time	%area	Carbon no.	peak	time	%area	Carbon no.	peak	time	%area	Carbon no.
1	7.988	0.0329	3	17	14.071	4.423	6	33	19.487	0.256	7
2	8.398	0.335	4	18	14.523	2.874	6	34	19.809	0.681	7
3	8.608	1.436	4	19	15.196	0.477	7	35	19.957	0.316	8
4	8.75	1.306	4	20	15.493	1.257	7	36	20.233	1.803	8
5	8.917	2.369	4	21	15.753	1.139	7	37	20.461	0.486	8
6	9.397	0.811	4	22	16.116	2.834	7	38	20.649	1.087	8
7	9.763	1.154	5	23	16.509	0.366	7	39	20797	1.452	8
8	10.182	2.488	5	24	16.688	0.707	7	40	21.193	0.759	8
9	10.415	1.892	5	25	17.108	1.962	7	41	21.39	0.394	8
10	10.748	11.902	5	26	17.384	0.468	7	42	21.78	0.352	8
11	11.813	0.978	6	27	17.503	0.966	7	43	21.992	0.77	8
12	12.194	3.308	6	28	17.748	5.326	7	44	22.255	1.472	8
13	12.653	0.311	6	29	18.081	1.841	7	45	22.39	1.424	8
14	12.856	2.208	6	30	18.287	3.016	7	46	22.542	0.902	8
15	13.531	4.226	6	31	19.158	0.21	7	47	22.767	1.033	8
16	13.663	4.46	6	32	19.322	0.259	7	48	22.967	0.617	8

peak	time	%area	Carbon no.	peak	time	%area	Carbon no.	peak	time	%area	Carbon no.
49	23.306	0.111	9	80	29.731	0.167	10	111	36.112	0.071	11
50	23.636	0.289	9	81	29.808	0.428	10	112	36.479	0.06	11
51	23.844	0.269	9	82	30.184	0.351	10	113	36.817	0.085	11
52	23.974	0.416	9	83	30.406	0.065	10	114	37.009	0.076	11
53	24.152	0.316	9	84	30.61	0.367	10	115	37.237	0.061	11
54	24.521	0.627	9	85	30.932	0.266	10	116	37.464	0.06	11
55	24.808	1.071	9	86	31.075	0.287	10	117	37.819	0.054	11
56	25.04	0.372	9	87	31.323	0.101	10	118	37.937	0.074	11
57	25.195	0.222	9	88	31.501	0.185	10	119	38.388	0.085	12+
58	25.345	0.553	9	89	31.661	0.086	10	120	38.551	0.029	12+
59	25.456	0.42	9	90	31.789	0.171	10	121	38.702	0.046	12+
60	25.569	0.498	9	91	32.113	0.095	11	122	38.843	0.054	12+
61	25.767	0.43	9	92	32.244	0.144	11	123	39.07	0.06	12+
62	26.017	0.669	9	93	32.515	0.124	11	124	39.369	0.062	12+
63	26.289	0.244	9	94	32.657	0.146	11	125	39.84	0.047	12+
64	26.417	0.573	9	95	32.975	0.159	11	126	40.145	0.019	12+
65	26.552	0.228	9	96	33.211	0.136	11	127	40.285	0.017	12+
66	26.748	0.558	9	97	33.381	0.201	11	128	40.566	0.017	12+
67	26.682	0.543	9	98	33.634	0.106	11	129	40.786	0.039	12+
68	27.098	0.222	9	99	33.732	0.121	11	130	41.003	0.05	12+
69	27.205	0.325	9	100	33.95	0.151	11	131	41.464	0.043	12+
70	27.513	0.253	9	101	34.115	0.085	11	132	42.011	0.014	12+
71	27.719	0.125	9	102	34.279	0.21	11	133	42.275	0.023	12+
72	27.84	0.246	9	103	34.619	0.129	11	134	43.017	0.016	12+
73	28.106	0.199	9	104	34.863	0.065	11	135	44.386	0.013	12+
74	28.263	0.268	9	105	34.97	0.031	11	136	44.61	0.014	12+
75	28.628	0.442	10	106	35.131	0.102	11	137	46.224	0.015	12+
76	28.777	0.183	10	107	35.312	0.038	11	138	47.561	0.015	12+
77	29.098	0.555	10	108	35.44	0.073	11	139	47.994	0.013	12+
78	29.407	0.412	10	109	35.621	0.125	11	140	50.592	0.015	12+
79	29.604	0.268	10	110	35.963	0.087	11				

Figure D.2 Chromatogram of liquid products from cracking reaction of polyethylene at 430 °C under nitrogen flow

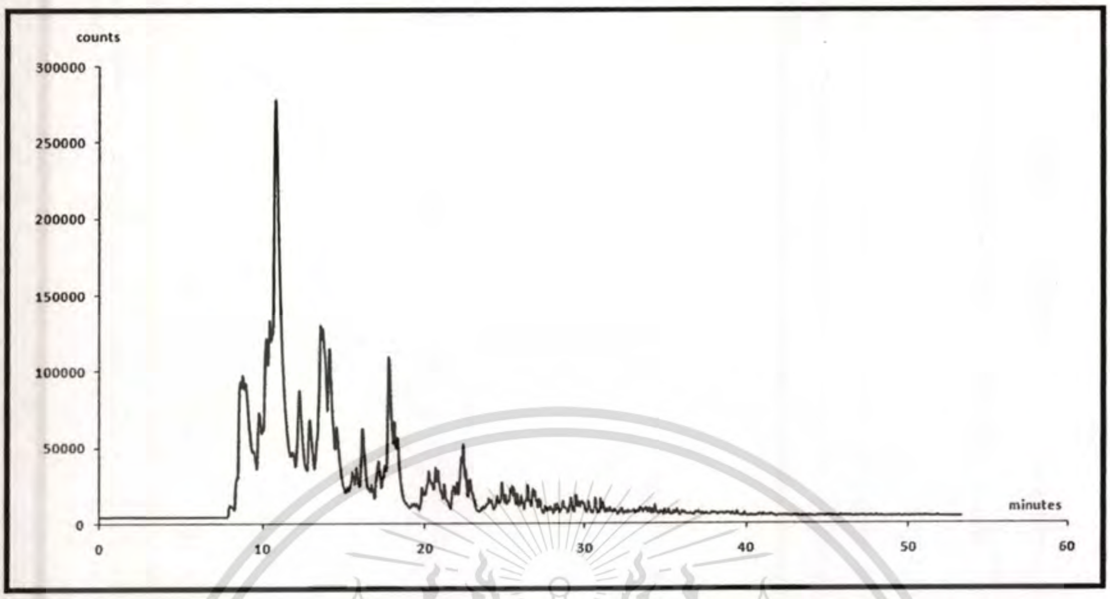

Reaction parameters; reactor screw speed, 66 rpm; catalyst content, 1.0 %wt.; polyethylene feed rate, 635.6 g/hr.; viscosity of polyethylene feed, 4.0 poise.

peak	time	%area	Carbon no.	peak	time	%area	Carbon no.	peak	time	%area	Carbon no.
1	7.995	0.29	3	17	14.072	4.505	6	33	19.491	0.183	7
2	8.407	0.468	4	18	14.52	2.968	7	34	19.816	0.41	8
3	8.615	2.02	4	19	15.193	0.44	7	35	19.96	0.209	8
4	8.759	2.029	4	20	15.494	1.097	7	36	20.237	1.123	8
5	8.923	4.025	4	21	15.754	0.954	7	37	20.462	0.314	8
6	9.395	1.413	5	22	16.12	2.282	7	38	20.655	0.661	8
7	9.768	2.185	5	23	16.506	0.327	7	39	20.801	0.933	8
8	10.184	4.247	5	24	16.687	0.578	7	40	21.199	0.731	8
9	10.413	3.145	5	25	17.112	1.444	7	41	21.789	0.548	8
10	10.75	19.006	6	26	17.385	0.35	7	42	21.998	0.454	8
11	11.8	1.417	6	27	17.506	0.647	7	43	22.261	0.819	8
12	12.195	4.345	6	28	17.755	3.706	7	44	22.396	0.864	8
13	12.643	0.428	6	29	18.081	1.317	7	45	22.546	0.555	8
14	12.855	2.597	6	30	18.289	2.225	7	46	22.844	1.073	8
15	13.535	4.222	6	31	19.163	0.139	7	47	23.642	0.174	9
16	13.667	4.625	6	32	19.323	0.183	7	48	23.852	0.159	9

peak	time	%area	Carbon no.	peak	time	%area	Carbon no.	peak	time	%area	Carbon no.
49	23.983	0.239	9	81	31.339	0.068	10	113	38.103	0.036	12+
50	24.16	0.201	9	82	31.517	0.116	10	114	38.315	0.038	12+
51	24.531	0.368	9	83	31.679	0.055	10	115	38.41	0.042	12+
52	24.819	0.6	9	84	31.806	0.114	10	116	38.575	0.027	12+
53	25.048	0.211	9	85	32.131	0.063	11	117	38.728	0.044	12+
54	25.356	0.447	9	86	32.262	0.098	11	118	38.868	0.051	12+
55	25.463	0.247	9	87	32.534	0.081	11	119	39.096	0.053	12+
56	25.578	0.29	9	88	32.675	0.096	11	120	39.395	0.077	12+
57	25.778	0.292	9	89	32.994	0.112	11	121	39.867	0.04	12+
58	26.028	0.344	9	90	33.23	0.093	11	122	40.173	0.014	12+
59	26.303	0.132	9	91	33.401	0.142	11	123	40.312	0.015	12+
60	26.428	0.335	9	92	33.654	0.074	11	124	40.599	17	12+
61	26.561	0.133	9	93	33.752	0.089	11	125	40.805	0.041	12+
62	26.762	0.315	9	94	33.969	0.108	11	126	41.034	0.032	12+
63	26.871	0.321	9	95	34.134	0.062	11	127	41.337	0.026	12+
64	27.109	0.132	9	96	34.298	0.154	11	128	41.498	0.046	12+
65	27.216	0.192	9	97	34.637	0.097	11	129	42.05	0.018	12+
66	27.527	0.148	9	98	34.884	0.05	11	130	42.303	0.034	12+
67	27.732	0.073	9	99	34.989	0.024	11	131	43.047	0.035	12+
68	27.854	0.146	9	100	35.151	0.081	11	132	43.919	0.012	12+
69	28.12	0.118	9	101	35.335	0.03	11	133	44.416	0.014	12+
70	28.276	0.162	9	102	35.462	0.059	11	134	44.639	0.016	12+
71	28.64	0.372	10	103	35.642	0.102	11	135	45.043	0.025	12+
72	29.113	0.332	10	104	35.982	0.07	11	136	45.816	0.013	12+
73	29.424	0.251	10	105	36.134	0.062	11	137	46.254	0.017	12+
74	29.619	0.163	10	106	36.502	0.066	11	138	46.425	0.01	12+
75	29.822	0.369	10	107	36.841	0.068	11	139	47.103	0.023	12+
76	30.199	0.219	10	108	37.02	0.069	11	140	47.571	0.013	12+
77	30.423	0.04	10	109	37.26	0.056	11	141	48.025	0.014	12+
78	30.626	0.231	10	110	37.487	0.056	11	142	48.226	0.011	12+
79	30.947	0.177	10	111	37.845	0.06	11	143	49.887	0.01	12+
80	31.091	0.18	10	112	37.958	0.036	12+	144	51.802	0.012	12+

Figure D.3 Chromatogram of liquid products from cracking reaction of polyethylene at 430 °C under nitrogen flow

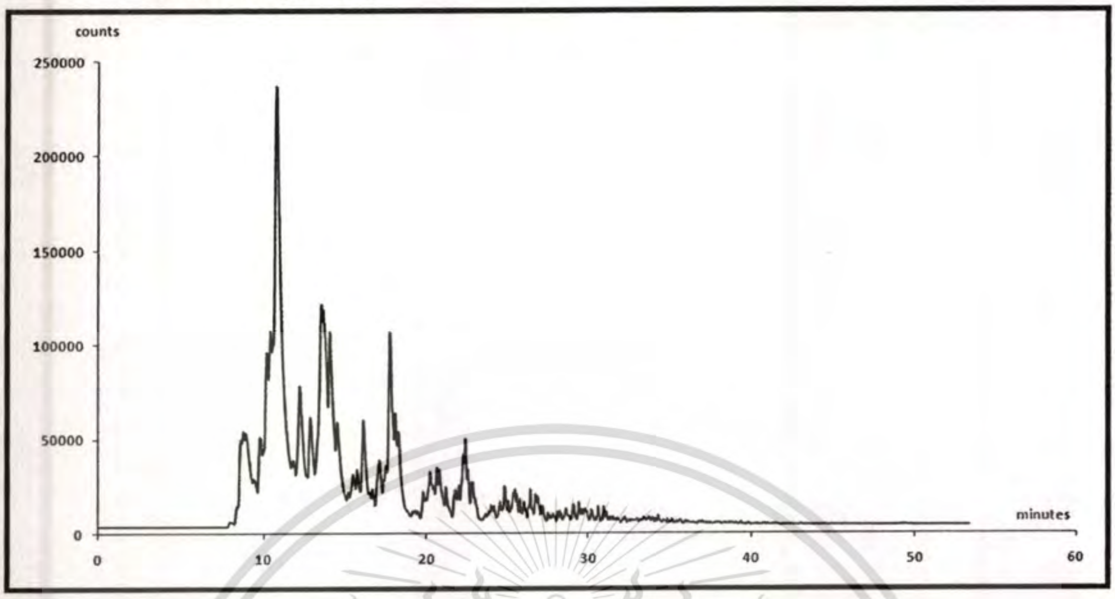

Reaction parameters; reactor screw speed, 46 rpm; catalyst content, 1.0 %wt.; polyethylene feed rate, 639.5 g/hr.; viscosity of polyethylene feed, 4.0 poise.

peak	time	%area	Carbon no.	peak	time	%area	Carbon no.	peak	time	%area	Carbon no.
1	8.002	0.115	3	17	14.517	3.264	6	33	19.949	0.239	8
2	8.617	1.438	4	18	15.189	0.486	7	34	20.224	1.292	8
3	8.763	1.314	4	19	15.489	1.221	7	35	20.449	0.36	8
4	8.927	2.688	4	20	15.748	1.068	7	36	20.641	0.757	8
5	9.408	1.001	4	21	16.113	2.589	7	37	20.788	1.093	8
6	9.771	1.767	5	22	16.499	0.37	7	38	21.183	0.844	8
7	10.186	3.871	5	23	16.68	0.644	7	39	21.773	0.631	8
8	10.413	3.005	5	24	17.104	1.654	7	40	21.983	0.52	8
9	10.75	18.717	5	25	17.497	1.131	7	41	22.245	0.952	8
10	11.802	1.428	6	26	17.745	4.27	7	42	22.38	0.988	8
11	12.193	4.546	6	27	18.072	1.496	7	43	22.53	0.635	8
12	12.644	0.446	6	28	18.297	2.535	7	44	22.759	0.323	8
13	12.853	2.788	6	29	19.152	0.162	7	45	22.829	0.903	8
14	13.532	4.675	6	30	19.312	0.215	7	46	23.625	0.198	9
15	13.661	5.068	6	31	19.479	0.208	7	47	23.834	0.085	9
16	14.068	4.978	6	32	19.803	0.473	7	48	23.965	0.265	9

peak	time	%area	Carbon no.	peak	time	%area	Carbon no.	peak	time	%area	Carbon no.
49	24.142	0.232	9	75	30.172	0.214	10	101	35.425	0.037	11
50	24.513	0.473	9	76	30.397	0.04	10	102	35.605	0.064	11
51	24.799	0.611	9	77	30.598	0.224	10	103	35.943	0.044	11
52	25.029	0.233	9	78	30.918	0.171	10	104	36.095	0.035	11
53	25.336	0.496	9	79	31.063	0.169	10	105	36.462	0.028	11
54	25.444	0.286	9	80	31.309	0.091	10	106	36.804	0.07	11
55	25.557	0.321	9	81	31.488	0.078	10	107	36.993	0.037	11
56	25.758	0.327	9	82	31.65	0.051	10	108	37.221	0.024	11
57	26.007	0.378	9	83	31.776	0.098	10	109	37.447	0.022	11
58	26.407	0.515	9	84	32.098	0.056	11	110	37.802	0.023	11
59	26.539	0.145	9	85	32.232	0.086	11	111	37.922	0.014	11
60	26.74	0.342	9	86	32.501	0.07	11	112	38.06	0.016	12+
61	26.849	0.345	9	87	32.644	0.075	11	113	38.364	0.041	12+
62	27.087	0.143	9	88	32.964	95	11	114	38.686	0.018	12+
63	27.194	0.026	9	89	33.197	0.077	11	115	38.824	0.021	12+
64	27.504	0.158	9	90	33.367	0.116	11	116	39.053	0.019	12+
65	27.71	0.078	9	91	33.619	0.058	11	117	39.351	0.017	12+
66	27.832	0.158	9	92	33719	0.072	11	118	39.821	0.013	12+
67	28.099	126	9	93	33.935	0.084	11	119	40.266	0.02	12+
68	28.253	0.175	9	94	34.099	0.047	11	120	40.766	0.019	12+
69	28.615	0.272	10	95	34.264	0.116	11	121	40.983	0.023	12+
70	28.767	0.115	10	96	34.602	0.073	11	122	41.447	0.019	12+
71	29.087	0.34	10	97	34.847	0.037	11	123	42.254	0.019	12+
72	29.399	0.257	10	98	34.953	0.017	11	124	42.993	0.023	12+
73	29.593	0.161	10	99	35.115	0.058	11				
74	29.796	0.366	10	100	35.3	0.02	11				

Figure D.4 Chromatogram of liquid products from cracking reaction of polyethylene at 430 °C under nitrogen flow

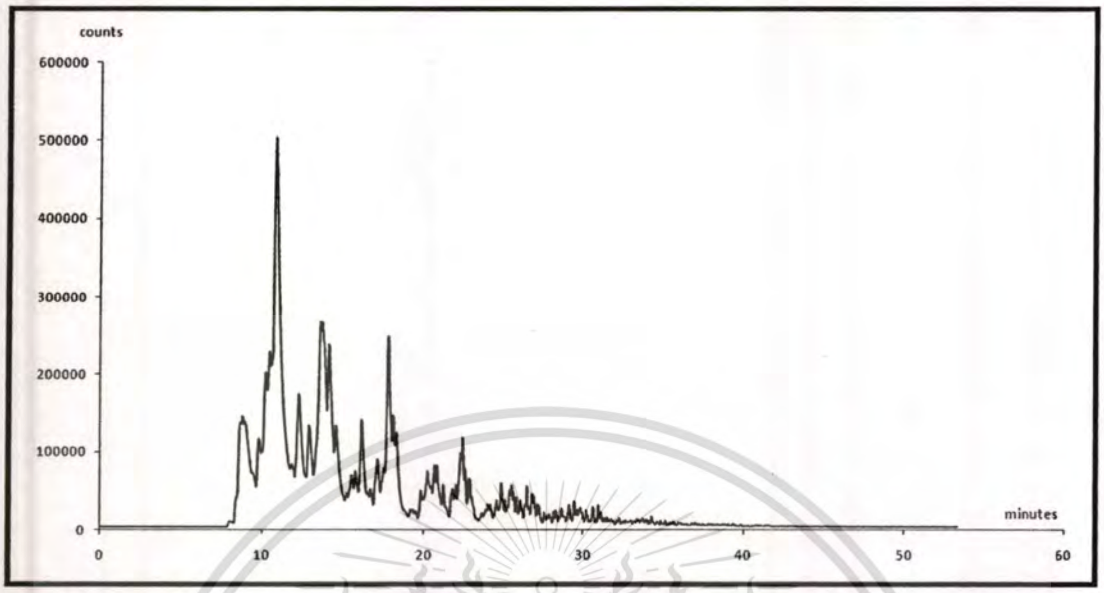

Reaction parameters; reactor screw speed, 46 rpm; catalyst content, **2.0** %wt.; polyethylene feed rate, 632.2 g/hr.; viscosity of polyethylene feed, 4.0 poise.

peak	time	%area	Carbon no.	peak	time	%area	Carbon no.	peak	time	%area	Carbon no.
1	8.026	0.131	3	17	14.531	3.176	6	33	19.96	0.237	8
2	8.639	1.781	4	18	15.199	0.477	7	34	20.239	1.328	8
3	8.773	1.6	4	19	15.501	1.197	7	35	20.462	0.363	8
4	8.931	3.098	4	20	15.759	1.057	7	36	20.658	0.793	8
5	9.399	1.056	4	21	16.13	2.628	7	37	20.808	1.153	8
6	9.784	1.796	5	22	16.511	0.368	7	38	21.2	0.88	8
7	9.991	0.593	5	23	16.691	0.656	7	39	21.786	0.659	8
8	10.197	2.92	5	24	17.117	0.1655	7	40	21.999	0.539	8
9	10.424	2.728	5	25	17.51	1.112	7	41	22.268	1.02	8
10	10.763	17.377	5	26	17.775	4.265	7	42	22.404	0.992	8
11	11.808	1.312	6	27	18.094	1.512	7	43	22.553	0.629	8
12	12.204	4.828	6	28	18.299	2.472	7	44	22.782	1.212	8
13	12.864	2.659	6	29	19.167	0.185	7	45	23.301	0.09	9
14	13.547	4.301	6	30	19.319	0.236	7	46	23.639	0.228	9
15	13.67	4.908	6	31	19.489	0.22	7	47	23.847	0.217	9
16	14.083	4.767	6	32	19.818	0.504	7	48	23.98	0.281	9

peak	time	%area	Carbon no.	peak	time	%area	Carbon no.	peak	time	%area	Carbon no.
49	24.159	0.262	9	80	30.936	0.199	10	111	37.824	0.043	12+
50	24.528	0.453	9	81	31.079	0.183	10	112	37.94	0.022	12+
51	24.815	0.718	9	82	31.327	0.075	10	113	38.082	0.028	12+
52	25.047	0.25	9	83	31.507	0.121	10	114	38.389	0.052	12+
53	25.353	0.554	9	84	31.67	0.061	10	115	38.549	0.02	12+
54	25.465	0.327	9	85	31.793	0.118	10	116	38.709	0.207	12+
55	25.577	0.34	9	86	32.114	0.07	11	117	38.844	0.036	12+
56	25.776	0.314	9	87	32.252	0.102	11	118	39.077	0.034	12+
57	26.023	0.459	9	88	32.518	0.086	11	119	39.373	0.048	12+
58	26.297	0.167	9	89	32.661	0.093	11	120	39.846	0.034	12+
59	26.425	0.391	9	90	32.984	0.112	11	121	40.152	0.018	12+
60	26.559	0.165	9	91	33.216	0.091	11	122	40.287	0.012	12+
61	26.757	0.369	9	92	33.385	0.131	11	123	40.55	0.014	12+
62	26.87	0.368	9	93	33.739	0.147	11	124	40.786	0.027	12+
63	27.105	0.163	9	94	33.956	0.095	11	125	41.007	0.02	12+
64	27.211	0.231	9	95	34.118	0.055	11	126	41.313	0.018	12+
65	27.518	0.184	9	96	34.284	0.134	11	127	41.469	0.032	12+
66	27.726	0.093	9	97	34.621	0.089	11	128	42.01	0.013	12+
67	27.849	0.176	9	98	34.866	0.044	11	129	42.282	0.011	12+
68	28.114	0.147	9	99	34.972	0.022	11	130	42.49	0.009	12+
69	28.269	0.204	9	100	35.135	0.071	11	131	43.016	0.024	12+
70	28.63	0.304	10	101	35.32	0.028	11	132	43.705	0.004	12+
71	28.783	0.133	10	102	35.444	0.048	11	133	43.886	0.008	12+
72	29.104	0.327	10	103	35.624	0.081	11	134	44.385	0.009	12+
73	29.257	0.055	10	104	35.962	0.058	11	135	44.611	0.008	12+
74	29.418	0.28	10	105	36.114	0.064	11	136	45.02	0.011	12+
75	29.612	0.18	10	106	36.478	0.064	11	137	45.779	0.005	12+
76	29.817	0.411	10	107	36.825	0.053	11	138	46.009	0.005	12+
77	30.192	0.241	10	108	37.014	0.053	12+	139	47.073	0.005	12+
78	30.416	0.05	10	109	37.241	0.044	12+	140	47.554	0.005	12+
79	30.616	0.245	10	110	37.468	0.04	12+	141	68.469	0.009	12+

Figure D.5 Chromatogram of liquid products from cracking reaction of polyethylene at 430 °C under nitrogen flow

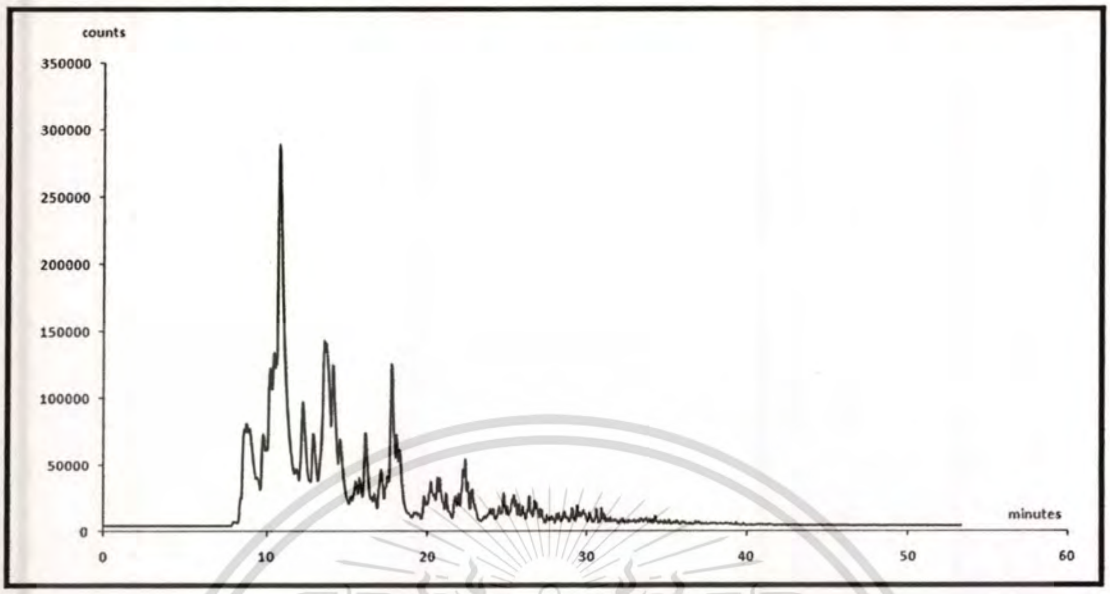

Reaction parameters; reactor screw speed, 46 rpm; catalyst content, 2.0 %wt.; polyethylene feed rate, 442.3 g/hr.; viscosity of polyethylene feed, 4.0 poise.

peak	time	%area	Carbon no.	peak	time	%area	Carbon no.	peak	time	%area	Carbon no.
1	7.993	0.116	3	17	14.062	4.72	6	33	19.791	0.458	7
2	8.61	1.899	4	18	14.511	3.119	6	34	19.936	0.213	8
3	8.75	1.651	4	19	15.181	0.472	7	35	20.21	1.188	8
4	8.913	3.237	4	20	15.48	1.188	7	36	20.436	0.326	8
5	9.391	1.141	4	21	15.74	1.03	7	37	20.629	0.698	8
6	9.769	2.137	5	22	16.106	2.554	7	38	20.778	0.1013	8
7	9.968	0.684	5	23	16.493	0.353	7	39	21.171	0.766	8
8	10.18	3.408	5	24	16.67	0.626	7	40	21.758	0.576	8
9	10.405	3.092	5	25	17.091	1.589	7	41	21.969	0.465	8
10	10.746	18.931	5	26	17.486	1.074	7	42	22.231	0.871	8
11	11.793	1.395	6	27	17.738	3.988	7	43	22.367	0.842	8
12	12.189	4.655	6	28	18.063	1.399	7	44	22.519	0.539	8
13	12.633	0.42	6	29	18.27	2.303	7	45	22.817	1.116	8
14	12.848	2.742	6	30	19.142	0.171	7	46	23.611	0.192	9
15	13.527	4.427	6	31	19.295	0.214	7	47	23.817	0.185	9
16	13.649	4.914	6	32	19.467	0.2	7	48	23.95	0.234	9

peak	time	%area	Carbon no.
49	24.13	0.218	9
50	24.498	0.375	9
51	24.783	0.604	9
52	25.015	0.207	9
53	25.32	0.457	9
54	25.43	0.273	9
55	25.543	0.284	9
56	25.743	0.262	9
57	25.99	0.381	9
58	26.264	0.141	9
59	26.392	0.323	9
60	26.526	0.139	9
61	26.722	0.309	9
62	26.835	0.307	9
63	27.072	0.138	9
64	27.179	0.093	9
65	27.488	0.153	9
66	17.694	0.077	9
67	27.818	0.148	9
68	28.083	0.125	9
69	28.238	0.175	9
70	283598	0.264	10
71	283751	0.115	10
72	29.071	0.337	10
73	29.385	0.248	10
74	29.578	0.162	10
75	29.704	0.101	10
76	29.782	0.269	10
77	30.156	0.217	10
78	30.382	0.045	10
79	30.582	0.225	10
80	30.901	0.179	10
81	31.045	0.171	10
82	31.292	0.1	10
83	31.472	0.083	10
84	31.635	0.057	10
85	31.758	0.109	10
86	32.078	0.066	11
87	32.216	0.096	11
88	32.483	0.082	11
89	32.626	0.087	11
90	32.949	0.112	11
91	33.179	0.09	11
92	33.35	0.131	11
93	33.604	0.063	11
94	33.701	0.084	11
95	33.919	0.097	11
96	34.081	0.056	11
97	34.246	0.137	11
98	34.582	0.09	11
99	34.829	0.066	11
100	35.097	0.072	11
101	35.281	0.027	11
102	35.405	0.048	11
103	35.585	0.084	11
104	35.922	0.06	11
105	36.074	6	11
106	36.44	0.069	11
107	36.783	0.054	11
108	36.972	0.057	11
109	37.202	3045	11
110	37.427	0.044	11
111	37.783	0.069	11
112	38.041	0.031	12+
113	38.347	0.058	12+
114	38.502	0.021	12+
115	38.665	0.029	12+
116	38.805	0.04	12+
117	39.034	0.039	12+
118	39.329	0.059	12+
119	39.799	0.031	12+
120	40.105	0.017	12+
121	40.242	0.012	12+
122	40.534	0.014	12+
123	40.743	0.028	12+
124	40.961	0.021	12+
125	41.261	0.018	12+
126	41.447	0.034	12+
127	41.963	0.015	12+
128	42.231	0.012	12+
129	42.447	0.009	12+
130	42.977	0.026	12+
131	44.548	0.009	12+
132	44.988	0.014	12+
133	47.029	0.011	12+
134	47.953	0.01	12+

Figure D.6 Chromatogram of liquid products from cracking reaction of polyethylene at 430 °C under nitrogen flow

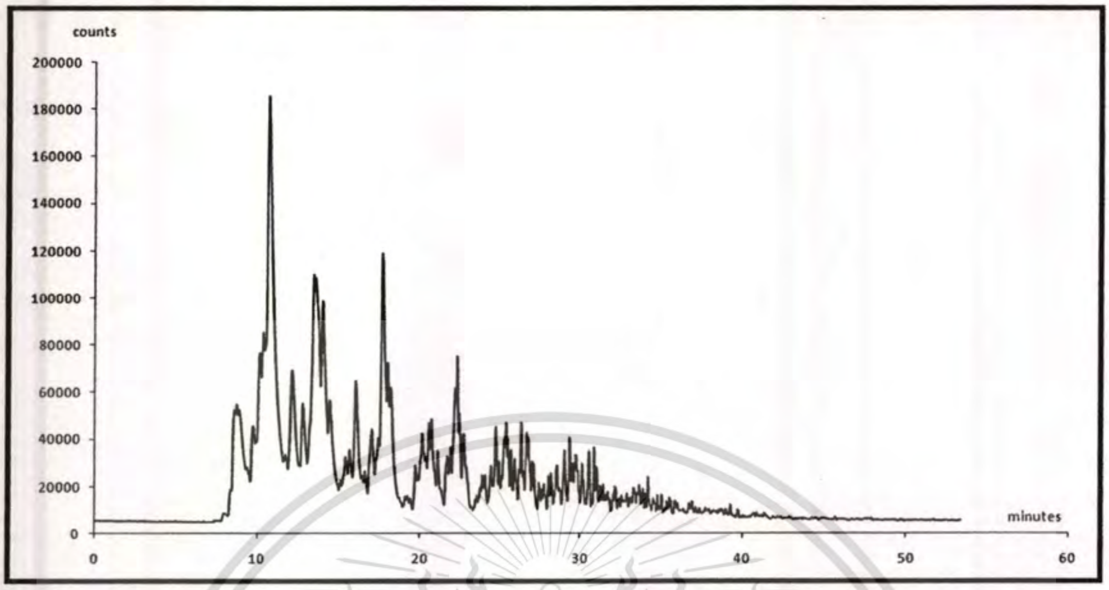

Reaction parameters; reactor screw speed, 46 rpm; catalyst content, 2.0 %wt.; polyethylene feed rate, **771.3** g/hr.; viscosity of polyethylene feed, 4.0 poise.

peak	time	%area	Carbon no.	peak	time	%area	Carbon no.	peak	time	%area	Carbon no.
1	7.959	0.19	3	17	14.002	3.854	6	33	19.406	0.219	7
2	8.568	1.332	4	18	14.451	2.616	6	34	19.732	0.52	7
3	8.711	1.079	4	19	15.119	0.405	7	35	19.875	0.251	7
4	8.874	2.188	4	20	15.421	1.021	7	36	20.153	1.417	8
5	9.344	0.747	4	21	15.678	0.911	7	37	20.377	0.397	8
6	9.719	1.301	5	22	16.046	2.332	7	38	20.571	0.863	8
7	9.929	0.44	5	23	16.43	0.342	7	39	20.719	1.313	8
8	10.132	2.141	5	24	16.61	0.59	7	40	21.113	1.013	8
9	10.36	1.979	5	25	17.044	1.529	7	41	21.701	0.773	8
10	10.695	12.484	5	26	17.305	0.356	7	42	21.912	0.647	8
11	11.746	0.977	6	27	17.425	0.693	7	43	22.178	1.227	8
12	12.134	3.33	6	28	17.677	4.035	7	44	22.313	1.26	8
13	12.583	0.335	6	29	18.003	1.444	7	45	22.462	0.81	8
14	12.788	2.062	6	30	18.208	2.452	7	46	22.693	1.662	8
15	13.466	3.484	6	31	19.083	0.198	7	47	23.554	0.294	9
16	13.595	3.9	6	32	19.234	0.244	7	48	23.763	0.295	9

peak	time	%area	Carbon no.	peak	time	%area	Carbon no.	peak	time	%area	Carbon no.
49	23.895	0.393	9	84	31.704	0.302	10	119	38.732	0.12	12+
50	24.074	0.371	9	85	32.023	0.182	11	120	38.965	0.114	12+
51	24.443	0.654	9	86	32.159	0.271	11	121	39.259	0.188	12+
52	24.731	1.079	9	87	32.426	0.228	11	122	39.727	0.098	12+
53	24.962	0.385	9	88	32.571	0.232	11	123	39.89	0.021	12+
54	25.269	0.841	9	89	32.894	0.327	11	124	40.033	0.042	12+
55	25.38	0.553	9	90	33.124	0.248	11	125	40.169	0.045	12+
56	25.491	0.553	9	91	33.294	0.364	11	126	40.456	0.055	12+
57	25.693	0.586	9	92	33.544	0.182	11	127	40.676	0.098	12+
58	25.94	0.692	9	93	33.645	0.233	11	128	40.884	0.077	12+
59	26.341	0.957	9	94	33.864	0.272	11	129	41.188	0.064	12+
60	26.473	0.279	9	95	34.024	0.158	11	130	41.343	0.119	12+
61	26.674	0.665	9	96	34.19	0.387	11	131	41.885	0.061	12+
62	26.787	0.686	9	97	34.525	0.259	11	132	42.15	0.045	12+
63	27.022	0.298	9	98	34.769	0.13	11	133	42.363	0.04	12+
64	27.128	0.43	9	99	34.875	0.065	11	134	42.89	0.109	12+
65	27.437	0.341	9	100	35.036	0.209	11	135	43.243	0.021	12+
66	27.643	0.176	9	101	35.219	0.082	11	136	43.396	0.022	12+
67	27.767	0.348	9	102	35.345	0.141	11	137	43.568	0.023	12+
68	28.032	0.294	9	103	35.525	0.242	11	138	43.75	0.044	12+
69	28.186	0.411	9	104	35.861	0.176	11	139	44.248	0.045	12+
70	28.548	0.641	10	105	36.013	0.164	11	140	44.477	0.041	12+
71	28.702	0.274	10	106	36.243	0.064	11	141	44.889	0.082	12+
72	29.025	0.828	10	107	36.376	0.163	11	142	45.421	0.023	12+
73	29.334	0.635	10	108	36.719	0.161	11	143	45.656	0.035	12+
74	29.529	0.408	10	109	36.908	0.169	11	144	46.105	0.044	12+
75	29.734	0.964	10	110	37.136	0.135	11	145	46.26	0.021	12+
76	30.106	0.57	10	111	37.362	0.128	11	146	46.66	0.026	12+
77	30.329	0.115	10	112	37.715	0.139	11	147	46.954	0.02	12+
78	30.531	0.595	10	113	37.832	0.065	11	148	47.085	0.016	12+
79	30.849	0.482	10	114	37.969	0.093	12+	149	47.24	0.009	12+
80	30.994	0.461	10	115	38.182	0.085	12+	150	47.496	0.028	12+
81	31.24	0.276	10	116	38.276	0.084	12+	151	47.658	0.027	12+
82	31.419	0.225	10	117	38.436	0.065	12+	152	47.881	0.018	12+
83	31.581	0.156	10	118	38.595	0.086	12+	153	48.082	0.01	12+

peak	time	%area	Carbon no.
154	48.293	0.024	12+
155	48.719	0.029	12+
156	49.302	0.02	12+
157	49.754	0.009	12+
158	50.109	0.01	12+
159	50.476	0.015	12+
160	50.929	0.025	12+
161	51.668	0.02	12+
162	53.606	0.011	12+
163	68.355	0.07	12+
164	70.027	0.013	12+
165	70.736	0.018	12+
166	71.258	0.012	12+

Figure D.7 Chromatogram of liquid products from cracking reaction of polyethylene at 430 °C under nitrogen flow

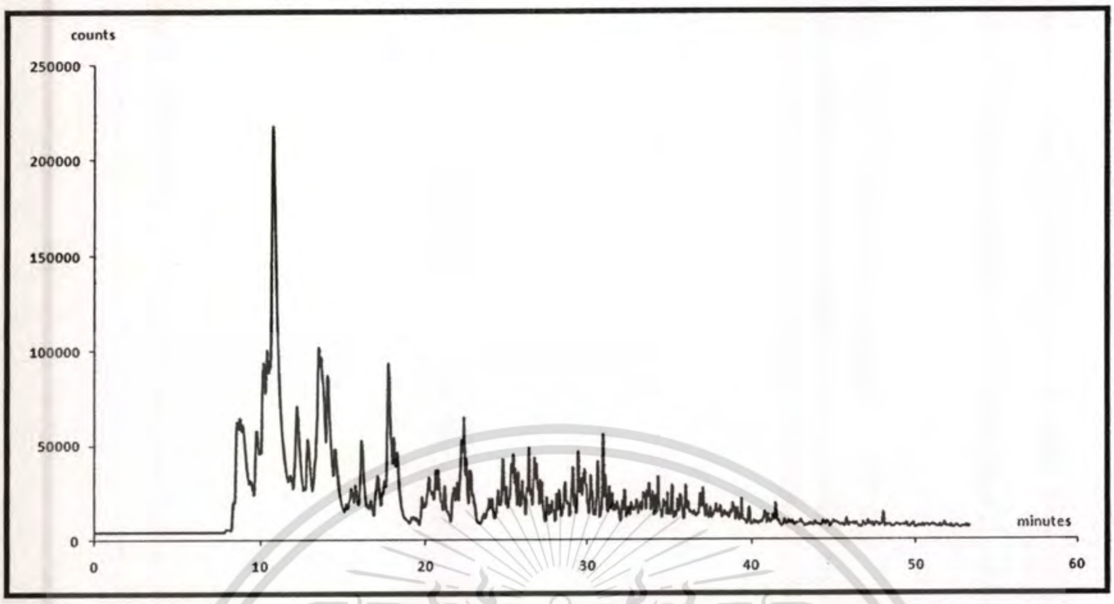

Reaction parameters; reactor screw speed, 46 rpm; catalyst content, 2.0 %wt.; polyethylene feed rate, **865.6** g/hr.; viscosity of polyethylene feed, 4.0 poise.

peak	time	%area	Carbon no.	peak	time	%area	Carbon no.	peak	time	%area	Carbon no.
1	7.987	0.053	3	**17**	14.057	3.027	6	**33**	19.471	0.145	7
2	8.396	0.257	4	**18**	14.508	1.982	6	**34**	19.732	0.359	7
3	8.599	1.251	4	**19**	18.18	0.304	7	**35**	19.941	0.176	8
4	8.749	1.214	4	**20**	15.478	0.771	7	**36**	20.216	0.997	8
5	8.916	2.351	4	**21**	15.738	0.659	7	**37**	20.442	0.289	8
6	9.396	0.84	4	**22**	16.103	1.654	7	**38**	20.633	0.604	8
7	9.758	1.577	5	**23**	16.497	0.234	7	**39**	20.782	0.902	8
8	9.971	0.515	5	**24**	16.672	0.407	7	**40**	21.177	0.731	8
9	10.169	2.483	5	**25**	17.096	1.073	7	**41**	21.766	0.592	8
10	10.4	2.194	5	**26**	17.368	0.255	7	**42**	21.976	0.492	8
11	10.738	12.957	5	**27**	17.487	0.475	7	**43**	22.238	0.952	8
12	11.794	0.0971	6	**28**	17.732	2.8	7	**44**	22.377	0.98	8
13	12.182	3.08	6	**29**	18.064	961	7	**45**	22.527	0.617	8
14	12.841	2.119	6	**30**	18.271	1.619	7	**46**	22.755	0.756	8
15	13.519	3.023	6	**31**	19.144	0.123	7	**47**	22.948	0.447	8
16	13.651	3.126	6	**32**	19.301	0.158	7	**48**	23.278	0.089	9

peak	time	%area	Carbon no.	peak	time	%area	Carbon no.	peak	time	%area	Carbon no.
49	23.619	0.228	9	84	31.065	0.552	10	119	38.067	0.336	12+
50	23.825	0.229	9	85	31.317	0.372	10	120	38.316	0.329	12+
51	23.959	0.312	9	86	31.495	0.266	10	121	38.531	0.138	12+
52	24.139	0.294	9	87	31.655	0.179	10	122	38.7	0.164	12+
53	24.507	0.544	9	88	31.779	0.361	10	123	38.833	0.318	12+
54	24.795	0.945	9	89	32.097	0.233	11	124	39.086	0.254	12+
55	25.027	0.326	9	90	32.242	0.355	11	125	39.362	0.405	12+
56	25.332	0.77	9	91	32.502	0.289	11	126	39.825	0.24	12+
57	25.444	0.481	9	92	32.649	0.346	11	127	39.991	0.047	12+
58	25.556	0.48	9	93	32.974	0.384	11	128	40.136	0.088	12+
59	25.758	0.494	9	94	33.203	0.34	11	129	40.277	0.097	12+
60	26.004	0.695	9	95	33.373	0.272	11	130	40.564	0.125	12+
61	26.406	0.91	9	96	33.464	0.232	11	131	40.786	0.251	12+
62	26.539	0.272	9	97	33.614	0.282	11	132	40.993	0.172	12+
63	26.739	0.649	9	98	33.728	0.355	11	133	41.3	0.162	12+
64	26.852	0.679	9	99	33.948	0.388	11	134	41.446	0.362	12+
65	27.087	0.287	9	100	34.11	0.239	11	135	41.996	0.16	12+
66	27.194	0.414	9	101	34.276	0.574	11	136	42.261	0.12	12+
67	27.501	0.334	9	102	34.609	0.256	11	137	42.471	0.102	12+
68	27.709	0.167	9	103	34.719	0.173	11	138	42.738	0.099	12+
69	27.833	0.331	9	104	34.852	0.219	11	139	42.997	0.224	12+
70	28.098	0.284	9	105	34.962	0.11	11	140	43.356	0.059	12+
71	28.252	0.405	9	106	35.128	0.392	11	141	43.512	0.073	12+
72	28.616	0.657	10	107	35.3	0.134	11	142	43.683	0.072	12+
73	28.768	0.28	10	108	35.438	0.283	11	143	43.864	0.1	12+
74	29.092	0.744	10	109	35.614	0.461	11	144	44.06	0.079	12+
75	29.242	0.128	10	110	35.949	0.395	11	145	44.351	0.0135	12+
76	29.405	0.689	10	111	36.108	0.207	11	146	44.596	0.135	12+
77	29.599	0.454	10	112	36.237	0.244	11	147	45.006	0.146	12+
78	29.727	0.312	10	113	36.475	0.223	11	148	45.149	0.141	12+
79	29.804	0.763	10	114	36.82	0.467	11	149	45.526	0.084	12+
80	30.178	0.651	10	115	37.006	0.402	11	150	45.762	0.13	12+
81	30.401	0.126	10	116	37.231	0.262	11	151	45.995	0.103	12+
82	30.605	0.676	10	117	37.461	0.187	11	152	46.211	0.063	12+
83	30.924	0.684	10	118	37.807	0.425	11	153	46.368	0.118	12+

peak	time	%area	Carbon no.	peak	time	%area	Carbon no.	peak	time	%area	Carbon no.
154	46.765	0.102	12+	176	51.351	0.029	12+	198	57.405	0.044	12+
155	47.058	0.092	12+	177	51.492	0.046	12+	199	57.742	0.036	12+
156	47.194	0.064	12+	178	51.757	0.092	12+	200	57.931	0.01	12+
157	47.337	0.056	12+	179	51.947	0.05	12+	201	58.252	0.027	12+
158	47.532	0.113	12+	180	52.172	0.053	12+	202	58.508	0.01	12+
159	47.752	0.045	12+	181	52.513	0.098	12+	203	58.797	0.01	12+
160	47.983	0.158	12+	182	52.888	0.048	12+	204	59.043	0.014	12+
161	48.184	0.049	12+	183	53.038	0.029	12+	205	59.396	0.011	12+
162	48.393	0.087	12+	184	53.171	0.037	12+	206	60.089	0.073	12+
163	48.595	0.041	12+	185	53.393	0.054	12+	207	60.869	0.015	12+
164	48.796	0.119	12+	186	53.776	0.0123	12+	208	62.164	0.012	12+
165	49.093	0.039	12+	187	53.984	0.051	12+	209	63.877	0.01	12+
166	49.197	0.047	12+	188	54.256	0.028	12+	210	64.09	0.008	12+
167	49.399	0.108	12+	189	54.373	0.023	12+	211	64.747	0.008	12+
168	49.726	0.054	12+	190	54.563	0.059	12+	212	67.585	0.031	12+
169	49.847	0.058	12+	191	54.827	0.051	12+	213	68.463	0.018	12+
170	50.207	0.081	12+	192	55.172	0.042	12+	214	72.029	0.008	12+
171	50.396	0.057	12+	193	55.424	0.057	12+	215	73.678	0.011	12+
172	50.584	0.048	12+	194	55.97	0.04	12+	216	74.153	0.026	12+
173	50.706	0.058	12+	195	56.164	0.022	12+	217	79.467	0.015	12+
174	51.014	0.089	12+	196	56.437	0.045	12+				
175	51.162	0.059	12+	197	57.079	0.081	12+				

Figure D.8 Chromatogram of liquid products from cracking reaction of polyethylene at 430 °C under nitrogen flow

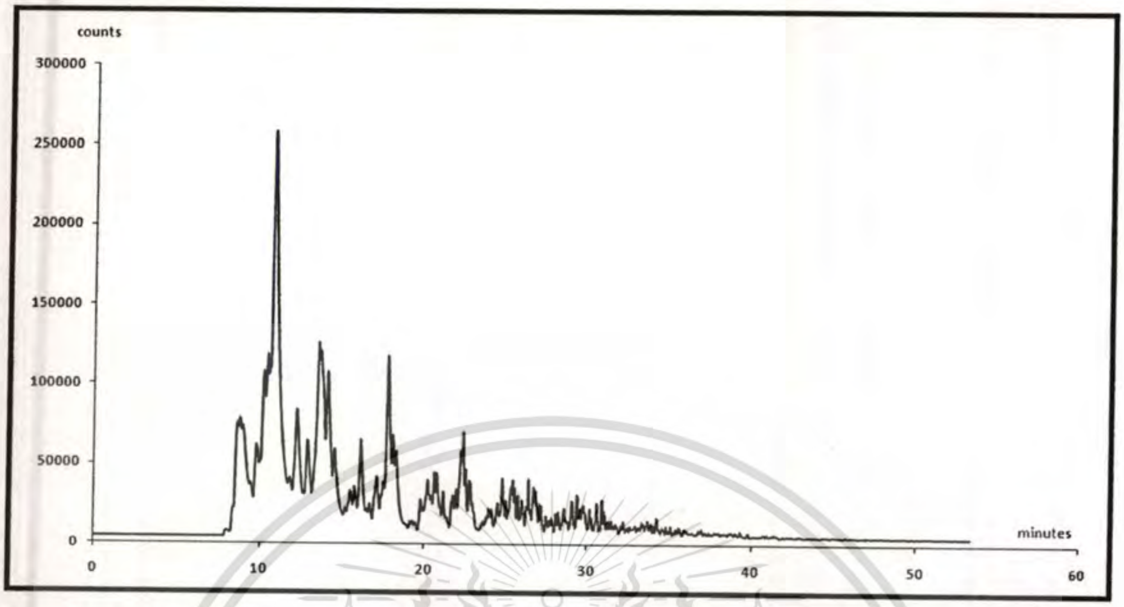

Reaction parameters; reactor screw speed, 46 rpm; catalyst content, 2.0 %wt.; polyethylene feed rate, 607.7 g/hr.; viscosity of polyethylene feed, 20.3 poise.

peak	time	%area	Carbon no.	peak	time	%area	Carbon no.	peak	time	%area	Carbon no.
1	7.982	0.145	3	17	14.046	4.003	6	33	19.777	0.484	7
2	8.6	1.899	4	18	14.497	2.596	6	34	19.924	0.225	8
3	8.742	1.599	4	19	15.168	0.403	7	35	20.199	1.85	8
4	8.906	3.68	4	20	15.466	1.018	7	36	20.426	0.356	8
5	9.385	1.083	4	21	15.725	0.879	7	37	20.617	0.79	8
6	9.752	1.775	5	22	16.09	2.178	7	38	20.766	1.139	8
7	9.969	0.599	5	23	16.481	0.305	7	39	21.16	0.606	8
8	10.167	3.02	5	24	16.657	0.539	7	40	21.353	0.284	8
9	10.395	2.736	5	25	17.078	1.415	7	41	21.746	0.709	8
10	10.732	16.458	5	26	17.472	0.991	7	42	21.959	0.584	8
11	11.784	1.231	6	27	17.72	3.71	7	43	22.222	1.133	8
12	12.172	3.912	6	28	18.05	1.295	7	44	22.359	1.099	8
13	12.629	0.357	6	29	18.257	2.152	7	45	22.51	0.705	8
14	12.832	2.334	6	30	19.128	0.165	7	46	22.737	1.36	8
15	13.51	3.936	6	31	19.283	0.206	7	47	23.262	0.097	8
16	13.638	4.129	6	32	19.455	0.19	7	48	23.6	0.254	9

peak	time	%area	Carbon no.
49	23.808	0.251	9
50	23.94	0.343	9
51	24.119	0.306	9
52	24.488	0.552	9
53	24.773	0.941	9
54	25.006	0.324	9
55	25.311	0.719	9
56	25.423	0.349	9
57	25.535	0.455	9
58	25.735	0.421	9
59	25.981	0.624	9
60	26.255	0.23	9
61	26.384	0.545	9
62	26.518	0.229	9
63	26.715	0.532	9
64	26.829	0.533	9
65	27.064	0.233	9
66	27.171	0.329	9
67	27.478	0.262	9
68	27.685	0.133	9
69	27.808	0.257	9
70	28.073	0.218	9
71	28.228	0.302	9
72	28.59	0.469	10
73	28.743	0.201	10
74	29.064	0.516	10
75	29.216	0.086	10
76	29.375	0.453	10
77	29.57	0.295	10
78	29.775	0.673	10
79	30.148	0.395	10
80	30.372	0.08	10
81	30.573	0.408	10
82	30.891	0.333	10
83	31.036	0.314	10
84	31.283	0.18	10
85	31.462	0.151	10
86	31.625	0.101	10
87	31.748	0.197	10
88	32.068	0.118	11
89	32.205	0.175	11
90	32.472	0.148	11
91	32.616	144	11
92	32.938	0.212	11
93	33.17	0.16	11
94	33.338	0.235	11
95	33.592	0.114	11
96	33.691	0.154	11
97	33.909	173	11
98	34.071	0.1	11
99	34.236	0.245	11
100	34.572	0.161	11
101	34.817	0.081	11
102	34.923	0.039	11
103	35.085	0.131	11
104	35.269	0.049	11
105	35.394	0.087	11
106	35.573	0.148	11
107	35.911	0.106	11
108	36.062	0.129	11
109	36.427	0.101	11
110	36.77	0.098	11
111	36.96	0.102	11
112	37.188	0.078	11
113	37.414	0.074	11
114	37.768	0.081	11
115	37.885	0.039	11
116	38.024	0.056	12+
117	38.235	0.047	12+
118	38.332	0.049	12+
119	38.49	0.037	12+
120	38.651	0.051	12+
121	38.787	0.07	12+
122	39.021	0.065	12+
123	39.315	0.102	12+
124	39.786	0.053	12+
125	39.946	0.009	12+
126	40.09	0.019	12+
127	40.226	0.02	12+
128	40.513	0.025	12+
129	40.731	0.05	12+
130	40.943	0.037	12+
131	41.25	0.032	12+
132	41.404	0.06	12+
133	14.946	0.026	12+
134	42.213	0.021	12+
135	42.425	0.018	12+
136	42.95	0.047	12+
137	43.632	0.009	12+
138	43.817	0.016	12+
139	44.316	0.016	12+
140	44.541	0.017	12+
141	44.953	0.024	12+
142	45.715	0.011	12+
143	46.163	0.014	12+
144	47.012	0.008	12+
145	47.495	0.011	12+
146	47.936	0.011	12+
147	51.719	0.008	12+
148	68.446	0.014	12+

Figure D.9 Chromatogram of liquid products from cracking reaction of polyethylene at 430 °C under nitrogen flow

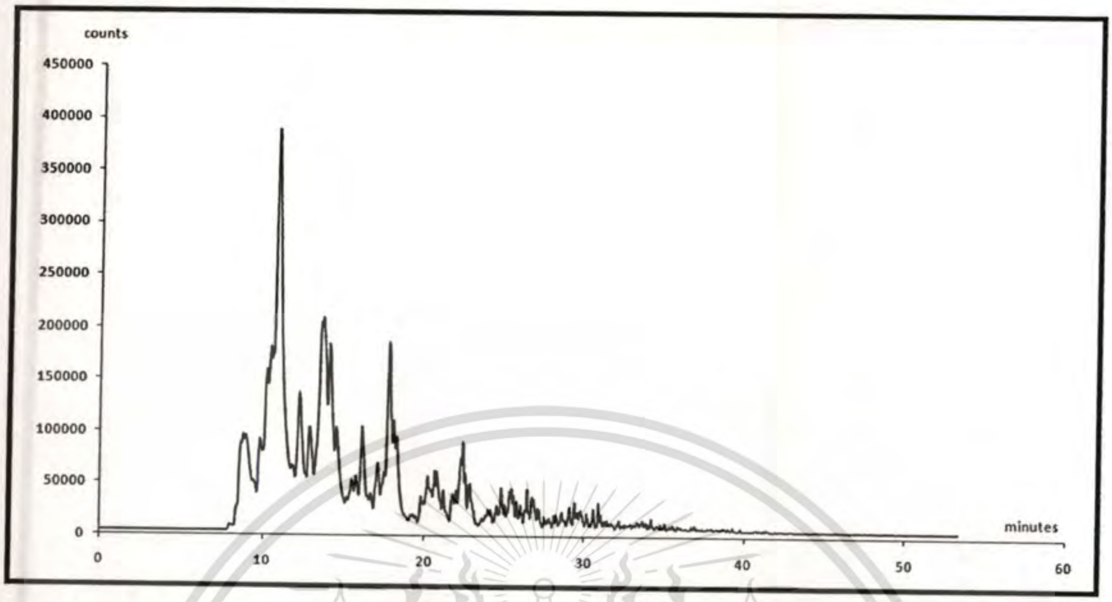

Reaction parameters; reactor screw speed, 46 rpm; catalyst content, 2.0 %wt.; polyethylene feed rate, 639.9 g/hr.; viscosity of polyethylene feed, **2.7** poise.

peak	time	%area	Carbon no.	peak	time	%area	Carbon no.	peak	time	%area	Carbon no.
1	7.987	0.135	3	17	15.164	0.466	7	33	20.195	1.267	8
2	8.611	1.397	4	18	15.466	1.172	7	34	20.415	0.38	8
3	8.749	1.321	4	19	15.724	1.034	7	35	20.613	0.757	8
4	8.908	2.766	4	20	16.095	2.566	7	36	20.762	1.121	8
5	9.376	0.971	4	21	16.469	0.358	7	37	21.156	0.858	8
6	9.766	1.794	5	22	16.653	0.644	7	38	21.741	0.634	8
7	10.176	3.528	5	23	17.081	1.62	7	39	21.952	0.522	8
8	10.398	2.765	5	24	17.472	1.62	7	40	22.22	0.976	8
9	10.742	17.811	5	25	17.735	4.131	7	41	22.354	0.984	8
10	11.776	1.29	6	26	18.049	1.48	7	42	22.502	0.621	8
11	12.18	4.946	6	27	18.255	2.436	7	43	22.799	1.281	8
12	12.36	2.7	6	28	19.126	0.172	7	44	23.591	0.218	9
13	13.518	4.133	6	29	19.277	0.229	7	45	23.801	0.208	9
14	13.363	5.027	6	30	19.448	0.213	7	46	23.932	0.272	9
15	14.049	4.817	6	31	19.777	0.475	7	47	24.111	0.26	9
16	14.496	3.231	6	32	19.916	0.226	8	48	24.48	0.497	9

peak	time	%area	Carbon no.	peak	time	%area	Carbon no.	peak	time	%area	Carbon no.
49	24.767	0.66	9	83	32.053	0.081	11	117	39.765	0.038	12+
50	24.998	0.25	9	84	32.192	0.124	11	118	39.925	0.007	12+
51	25.303	0.577	9	85	32.457	0.1	11	119	40.068	0.014	12+
52	25.413	0.33	9	86	32.6	0.117	11	120	40.204	0.015	12+
53	25.525	0.344	9	87	32.922	0.126	11	121	40.492	0.018	12+
54	25.726	0.36	9	88	33.153	0.108	11	122	40.717	0.037	12+
55	25.973	0.418	9	89	33.323	0.162	11	123	40.921	0.026	12+
56	26.248	0.164	9	90	33.676	0.186	11	124	41.228	0.025	12+
57	26.374	0.579	9	91	33.892	0.117	11	125	41.377	0.043	12+
58	26.706	0.38	9	92	34.054	0.067	11	126	41.923	0.018	12+
59	26.818	0.384	9	93	34.219	0.165	11	127	42.189	0.015	12+
60	27.054	0.168	9	94	34.555	0.112	11	128	42.398	0.012	12+
61	27.16	0.236	9	95	34.798	0.055	11	129	42.924	0.033	12+
62	27.468	0.188	9	96	35.067	0.095	11	130	43.434	0.006	12+
63	27.674	0.094	9	97	35.253	0.035	11	131	43.61	0.006	12+
64	27.798	0.183	9	98	35.375	0.06	11	132	43.789	0.012	12+
65	28.063	0.153	9	99	35.556	0.1	11	133	44.29	0.011	12+
66	28.218	0.212	9	100	35.892	0.073	11	134	44.518	0.012	12+
67	28.577	0.325	10	101	36.045	0.083	11	135	44.926	0.018	12+
68	28.731	0.14	10	102	36.405	0.074	11	136	45.692	0.008	12+
69	29.053	0.354	10	103	36.751	0.069	11	137	46.136	0.01	12+
70	29.203	0.059	10	104	36.941	0.073	11	138	46.297	0.006	12+
71	29.365	0.317	10	105	37.168	0.054	11	139	46.696	0.006	12+
72	29.557	0.202	10	106	37.393	0.05	11	140	46.988	0.007	12+
73	29.761	0.463	10	107	37375	0.056	11	141	47.473	0.008	12+
74	30.135	0.27	10	108	37.863	0.026	11	142	47.913	0.009	12+
75	30.358	0.054	10	109	38.001	0.042	12+	143	48.116	0.006	12+
76	30.559	0.275	10	110	38.214	33	12+	144	50.645	0.006	12+
77	30.877	0.252	10	111	38.311	0.034	12+	145	50.959	0.007	12+
78	31.022	0.213	10	112	38.468	0.027	12+	146	51.697	0.008	12+
79	31.269	0.124	10	113	38.632	0.036	12+	147	68.414	0.011	12+
80	31.448	0.103	10	114	38.764	0.051	12+				
81	31.61	0.067	10	115	39.001	0.047	12+				
82	31.733	0.132	10	116	39.293	0.073	12+				

APPENDIX E

GAS CHROMATOGRAPH/MASS SPECTROMETER CONDITION

Condition for heavy liquid products

Column parameters
- Type : HP-1 capillary column
- Length (meters) : 30
- I.D. (mm) : 0.25
- Film thickness (μm) : 0.25

Carrier gas : Nitrogen

Average velocity : 28 cm/sec

Injector temperature : 220°C

FID detector temperature : 220°C

Split ratio : 100

Amount injected (μl) : 0.1

Scan parameters
- Low Mass : 30
- High Mass : 350

Column oven condition

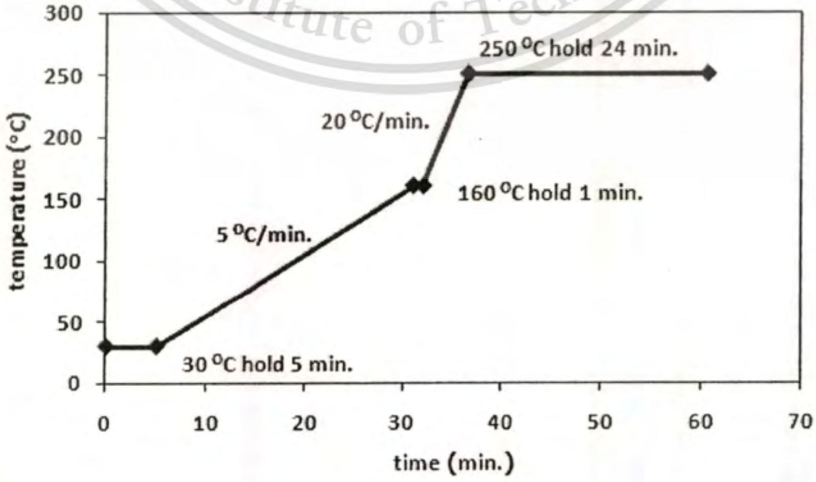

Figure E.1 Chromatogram GC-MS of liquid products from cracking reaction of polyethylene at 430 °C under nitrogen flow

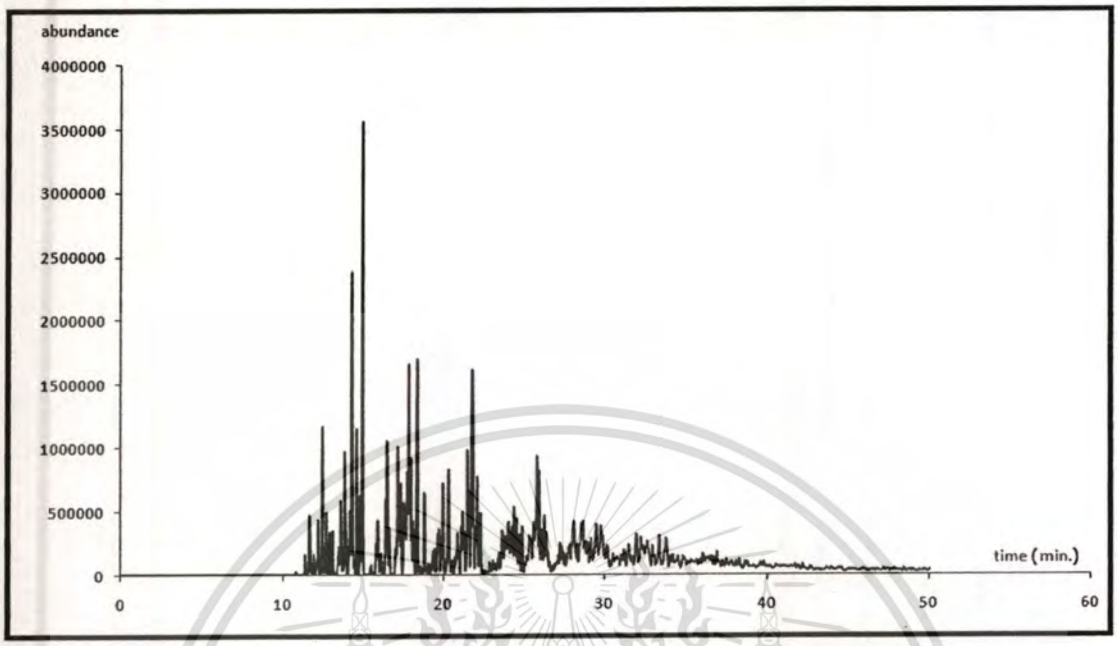

Reaction parameters; reactor screw speed, **66.26** rpm; catalyst content, 1.0 %wt.; polyethylene feed rate, 635.59 g/hr.; viscosity of polyethylene feed, 4.00 poise

peak	RT.	Name	Carbon no.	% area
1	10.873	propene	3	0.049
2	11.408	isobutane	4	0.296
3	11.685	2-methyl propene	4	0.971
4	11.947	2-butene	4	0.284
5	12.243	isobutane	4	0.87
6	12.498	2-methyl propene	4	1.829
7	12.627	n-butane	4	0.033
8	12.752	1-butene	4	0.773
9	12.961	2-butane	4	0.524
10	13.135	2-metyl butane	5	0.636
11	13.5	2-pentene	5	0.489
12	13.621	2-ethyl propene	5	1.071
13	13.875	2-methyl butane	5	2.297
14	14.164	2-pentene	5	0.887
15	14.312	2-ethyl propene	5	4.502
16	14.445	pentane	5	0.092

peak	RT.	Name	Carbon no.	% area
17	14.612	2-pentene	5	1.759
18	14.824	2-pentene	5	0.955
19	14.957	2-metyl-butene	5	5.753
20	15.462	4-methyl-1-pentene	6	0.027
21	15.534	3-methyl-1-pentene	6	0.052
22	15.819	2,3-dimethyl-1-butene	6	0.429
23	15.917	2,3-dimethyl-2-butene	6	0.76
24	16.058	4-methyl-1-pentene	6	0.203
25	16.122	3-methyl-1-pentene	6	0.265
26	16.396	2-methyl-2-pentene	6	0.928
27	16.472	4-methyl-2-pentene	6	1.687
28	16.612	2-methyl-2-pentene	6	0.695
29	17.003	3-methylpentane	6	0.409
30	17.136	2-methyl-1-pentene	6	1.927
31	17.242	3-hexene	6	0.54
32	17.337	2-methyl-2-pentene	6	1.239
33	17.527	3-methyl-2-pentene	6	1.157
34	17.622	cis-3-hexene	6	0.971
35	17.732	cis-3-hexene	6	1.34
36	17.823	4-methyl-trans-2-pentene	6	3.647
37	17.99	3-methyl-2-pentene	6	1.496
38	18.111	3-hexene	6	0.688
39	18.347	3-methyl-2-pentene	6	2.776
40	18.533	2,4-dimethyl-2-pentene	7	0.103
41	18.791	2,3-dimethyl-2-butene	6	1.081
42	19.049	2,4-dimethyl-1-pentene	7	0.146
43	19.322	2,4-dimethyl-2-pentene	7	0.466
44	19.444	2,4-dimethyl-1-pentene	7	0.334
45	19.705	2,4-dimethyl-2-pentene	7	1.135
46	19.952	2-methyl-trans-3-hexene	7	1.65
47	20.298	3-heptene	7	2.125
48	20.514	2-heptene	7	0.254
49	20.696	3-methyl-2-hexane	7	0.206
50	20.855	methyl-cyclohexane	7	1.063

peak	RT.	Name	Carbon no.	% area
51	21.098	2-methyl-1-hexene	7	0.303
52	21.189	methyl-cyclohexane	7	0.262
53	21.265	3-heptane	7	0.586
54	21.489	2-methyl-2-hexene	7	2.853
55	21.789	2-methyl-2-hexene	7	4.589
56	22.009	cis-2-methyl-3-hexene	7	0.611
57	22.116	3-methyl-2-hexene	7	1.47
58	22.324	3,4-dimethyl-2-pentene	7	1.109
59	22.469	5,5-dimethyl-2-hexene	8	0.035
60	22.62	methyl-cyclohexane	7	0.062
61	22.875	methyl-cyclohexane	7	0.163
62	23.099	2,5-dimethylhexane	8	0.144
63	23.224	2,4-dimethylhexane	8	0.112
64	23.391	2,4-dimethyl-3-hexene	8	0.134
65	23.471	2,3-dimethyl-2-hexene	8	0.223
66	23.672	2,3-dimethyl-2-hexene	8	0.79
67	23.831	2-methyl-trans-3-heptene	8	0.813
68	24.017	2-methyl-trans-3-heptene	8	0.643
69	24.082	3-methyl-3-heptene	8	0.6
70	24.199	trans-4-methyl-2-heptene	8	0.364
71	24.283	3,5-dimethyl-2-hexene	8	0.552
72	24.397	2,5-dimethyl-2-hexene	8	0.72
73	24.465	3,5-dimethyl-2-hexene	8	0.392
74	24.568	2-methylheptane	8	0.548
75	24.761	cyclooctane	8	0.416
76	24.917	3-methyl-4-methylenehexane	8	0.584
77	25.11	5-methyl-2-heptene	8	0.065
78	25.205	6-methyl-2-heptene	8	0.246
79	25.357	4-methyl-3-heptene	8	0.66
80	25.433	5-methyl-3-heptene	8	0.725
81	25.627	4-methyl-3-heptene	8	0.91
82	25.847	4-octene	8	2.586
83	25.972	4-methyleneheptane	8	1.556

peak	RT.	Name	Carbon no.	% area
84	26.12	4-octene	8	0.848
85	26.302	3-methyl-2-heptene	8	0.793
86	26.427	2,3-dimethyl-1,4-hexadiene	8	0.825
87	26.61	2,6-dimethyl-2,4-heptadiene	9	0.083
88	26.834	1-ethylcyclohexene	8	0.062
89	27.152	1-methyl-4-methylene-cyclohexane	8	0.363
90	27.262	propylcyclohexane	9	0.434
91	27.376	3-ethylcyclohexone	8	0.336
92	27.464	3-ethyl-3-heptene	9	0.092
93	27.562	1-ethyl-2-methylcyclopentene	8	0.112
94	27.801	4-ethyl-3-heptene	9	0.081
95	27.877	3-nonene	9	0.089
96	28.006	4-nonene	9	0.087
97	28.124	1,2,3-trimethylcyclohexane	9	0.412
98	28.23	4-ethyl-3-heptene	9	0.042
99	28.325	4-nonene	9	0.424
100	28.481	2-methyl-2-octene	9	0.076
101	28.595	2,6-dimethyl-3-heptene	9	0.23
102	28.652	p-xylene	8	0.659
103	29.126	trans-4-nonene	9	0.878
104	29.46	trans-4-nonene	9	1.73
105	29.79	1,2,3-trimethylcyclohexane	9	1.399
106	30.01	propylcyclohexane	9	0.029
107	30.166	3-ethyl-2-methyl-1,3-hexadiene	9	0.506
108	30.557	4-ethyl-2-propyl-furan	9	0.017
109	30.686	2-methyl-3-ethyl-2-heptene	10	0.145
110	30.792	cis-3-decene	10	0.174
111	31.077	3-ethyl-2-methyl-1,3-hexadiene	9	0.49
112	31.236	1,1-dimethyl-4-methylenecyclohexane	9	0.843
113	31.502	4-decene	10	0.987
114	31.984	4-decene	10	1.083
115	32.257	1,2,4,5-tetramethylcyclohexane	10	0.528
116	32.443	cyclohexanone	8	0.031
117	32.58	1,2,4,5-tetramethylcyclohexane	10	0.248

peak	RT.	Name	Carbon no.	% area
118	32.72	2,6-dimethyl-2-octene	10	0.694
119	32.994	5-decene	10	0.931
120	33.396	5-methyl-4-nonene	10	0.052
121	33.707	2,6-dimethyl-4-octene	10	0.429
122	33.81	1,2,5-trimethylbenzene	10	0.142
123	34.075	1-(3-methyl-2-furyl)-2-propanone	8	0.1
124	34.246	3-methyl-3-nonene	10	0.325
125	34.516	1-methyl-1-(2-methyl-2-propenyl)cyclopentane	10	0.358
126	34.975	5-undecene	11	0.135
127	36.08	5-undecene	11	0.125
128	36.622	2-isopropyl-1-octene	11	0.17
129	36.945	2-undecene	11	0.126
130	37.283	6-undecene	11	0.178
131	37.533	5-methyl-1-decene	11	0.2
132	38.296	4-undecene	11	0.125
133	38.661	6-undecene	11	0.062
134	38.797	5-undecene	11	0.069
135	39.613	1,2,4,5-trimethylbenzene	11	0.079
136	39.807	1,2,3,5-trimethylbenzene	11	0.083
137	41.724	6-dodecene	12	0.178
138	42.187	6-dodecene	12	0.156
139	42.68	6-tridecene	13	0.087
140	43.682	2-dodecene	12	0.065
141	43.929	4-dodecene	12	0.3

APPENDIX F

NMR DATA

A nuclear magnetic resonance (NMR) technique has been developed for determining the octane number from the composition of gasoline. Since the determination of gasoline octane number using the ASTM test engine required large quantities of the samples. The NMR technique can be used for limited amounts of samples. These measurements are performed using a Bruker AVANCE DPX300 NMR spectrometer with 300-MHz proton resonance frequency. A typical NMR spectrum of liquid product and a commercial gasoline 91 are shown in Figures F.1 and F.2, respectively.

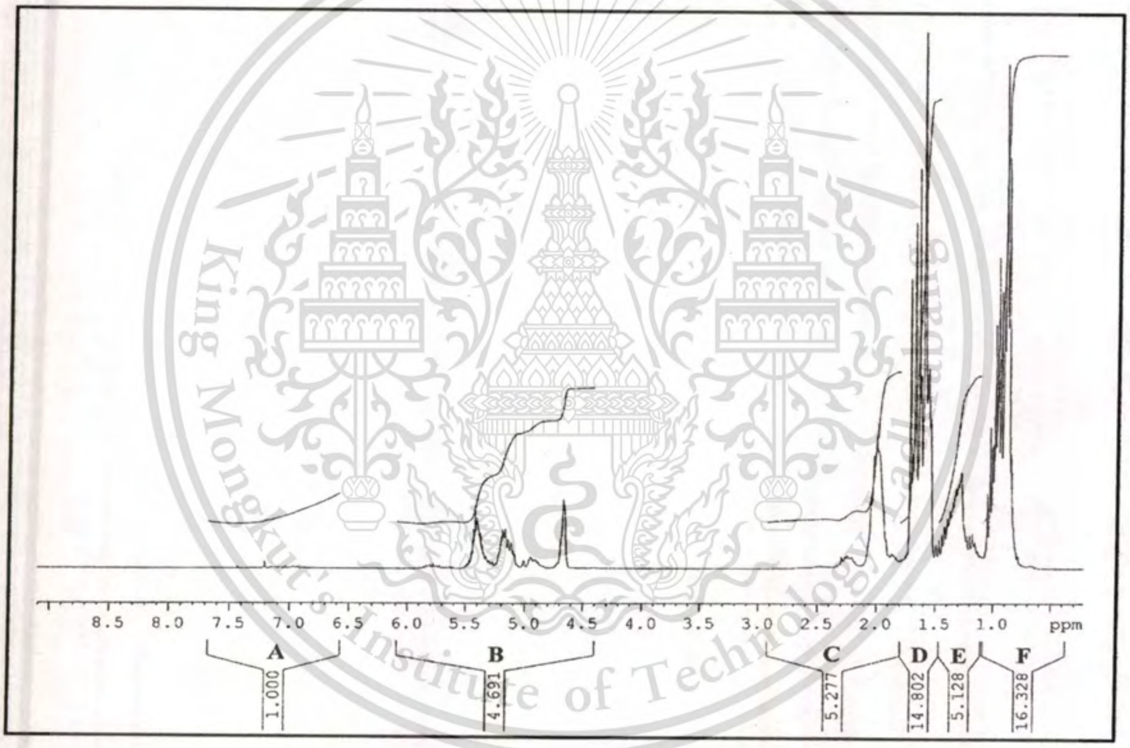

Figure F.1 NMR spectrum of liquid product

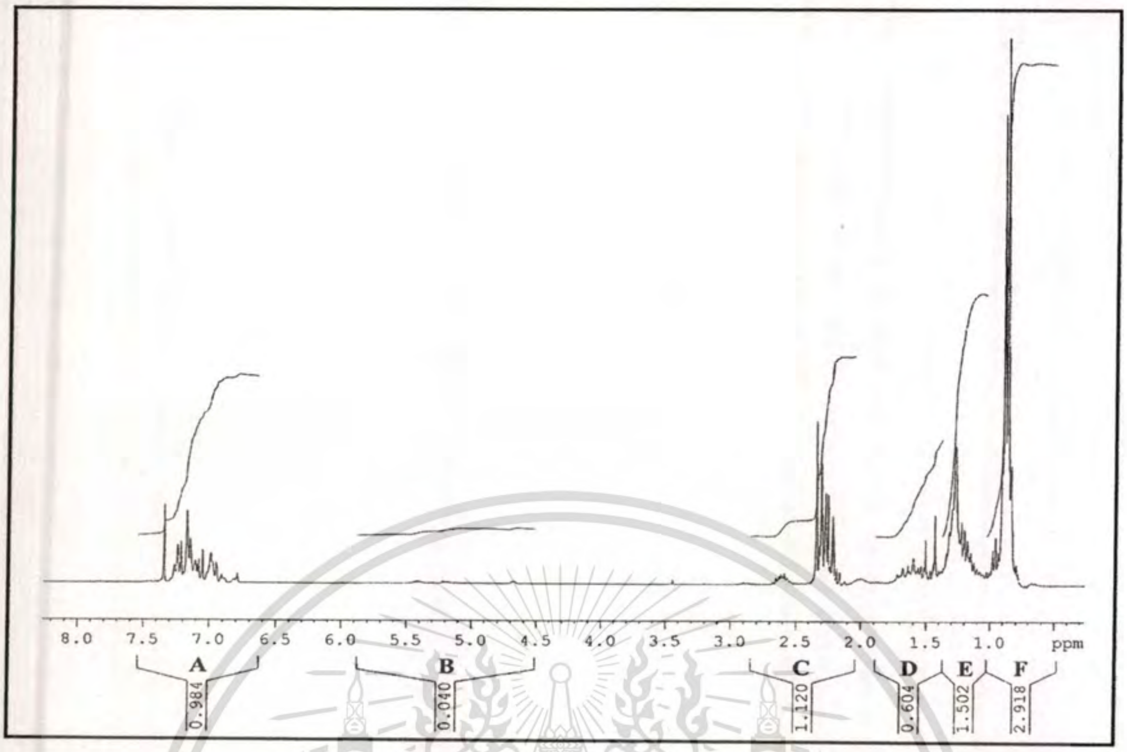

Figure F.2 NMR spectrum of commercial gasoline 91

The hydrocarbon species including aromatics, paraffins and olefins which are major components of petroleum products are estimated using literature correlations developed by Myers *et at.* [65]. In these equations, the chemical shift scale is divided into 6 regions (Figure F.3), marked as A to F. A, B, C, D, E and F representing the integrated area of the spectral regions are used for the octane number prediction as shown in Table F.1.

Table F.1 NMR spectral regions

Regions	Proton type	Chemical shift region (ppm)
A	Ring aromatics	6.6-8.0
B	Olefin	4.5-6.0
C	α-methyl	2.0-3.0
D	Methine (paraffins)	1.5-2.0
E	Methylene (paraffins)	1.0-1.5
F	Methyl (paraffins)	0.6-1.0

These equations include correction factors for the varying densities of the different hydrocarbon types which can be defined by the relations:

$$\text{Aromatics, vol.\%} = \left[\frac{0.97\left(A + \frac{C}{3}\right) \times 100}{0.97\left(A + \frac{C}{3}\right) + 1.02\left(D - 2B + \frac{E}{2} + \frac{F}{3}\right) + 3.33B} \right] \text{--------(1)}$$

$$\text{Paraffins, vol.\%} = \left[\frac{1.02\left(D - 2B + \frac{E}{2} + \frac{F}{3}\right) \times 100}{0.97\left(A + \frac{C}{3}\right) + 1.02\left(D - 2B + \frac{E}{2} + \frac{F}{3}\right) + 3.33B} \right] \text{--------(2)}$$

$$\text{Olefins, vol.\%} = \left[\frac{3.33B \times 100}{0.97\left(A + \frac{C}{3}\right) + 1.02\left(D - 2B + \frac{E}{2} + \frac{F}{3}\right) + 3.33B} \right] \text{--------(3)}$$

In addition, Myers *et al.* [66] also developed correlations for an 'isoparaffin index', and octane number. The isoparaffin index represents the estimated yields of branching which are the measured ratios of CH_3/CH_2 in the paraffins. The CH_3/CH_2 ratio is thus taken as a principal entry in an equation to calculate the octane number. The octane rating of gasoline (sample) is primarily arised from its isoparaffin and aromatic contents. By increasing the aromatic content, the blender can increase the octane quality to the required level. Aromatics are used because their individual octane ratings tend to be high. Another possible contributor to the high octane number would be the olefins. However, among the three hydrocarbon types (paraffins, aromatics, and olefins), olefin concentration is usually low (~10%) in petroleum fraction, which is fortunate because the olefin groups are determined with the least precision. Thus, olefin concentration is ignored in the linear regression analysis. A multiple linear equation is developed to express the octane number as a linear combination of the isoparaffin index, the aromatic content (vol%), the lead content (g/gal), and the sulfur content (wt%)

$$\text{Isoparaffin index} = CH_3/CH_2 = (F/3)\,/\,(E/2) \quad \text{--------(4)}$$

$$\text{RON} = 80.2 + 8.9\,(\text{isoparaffin index}) + 0.107\,\text{aromatics (vol.\%)} + 2.93\,\text{lead (g/gal)} - 13.4\,\text{sulfur (wt\%)} \quad \text{--------(5)}$$

$$\text{MON} = 70.8 + 10.0\,(\text{isoparaffin index}) + 0.101\,\text{aromatics (vol.\%)} + 3.27\,\text{lead (g/gal)} - 11.1\,\text{sulfur (wt\%)} \quad \text{--------(6)}$$

In the case of cracking of polyethylene, lead and sulfur contents are assumed to be negligible in the final gasoline range products. Therefore, equations (5) and (6) can be rewritten as:

$$\text{RON} = 80.2 + 8.9\ (\text{isoparaffin index}) + 0.107\ \text{aromatics (vol.\%} \quad \text{--------(7)}$$

$$\text{MON} = 70.8 + 10.0\ (\text{isoparaffin index}) + 0.101\ \text{aromatics (vol.\%)} \quad \text{--------(8)}$$

Table F.2 Intergrated area of the spectral regions of liquid product with commercial gasoline 91

Run	Viscosity of feds (poise)	MFI of feds (g/10min)	RSS (rpm)	Catalyst content (%wt.)	Feed rate (g/hr.)	A	B	C	D	E	F
1	4.0	24.6	130	1.0	633.8	0.254	13.404	18.171	44.207	23.139	62.698
2	4.0	24.6	66	1.0	635.6	1.000	3.960	5.627	13.789	5.215	16.223
3	4.0	24.6	46	1.0	639.5	0.065	23.514	25.422	66.236	24.82	82.06
4	4.0	24.6	46	2.0	632.2	1.000	4.691	5.277	14.802	5.128	16.328
5	4.0	24.6	46	2.0	442.3	2.499	33.143	36.917	94.865	26.523	113.8
6	4.0	24.6	46	2.0	771.3	5.113	948.28	1183.7	2780.9	1406.2	4088.5
7	4.0	24.6	46	2.0	865.6	6.358	106.99	121.38	287.56	161.89	412.99
8	20.3	4.8	46	2.0	607.7	0.604	0.859	0.563	12.386	0.456	2.671
9	2.7	36.8	46	2.0	639.9	4.086	38.797	42.918	111.01	33.212	119.38
Gasoline 91	-	-	-	-	-	0.984	0.040	1.12	0.604	1.502	2.918

Table F.3 The hydrocarbon types and octane number of liquid products from cracking of polyethylene in continuous process at 430 ^{O}C under nitrogen flow

Run	Viscosity of feds (poise)	MFI of feds (g/10min)	RSS (rpm)	Catalyst content (%wt.)	Feed rate (g/hr.)	Olefins content (%Vol)	Paraffins content (%Vol)	Aromatics content (%Vol)	RON	MON	Gasoline selectivity
1	4.0	24.6	130	1.0	633.8	43.92	50.05	6.02	96.92	89.47	82.0
2	4.0	24.6	66	1.0	635.6	43.75	46.99	9.26	99.65	92.47	82.0
3	4.0	24.6	46	1.0	639.5	53.36	41.00	5.64	100.42	93.41	86.0
4	4.0	24.6	46	2.0	632.2	48.83	42.81	8.37	99.99	92.87	86.0
5	4.0	24.6	46	2.0	442.3	53.55	39.48	6.97	106.4	100.11	86.0
6	4.0	24.6	46	2.0	771.3	48.18	45.91	5.91	98.08	90.78	-
7	4.0	24.6	46	2.0	865.6	50.92	42.59	6.49	96.03	88.46	-
8	20.3	4.8	46	2.0	607.7	18.28	76.82	4.91	115.48	110.35	88.0
9	2.7	36.8	46	2.0	639.9	54.14	38.39	7.48	102.33	95.52	86.0
Gasoline 91	-	-	-	-	-	3.56	61.26	35.18	95.49	87.3	100

AUTHOR BIOGRAPHY

Mr. Boonsueb Sontayamarn was born on May 29, 1982 in Chainat. He received a Bachelor Degree in Chemistry from the Department of Chemistry, Faculty of Science, Narasuan University in 2005. He has been a graduate student of the Program of Petrochemicals and Hydrocarbon Chemistry, Graduate School, King Mongkut's Institute of Technology since 2005.